Title
Regulation of Synaptic Glutamate Receptors by MAGUK Scaffolding Proteins

Author
Levy, Jonathan Ma

Publication Date
2015

Peer reviewed|Thesis/dissertation

Regulation of Synaptic Glutamate Receptors by MAGUK Scaffolding Proteins

by

Jonathan Ma Levy

DISSERTATION

Submitted in partial satisfaction of the requirements for the degree of

DOCTOR OF PHILOSOPHY

in

Neuroscience

in the

GRADUATE DIVISION

of the

UNIVERSITY OF CALIFORNIA, SAN FRANCISCO

Acknowledgements

First are my parents, who will always be mom and dad, and never Margaret and Bob. They have made me into who I am today simply by being who they are. They are two of the hardest-working, humblest people I will ever meet. They are stubbornly determined to be successful in the things that are important to them. By being themselves, they have pushed me towards a happy, fulfilling life. The impact of their love, loyalty, and unshakable support cannot be measured.

As a college undergraduate, I joined the lab of Liqun Luo, in large part because he had wonderful pictures of GFP-expressing neurons on his website. This shallow decision turned out wonderfully – Liqun and the rest of the lab, especially Eric Hoopfer and Oren Schuldiner, whom I worked with closely, are incredible biologists who were able to demonstrate to me how science should be done. Furthermore, the culture that Liqun promoted – a sense of camaraderie and a willingness to push others – made science incredibly fun and rewarding, and served as a template that I sought out again in graduate school.

My decision to join Roger's lab was, in many ways, similarly shallow. Electrophysiology was foreign to me, coming from a fly genetics lab, and one of the main draws initially was the chance to work with Seth Shipman and Adam Granger, two of my classmates who I'd gotten to know over the first year. Again, this decision turned out wonderfully. Roger has been the perfect mentor for me. His experimental rigor and scientific curiosity have demonstrated for me the qualities of a successful scientist. His loyalty, humility, and dedication are personal traits I hope to emulate.

The thesis committee, Mark Von Zastrow, Rob Edwards, Graeme Davis, and Hillel Adesnik, have been absolute rock stars. They have each pushed me to think about my work from angles I hadn't considered, using their own unique expertise. Their feedback has improved both this thesis and my rigor as a scientist.

The people in Roger's lab have been a huge part of my experience there. Roger, like Liqun, has fostered a productive and open lab culture. I was able to learn from the senior members when I joined: Tasso, Wei, Eric, Geoff, and Aaron in particular stand out. Their advice was incredibly useful for teaching me how to think about the synapse. I hope I have been similarly useful to the newer members of the lab, including Meryl, Sam, Sal, and Yin. They are all incredible and it is great to know that the future of the lab is secure.

The bulk of my experience in lab, however, has been defined by a core lab group: Carleton, Adam, John Gray, Bruce, Alex, Kate, Quynh Anh, Seth, and Stone.

Carleton was the first person I got to know well; my rotation rig was next to his. Carleton is an absolutely top-notch scientist and a good friend. His lab projects and weekend stories always seemed to be tinged with madness, in the very best ways possible. Alex was the first postdoc I got to know when I joined the lab. He had an incredible wealth of knowledge, which, like a child looking ahead to adulthood, I assumed would be bestowed on me when the time came. Now that the time has come, it turns out he was just incredibly well-read, with impeccable knowledge of the literature and his chosen techniques. John Gray was the lab's only M.D. for the bulk of my time there, and provided an incredible amount of medical knowledge, useful both for considering the applications of our scientific work and for settling inane arguments. Stone

became the lab's glutamate fast-application wizard, and was able to generate data at an incredible rate.

I leave the lab just ahead of two of its other members: Bruce and Quynh Anh. Both have been incredible labmates. QA is several years younger; it has been amazing to see her truly come into her own as a now-senior member of the lab. Bruce has been a perfect addition to the lab, and has become a sounding board for ideas as the now-senior postdoc in the lab. His advice, both on my day-to-day experiments and longer-term career decisions, has been incredibly valuable and invariably on point.

Seth, Adam, and Kate formed the grad student core of my Nicoll Lab experience. Seth and Adam are in my graduate school class, and we all started in the Nicoll Lab within a month or so. Kate joined the next year. Seth and I shared a small room, with Kate and Adam next to us. They were better friends and co-workers than I would have known to ask for. They were there every step of the way, through everything. It would lessen them to say only that their advice was incredibly useful, or that they pushed me to be more than I would otherwise be, or to otherwise enumerate their virtues; they are good friends whose judgement I trust in all areas, and have made me better in all the ways friends do. In particular, Seth and I shared a small, windowless room for roughly five years. It was a privilege.

Rebecca and Andrew happened to move out to San Francisco while I was battling through some of the most trying times of graduate school. It was wonderful having them nearby and seeing their relationship grow and flourish.

Finally, Mary Lyn has been there with me the entire time. She is simply the best.

Contributions

All experiments were designed in collaboration with Roger Nicoll and were made possible by a graduate fellowship from the American Heart Association. Xiaobing Chen and Tom Reese helped guide the direction of the experiments presented in Chapter 3, which has been previously published in *Neuron* and is reproduced with permission:

Levy, J.M., Chen, X., Reese, T.S., and Nicoll, R.A. (2015). Synaptic Consolidation Normalizes AMPAR Quantal Size following MAGUK Loss. Neuron *87*, 534-548.

Regulation of Synaptic Glutamate Receptors by PSD-95 MAGUK Proteins

Jonathan Ma Levy

Abstract

The nervous system is tasked with quickly gathering, interpreting, and responding to information about the outside world. To carry out this task, it has signaling cells called neurons, their support cells, and most importantly, the connections between neurons which can be used in a combinatorial manner to generate a wide array of behaviors. These connections occur at locations termed synapses. Glutamatergic synapses, consisting of a post-synaptic specialization with clustered glutamate receptors opposite a pre-synaptic terminal, are the sites of fast excitatory neurotransmission in the brain. Communication between neurons via synaptic transmission enables the nervous system to respond quickly to stimuli. Changes in synaptic strength and connectivity change these responses, through processes commonly termed learning and memory. The mechanisms controlling synapse growth and maintenance are therefore critically important for learning and memory. Proper formation of the post-synaptic specialization requires that glutamate receptors localize to the synapse and associate with the complex network of signaling and scaffolding molecules known as the post-synaptic density (PSD). Multiple lines of evidence demonstrate that the PSD scaffolding proteins themselves play an instructive role in regulating the localization of synaptic glutamate receptors. The primary protein family implicated in synaptic glutamate receptor localization is the four-member membrane-associated guanylyl kinase (MAGUK) family: PSD-93, PSD-95, SAP97, and SAP102. Here, we examine the role of the MAGUKs in several contexts. We find that MAGUKs are specifically responsible for creating functional synapses after initial spine formation by

filling functionally silent spines with glutamate receptors. Removal of the MAGUKs causes an initial reduction in synaptic strength, followed by activation of a compensatory program that consolidates weakened synapses to normalize synaptic strength. We next find that overexpression of the MAGUKs fills additional silent spines with glutamate receptors. Removal or overexpression of MAGUKs therefore does not affect synaptic strength, which appears to be tightly regulated. Combination of these two manipulations by simultaneous removal of endogenous MAGUKs and overexpression of recombinant MAGUK destroys existing PSDs, disrupts regulation of synaptic strength, and results in formation of very strong synapses. Finally, we examine the role of the MAGUKs *in vivo*, characterizing their role during development of the hippocampus.

Table of Contents

List of Figures and Tables

CHAPTER 1: General Introduction

The nervous system is responsible for receiving, processing, and responding to all information about the world. It is the only system that performs these vital tasks and its proper function is essential for life. The human nervous system performs these complicated tasks using a brain containing approximately 10^{11} neurons with 10^{14} independent connections, roughly equivalent to the number of stars in the Milky Way. In this network, computation requires fast communication between groups of neurons. This communication generally takes place at microscopic anatomical specializations called synapses, whose location, number, and composition are tightly regulated. Genetic and environmental factors that disrupt these carefully assembled structures, resulting in errors in information transfer between neurons, have been closely linked to a variety of diseases affecting the brain.

There are many types of synapses in the nervous system, with each type performing a specialized role determined by protein composition, location, and connectivity. For example, some synapses are designed for high-fidelity transmission of information, such as would be useful in relaying primary sensory information. One example of this synapse type is the Calyx of Held, which relays auditory information to the cerebellum. Other synapses are designed only to maximally activate when several coincident inputs are received, as would be useful when functioning as a coincidence detector to form associative memories. These synapses are found in the CA1 region of the hippocampus, a structure required to form declarative memories. A wide variety of sign-inverting synapses shape the flow of information by inhibiting neuronal activation. Finally, some synapses have the best nomenclature, like the “detonator synapses” located on thorny excrescences connecting dentate gyrus neurons to the CA3 region of the hippocampus. Fortunately, while differences in the protein composition of synapses produce a wide range of useful synapse types, the fundamental properties of individual synaptic

components generally hold true across synapse types, meaning individual synaptic components can be linked to specific processes.

Makeup of the excitatory synapse

The synapse is the protein-rich point of contact between neurons, and its components can be conceptually divided into two groups. First, structural components that physically hold the synapse together, comprised of the membranes of the pre- and post-synaptic neurons, the cell adhesion molecules that keep them apposed, and the cytoplasmic molecules that form a synaptic scaffold in support of functional components. Second, the functional components that allow for neurotransmission at the synapse, including the presynaptic proteins which underlie neurotransmitter release, the neurotransmitter receptors, and the postsynaptic net of signaling proteins that interpret and respond to signals generated by the neurotransmitter receptors. Importantly, these groups are not fully segregated – the structural components are regulated by neuronal activity, and the functional components require the structural scaffold for synaptic localization.

Fast excitatory transmission in the brain is mediated by release of the neurotransmitter glutamate from presynaptic terminals, with its release sensed by a large family of glutamate receptors. These glutamate receptors must be held opposite the sites of neurotransmitter release by structural components for signaling to occur. Importantly, these bonds must strike a careful balance: although they must be stable enough to hold receptors at synapses, they must also be transient enough to permit the addition or subtraction of receptors during learning.

Glutamate receptors at synapses

Glutamate receptors at the synapse can be divided into two classes: AMPA- and NMDA-type ionotropic receptors. These receptors have distinct methods of localizing to the synapse, likely due to differences in their function: AMPA receptors are ligand-gated, meaning that they open following glutamate binding, while NMDARs are both ligand- and voltage-gated, meaning they require binding of glutamate and depolarization of the post-synaptic neuron to open. It is thought that NMDARs act as coincidence detectors, only opening when the post-synaptic neuron has been depolarized due to current entering through AMPARs simultaneously at several synapses. Importantly, NMDARs are permeable to calcium, an important signaling molecule in long-term plasticity. Long-term plasticity has the function of adding or removing AMPARs from synapses, meaning that AMPAR localization must be more dynamic than NMDAR localization, which is relatively unchanged by calcium influx and plasticity. Consistent with this idea, AMPARs are located at the periphery of the post-synaptic density, where they may be easily added or removed, while NMDARs are ensconced at the center of the PSD.

AMPARs are tetramers comprised of the GluA subunits: GluA1, GluA2, and GluA3. AMPARs form a "dimer of homodimers," such that all three subunits may never be present in a single molecule. In hippocampal pyramidal neurons AMPARs are either GluA1/A2 or GluA2/A3 heteromers, containing two copies of each subunit present. AMPAR synaptic trafficking is a well-studied multi-step phenomenon, involving maturation in the endoplasmic reticulum followed by forward trafficking to the plasma membrane and subsequent lateral diffusion to synapses. In the endoplasmic reticulum they associate with chaperone proteins such as TARPs and cornichons. These interactions are required for protein maturation and forward trafficking to the plasma membrane, as removal of these chaperone proteins prevents surface expression of AMPARs. AMPARs on the cell surface do not directly interact with synaptic proteins for

localization, but rather rely primarily on interactions between TARPs and the MAGUK family of synaptic scaffolding proteins.

The MAGUKs are a class of membrane-associated cytoplasmic synaptic scaffolding proteins that link transmembrane proteins, such as NMDARs and TARPs, with the cytoplasmic scaffold. MAGUK abundance controls synaptic AMPAR number: overexpression of MAGUKs increases the number of synaptic AMPARs, and knockdown of family members decreases it. Overexpression of PSD-95 mimics the selective increase in AMPAR transmission seen during LTP, and furthermore occludes it: neurons overexpressing PSD-95 are not able to undergo further potentiation via LTP stimulus, suggesting that they are part of the same pathway. Finally, increases in PSD-95 content are seen following LTP induction. It is tempting, therefore to speculate that increases in synaptic PSD-95 abundance are a critical step in the LTP pathway.

MAGUK interactions at the synapse

MAGUKs are central scaffolding proteins at the synapse. They are anchored to the membrane and exist in the PSD, a 30-50 μm-thick electron-dense proteinaceous structure that contains the cytoplasmic tails of many membrane proteins, as well as abundant enzymes including CaMKII and SynGAP. They are one of the most abundant proteins at the synapse, with an estimated 400 copies per synapse (Sheng and Hoogenraad, 2007). Their interaction with the cytoplasmic tail of the TARPs has been shown to be critical in localizing AMPARs to synapses (Bats et al., 2007; Hafner et al., 2015). Furthermore, they interact with many of the other proteins at the synapse, including CaMKII. Although they interact with many proteins thought to have structural roles, such as GKAP and Shank, loss of the MAGUKs does not cause a reduction in the number of dendritic spines (Elias et al., 2006). It is therefore likely that the MAGUKs play a

specific role in localizing glutamate receptors to synapses, rather than act as a necessary component of the spine formation machinery.

Homeostatic Processes at the synapse

LTP and related plasticity mechanisms, such as LTD, acting via Ca^{2+} influx through NMDA receptors have been shown to quickly change synaptic strength at a defined set of synapses, meaning they are candidates for strengthening or weakening a very small subset of a neuron's synapses. LTP is a Hebbian process, meaning that only those synapses that are active during postsynaptic depolarization are potentiated. There are also forms of plasticity, however, that counteract changes in activity, with the purpose of normalizing overall activity rates. These changes are termed homeostatic, since they act to oppose changes in firing rates. For example, one form of homeostatic plasticity, multiplicative scaling, uniformly reduces overall synaptic strength in dissociated cortical pyramidal neurons in response to bicuculline, while preserving established differences in relative strengths. Multiplicative scaling has also been shown to be bidirectional, scaling synapses up after application of TTX to block activity *in vitro*, and has also been shown to act *in vivo*, increasing synaptic strength in visual cortex following reduction of input strength via monocular deprivation (Hengen et al., 2013; Lambo and Turrigiano, 2013). Other expressions of homeostatic plasticity that act to oppose activity-induced changes in firing rate include reduction in functional synapse number, and an associated loss of spines, in channelrhodopsin-expressing hippocampal pyramidal neurons following chronic photostimulation (Goold and Nicoll, 2010). Although the expression of homeostatic plasticity may have different results in different brain regions, or as a result of differing experimental paradigms, multiple lines of evidence show that the same molecules are involved, suggesting a common pathway with different outputs, rather than region- or input-specific pathways.

Homeostatic plasticity has been well-described and several of the proteins required have been identified. Plasticity relies on depolarization of the neuron causing calcium influx through L-type voltage gated calcium channels (Goold and Nicoll, 2010; Ibata et al., 2008; Thiagarajan et al., 2005). Selective block of these channels eliminates all homeostatic plasticity, in contrast with synaptic plasticity such as LTP, which relies on calcium influx through NMDA receptors. A simple model would be an inverse correlation between calcium current and synaptic strength, such that increases in calcium current due to greater neuronal depolarization cause a reduction in synaptic strength, and reductions cause an increase in synaptic strength. Interestingly, as might be expected if the amount of calcium entering through L-type channels determines the homeostatic set point, block of these channels causes an increase in synaptic strength, but blocks any further plasticity even in the presence of increased activity, for example by photostimulation (Goold and Nicoll, 2010). Furthermore, it is not simply a reduction in calcium conductance that blocks scaling, since block of other channel types that reduces calcium influx to the same degree does not prevent scaling. Instead, it is likely that L-type channels are specifically coupled to a specific downstream target, either by their perisomatic location or by direct physical tethering of second messengers, such as the interaction between the cytoplasmic tail of the L-type channel and calmodulin (CaM), a calcium-binding protein that is capable of activating downstream proteins after binding calcium.

Calcium entering through L-type channels activates calcium-dependent signaling cascades, such as the CaM-dependent activation of CaMKK. CaMKK activation is required for homeostatic plasticity: block of CaMKK activation by application of STO-609 blocks plasticity while specific expression of CaMKK L233F, a point-mutant that is insensitive to STO-609, rescues the expression of plasticity (Goold and Nicoll, 2010). CaMKK has two well-

characterized downstream targets: CaMK1 and CaMKIV. These targets are weakly activated by CaM-Ca^{2+} alone, and more strongly activated by the combination of CaM-Ca^{2+} and phosphorylation by CaMKK (Soderling, 1999). Block of CaMKIV, but not CAMK1, prevents homeostatic plasticity.

Activated CaMKIV is a nuclear-localized transcriptional regulator that acts through phosphorylation of nuclear targets, including the transcription factor CREB. Strengthening a role for protein synthesis in homeostatic plasticity, application of the transcriptional inhibitors actinomycin D or 5,6-dichloro-1-b-D-ribobenzimidazole (DRB), or the translational inhibitors cyclohexamide or anisomycin, block several forms of homeostatic plasticity (Goold and Nicoll, 2010; Ibata et al., 2008). Future work is needed to determine the relevant transcriptional changes produced by CREB phosphorylation, and determine whether less well-characterized targets of CaMKIV might play significant roles in plasticity.

Plasticity targets at the synapse

Although the homeostatic plasticity pathways leading to transcriptional regulation and translation are well-characterized, we do not know the identity or downstream targets of these newly-synthesized proteins. We do know, however, that the GluA2 AMPAR subunit is required for homeostatic plasticity (Gainey et al., 2009; Goold and Nicoll, 2010) but see (Altimimi and Stellwagen, 2013), and that removal of this subunit blocks homeostatic plasticity in cortex and hippocampus. There are two possible roles for GluA2: either in depolarizing the neuron to relieve the voltage block of L-type channels, or acting as a substrate for homeostatic plasticity at the synapse. The idea that GluA2 is responsible for depolarization is difficult to reconcile with the data that removal of GluA1, which reduces AMPAR transmission to a greater degree (Lu et

al., 2009), does not block homeostasis. GluA2 therefore acts downstream of L-type channel opening, meaning it is likely a substrate for removal by upstream effectors of the homeostatic pathway. It is still possible, however, that GluA2 loss blocks homeostasis not because the homeostatic pathway cannot act on GluA1 and GluA3, but rather because in the absence of GluA2 synapses are formed in a manner that prevents the homeostatic effector molecules from manipulating them.

The MAGUKs have been shown to play a necessary role in homeostatic plasticity. Specifically, loss of PSD-95 prevents scaling up and down in cortical cultures (Sun and Turrigiano, 2011), suggesting that PSD-95 must be present in the postsynaptic scaffold for homeostatic changes to take place. Although one simple mechanism would be that the abundance of PSD-95 at the synapse controls the number of AMAPRs, such that homeostatic effectors would add or remove PSD-95 molecules to add or subtract AMPARs. Direct manipulation of the levels of PSD-95 at the synapse, however, by overexpression of recombinant protein or knockdown of endogenous PSD-95, do not mimic synaptic scaling, suggesting that the abundance of PSD-95 is not the critical factor. Instead, it is likely that the homeostatic pathway modifies the interaction between the PSD-95 scaffold and AMPARs. In line with the hypothesis that homeostatic signaling might change the affinity of AMPARs for MAGUKs, scaling down is associated with an increase in the dissociation rate of AMPARs at synapses (Tatavarty et al., 2013).

The homeostatic plasticity pathway and default synaptic size

Although a number of proteins have been identified which contribute to homeostatic changes in synaptic strength, it is unclear whether these proteins are involved in controlling

default synaptic strength, or only in changing synaptic strength from the default in response to changes in activity. In rodents, average synaptic strength is conserved over the lifetime of the organism (Hsia et al., 1998), although at single synapses it can easily be modified by processes such as LTP. This conservation of synaptic strength suggests an active program to maintain it. Although manipulations such as incubation of neurons in TTX have been interpreted as layering a previously inactive homeostatic response on top of a previously-existing and mechanistically independent default synaptic strength set-point, it is possible *in vivo* that setting of default synaptic strength uses the homeostatic components and simply represents the signaling equilibrium between synapse assembly and disassembly.

If the homeostatic pathway is involved in setting default synaptic strength, perturbation of proteins involved in that pathway should be sufficient to cause changes in synaptic strength. For example, calcium signaling by L-type channels is required for many forms of homeostasis. Additionally, blockade of L-type channels by nifedipine, but not other channels expressed in the soma such as T-type channels (Avery and Johnston, 1996), causes an increase in synaptic strength, suggesting that L-type channel signaling is active in the absence of external perturbations (Thiagarajan et al., 2005). Additionally, the GluA2 subunit is required for distance-dependent scaling (Shipman et al., 2013). Synaptic currents in hippocampal pyramidal neurons are largely passively propagated, meaning that they dissipate in a distance-dependent manner. Therefore, without manipulation of synaptic currents, the amplitude of these currents upon reaching the soma would be inversely proportional to the distance of the synapse from the soma. To counteract this distance-dependent reduction in amplitude and prevent a bias in synaptic strength based on location of the synapse, the number of AMPARs at each synapse increases with distance from the soma, perfectly offsetting the reduction in amplitude caused by the

distance from the soma (Andrasfalvy and Magee, 2001; Magee and Cook, 2000; Smith et al., 2003). It is difficult to imagine how this program could be developed or maintained without active feedback, and indeed, it has been found that the GluA2 AMPAR subunit, which is required for homeostatic plasticity, is required for this distance-dependent scaling (Shipman et al., 2013).

In the following thesis, I first set out to determine whether the MAGUK family of synaptic scaffolding proteins is required to localize glutamate receptors to synapses, finding that removal of the MAGUKs causes loss of most of the post-synaptic glutamate receptors. Furthermore, each of the MAGUK family members plays an equal role in the localization of glutamate receptors. I address previous reports showing that one family member, SAP102, is not involved in synaptic transmission by demonstrating that these previous results were confounded by technical issues surrounding the method of SAP102 removal. Finally, I show that the loss of the MAGUKs results in all-or-none loss of excitatory synapses.

I next mechanistically describe the all-or-none synapse loss seen following MAGUK knockdown. Although MAGUKs are present rather uniformly at all synapses, suggesting their loss would cause a relatively uniform reduction in synaptic transmission, the remaining transmission instead is all-or-none, meaning many synapses are functionally eliminated while the remaining synapses appear to be functionally normal. I find that this all-or-none loss results from a compensatory program that consolidates synapses after they have been uniformly weakened by MAGUK knockdown. These processes are separable and I show that consolidation normalizes synaptic strength via signaling by the L-type calcium channel, acting through CaMKK on GluA2. These results are presented in Chapter 3.

Having now established techniques to knock down the MAGUKs in neurons, I combine MAGUK knockdown with overexpression of PSD-93 or PSD-95, finding that PSD-93, but not PSD-95, requires endogenous MAGUKs to localize AMPA receptors to synapses. This finding is supported by data that removal of all MAGUKs except PSD-93 mimics removal of all MAGUKs, indicating endogenous PSD-93 alone has little function. Structure-function experiments reveal that the extreme N-terminal 30 amino acids of PSD-95 is both necessary and sufficient for localization of synaptic AMPA receptors; exchange of PSD-93 and PSD-95 N-termini completely swaps functionality, conferring the ability to traffic synaptic AMPA receptors on PSD-93 and removing it from PSD-95. We also find that although overexpression of PSD-95 increases AMPAR-containing synapse number greatly, it has little effect on synapse strength at individual synapses, instead primarily unsilencing synapses. In contrast, PSD-95 overexpression and simultaneous removal of endogenous MAGUKs causes a large increase in synapse strength at individual synapses, indicating that the matrix of endogenous MAGUKs is required for proper regulation of synapse strength. These results are presented in Chapter 4.

Finally, in Chapter 5, I look at the role of MAGUKs *in vivo*. I find that in young animals and cultured slices, MAGUKs play very similar roles. Knockdown of the MAGUKs in CA1 of older animals, however, has little effect, suggesting that either the synapses or the MAGUKs themselves are much more stable than in young animals. Additionally, overexpression of PSD-95 has little effect in older animals, suggesting that synapses are much more resistant to changes due to fluctuations in MAGUK levels. Interestingly, dentate gyrus synapses are sensitive to MAGUKs at all time points tested, suggesting a spatial heterogeneity of function.

CHAPTER 2: Methods

Experimental Constructs

The triple MAGUK miRNA construct targeting PSD-93, PSD-95, and SAP102 was made using sequences that have been previously characterized (Elias et al., 2006). Targeting sequences GACTGCCTAGCCAAGGACTTA (PSD-93 rat/mouse), TCACGATCATCGCTCAGTATA (PSD-95 rat/mouse), CCAAGTCCATCGAAGCACTTA (SAP102 rat), and CCAAGTCCATTGAAGCACTTA (SAP102 mouse, single nucleotide change underlined) were subcloned into pCDNA6.2/EmGFP using the BLOCK-iT miRNA kit (Life Technologies) resulting in GFP followed by the miRNA. For triple knockdown, three chained miRNAs were subcloned into the 3'UTR of GFP. The resulting GFP-miRNA constructs were subcloned into pCAGGS or FUGW for biolistic and lentiviral expression, respectively. For calcium channel experiments, T1036Y mutation was made from human CaV1.2 cDNA (gift from D. Julius) by mutation using overlap-extension PCR with primers GGAACATCGTGATTGTCTACACCCTGCTGCAGTTCATG (Forward) and CATGAACTGCAGCAGGGTGTAGACAATCACGATGTTCC (Reverse) and subcloned into pCAGGS. CaMKK L223F (Goold and Nicoll, 2010) was subcloned into pCAGGS.

Electrophysiology in Slice Cultures

Organotypic hippocampal slice cultures were made as previously described in (Schnell et al., 2002). Slices from P6-P8 rats were biolistically transfected at 1-2DIV. Where specified, viral infections were performed via microinjection into the CA1 region using a Nanoject (Drummond Scientific). For drug incubations, nifedipine (20 μM) or STO-609 (3μM) were added at time of transfection. Recordings were performed at DIV 7-9 unless otherwise noted. Dual whole-cell

recordings in area CA1 were done by simultaneously recording responses from a fluorescent transfected neuron and neighboring untransfected control neuron. Pyramidal neurons were identified by morphology and location. Series resistance was monitored on-line, and recordings in which series increased to >30 MOhm or varied by >50% between neurons were discarded. Dual whole-cell recordings measuring evoked EPSCs used an external solution bubbled with 95% O_2/ 5% CO_2 consisting of (in mM) 119 NaCl, 2.5 KCl, 4 $CaCl_2$, 4 $MgSO_4$, 1 NaH_2PO_4, 26.2 $NaHCO_3$, 11 Glucose. 100 μM picrotoxin was added to block inhibitory currents and 0 – 2 μM 2-Chloroadenosine was used to control epileptiform activity. Intracellular solution contained 135 $CsMeSO_4$, 8 NaCl, 10 HEPES, 0.3 EGTA, 5 QX314-Cl, 4 MgATP, 0.3 Na_3GTP, 0.1 spermine. A bipolar stimulation electrode (FHC) was placed in stratum radiatum, and responses were evoked at 0.2 Hz. Peak AMPAR currents were recorded at -70 mV, and NMDAR current amplitudes 100 ms following the stimulus were recorded at +40 mV. Paired-pulse ratio was determined by delivering two stimuli 40 ms apart and dividing the peak response to stimulus 2 by the peak response to stimulus 1. Coefficient of variation analysis was generally performed as described previously (Gray et al., 2011), with the exception that pairs with fewer than 30 stable responses were discarded. mEPSCs were isolated by adding 0.5 – 1 μM TTX to the recording solution to block evoked potentials and were analyzed off-line with custom software (IGOR Pro). Paired whole-cell AMPAR currents were recorded following a puff of 100 nM S-AMPA delivered to the neuronal soma by a large-diameter (20-30 μM tip diameter) glass pipette in the presence of 1 μM TTX, 100 μM picrotoxin, 10 μM cyclothiazide, and 50 μM APV. Whole-cell NMDA responses were evoked at +40 mV by 200 μM NMDA / 200 μM glycine in the presence of 1μM TTX, 100 μM picrotoxin. In both cases, perfusion was 1 second in duration and was controlled by a Picospritzer II (General Valve Corporation). For Sr^{2+}-evoked asynchronous

EPSC recording, solution was as above with the equimolar substitution of $SrCl_2$ for $CaCl_2$. Stimulation was increased from 0.2 Hz to 2 Hz to optimize the frequency Sr^{2+}-evoked responses (Oliet et al., 1996). Sr^{2+}-evoked aEPSCs were analyzed off-line with custom software (IGOR Pro), and in all cases at least 100 quantal events were used. Intracellular solution for recording of calcium channel currents contained (in mM) 135 $CsMeSO_4$, 8 NaCl, 5 TEA-Cl, 10 HEPES, 4 MgATP, 0.3 Na_3GTP, 5 EGTA, 10 Phospho-creatine. Extracellular solution was as above with the equimolar substitution of $BaCl_2$ for $CaCl_2$, and $MgCl_2$ for $MgSO_4$. 10 TEA-Cl and 0.5 TTX were added to block potassium and sodium channels, respectively. Responses were collected with a Multiclamp 700A amplifier (Axon Instruments), filtered at 2 kHz, and digitized at 10 kHz.

Anatomy and Imaging

Slice cultures were maintained and transfected as described above. For spine density measurements, images were acquired at DIV 7-9 on a Zeiss LSM5 Pascal using a 63x water-immersion objective. Individual slices were immersed in HEPES-ACSF (140 NaCl, 5 KCl, 5 EGTA, 1.4 $MgSO_4$, 1 NaH_2PO_4, 10 glucose, and 10 HEPES, pH 7.2) and live-imaged using cytoplasmic GFP to identify transfected neurons. Spine density analysis was performed on the stretch of CA1 pyramidal neuron primary apical dendrite from 100 μm to 200 μm from the cell body. The entire 100 μm stretch was taken for analysis. Spine density analysis was performed manually on individual sections taken 400 nm apart by a blinded experimenter using Zeiss LSM Image Browser (Carl Zeiss), which were later reconstructed to form the z-stacks used as sample images. For spine morphology measurements, images were acquired at DIV 7-9 using super-resolution microscopy (N-SIM Microscope System, Nikon). For use with the available inverted

microscope and oil-immersion objective lens, slices were fixed in 4% PFA/4% sucrose in PBS and washed 3x with PBS. To amplify the GFP signal, slices were then blocked and permeabalized in 3% BSA in PBS containing 0.1% Triton-X and stained with primary antibody against GFP (2 μg/mL, Life Technologies A-11122) followed by washes in PBSTx and staining with Alexa 488-conjugated secondary (4μg/mL, Life Technologies A-11034). Slices were mounted in SlowFade Gold (Life Technologies) for imaging. Only dendrites in the top 20 μm of the slice were imaged. Some slices were further processed with an abbreviated SeeDB-based protocol (Ke et al., 2013) in an attempt to reduce spherical aberration, but no substantial improvement was seen. Images were acquired with a 100x oil objective in 3D-SIM mode using supplied SIM grating (3D EX V-R 100x/1.49) and processed and reconstructed using supplied software (NIS-Elements, Nikon). Morphological analysis was done on individual sections using ImageJ to perform geometric measurements on spines extending laterally from the dendrite. Spine neck widths were obtained from full width half-maximum (FWHM) measurements based on Gaussian fits of line profile plots (Tonnesen et al., 2014). Neck length was measured from the base of the spine to the base of the head. Head diameter was measured perpendicular to the spine neck axis through the thickest part of the spine head. Head diameter was obtained using full width tenth-maximum (FWTM) measurements based on Gaussian fits to approximate manual head measurement. We note that others (Tonnesen et al., 2014) have recently performed more precise morphological measurements; we are constrained by available tools and tissue preparation.

Immunoblotting

Rat primary hippocampal dissociated neurons (E18.5) were infected with lentivirus expressing MAGUK miRNA construct or GFP alone at DIV 4-7. Neurons were harvested at DIV17 – 18 in

Tris-buffered saline (25 mM Tris pH 7.4, 150 mM NaCl) plus 0.5% Triton-X and protease inhibitor mix (Roche Applied Sciences, cOmplete Protease Inhibitor Cocktail Tablets). Cell lysates were incubated at 4^{o} for 30 minutes and centrifuged for 15 minutes at 12000g. Proteins were resolved by SDS-PAGE and analyzed by western blot with antibodies against PSD-93 (0.4 μg/mL, Neuromab clone N18/30), PSD-95 (1 μg/mL, Neuromab K28/43), SAP102 (2 μg/mL, Neuromab N19/2), and actin (0.2 μg/mL, Millipore C4).

Lentivirus Production

3 T-75 flasks of rapidly-dividing HEK293T cells (ATCC) were transfected with FUGW-MAGUK miRNA or FUGW, plus helper plasmids pVSV-G and psPAX2 using FuGENE HD (Promega) according to the manufacturer's directions. 40 hours later, supernatant was collected, filtered and concentrated using the PEG-it Virus Precipitation Solution (System Biosciences) according to the manufacturer's directions. Resulting pellet was resuspended in 400 μL Opti-mem or PBS, flash-frozen, and stored at -80^{o} C.

Viral Injections

Rat viral injections were performed at P8. Rats were anesthetized with isoflurane and immobilized on a stereotaxic frame using ear and palate bars designed for young rats (David Kopf Instruments). 250 nl per hemisphere was injected at 500 nl/min via a Hamilton 88011 (Hamilton) syringe driven by a Micro4 microsyringe pump (WPI). All experiments were

performed in accordance with established protocols approved by the University of California San Francisco Institutional Animal Care and Use Committee.

Statistical analysis

Significance of evoked dual whole-cell recordings and aEPSC frequency compared to controls was determined using the Wilcoxon signed-rank sum test. Statistical comparisons between sets of paired data were done using the Mann-Whitney U test. Paired-pulse ratios, spine densities, surface currents, Ca^{2+}-channel currents and aEPSC amplitudes were analyzed with a Student's *t* test. For significance of coefficient of variation analysis, responses from each neuron were normalized to the mean response of that neuron creating a distribution with mean = 100%. These distributions were summed within datasets to create distributions of control and experimental responses with equal means such that any difference in CV would be due to a difference in variance. Equality of variances was then tested with the Brown-Forsythe Levene-type test using group medians.

CHAPTER 3: Synaptic consolidation normalizes AMPAR quantal size following MAGUK loss

Introduction

The glutamatergic synapse, consisting of a post-synaptic specialization with clustered glutamate receptors opposite a pre-synaptic terminal, is the site of fast excitatory neurotransmission in the brain. Proper formation of the post-synaptic specialization requires that glutamate receptors localize to the synapse and associate with the complex network of signaling and scaffolding molecules known as the post-synaptic density (PSD). The process of glutamate receptor trafficking and localization has been extensively studied, and multiple lines of evidence demonstrate that the PSD scaffolding proteins themselves play an instructive role in regulating the localization of synaptic glutamate receptors (El-Husseini et al., 2000; Schnell et al., 2002). The primary protein family implicated in synaptic glutamate receptor localization is the four-member membrane-associated guanylyl kinase (MAGUK) family (Elias and Nicoll, 2007; Opazo et al., 2012): PSD-93, PSD-95, SAP97, and SAP102.

The MAGUKs are membrane-associated cytoplasmic scaffolding proteins that are highly enriched at the PSD and are ideally situated to serve as a bridge between glutamate receptors and cytoplasmic structural proteins, such as polymerized actin, that form the protein backbone of the dendritic spine. MAGUKs are anchored to the plasma membrane at post-synaptic specializations primarily by N-terminal palmitoylation, directly and indirectly bind glutamate receptors via PDZ binding domains, and link these receptors to the cytoplasmic protein scaffold with C-terminal SH3 and GK domains (Kim and Sheng, 2004). Germline knockout of single MAGUKs has little or no effect, but these results are confounded by compensation within the MAGUK family (Elias et al., 2006). RNAi-mediated knockdown, an acute manipulation, does not suffer from this drawback and offers greater insight into the endogenous role of MAGUKs. Acute overexpression or RNAi-mediated knockdown of PSD-93 or PSD-95 results in correlated changes in the number

of synaptic AMPA-type glutamate receptors (AMPARs), demonstrating that MAGUKs play an instructive role in the localization of synaptic AMPARs (Chen et al., 2011; Ehrlich et al., 2007; Ehrlich and Malinow, 2004; Elias et al., 2006; Schluter et al., 2006).

Reductions in PSD-93 or PSD-95 by RNAi-mediated knockdown cause loss of AMPAR-containing synapses. Strikingly, there is no deficit in the number of AMPARs at the remaining synapses, which has been interpreted to mean that individual synapses may each contain either PSD-93 or PSD-95 (Elias et al., 2006) or that the MAGUKs may be required primarily for the development of AMPAR-containing synapses (Ehrlich et al., 2007). Additionally, removal of several other scaffolding proteins present at all PSDs, including GKAP (Shin et al., 2012) and Shank1 (Hung et al., 2008), also results in all-or-none loss of AMPAR-containing synapses rather than uniform loss of some AMPARs from every synapse. While this data might suggest that synapses are highly heterogeneous and these scaffolding proteins each play no role at a number of synapses, a plausible alternative would be that loss of ubiquitous synaptic proteins from all synapses triggers a compensatory reorganization in a process resembling a homeostatic rearrangement in an effort to maintain the number of AMPARs at each synapse. The most obvious candidate pathway for this reorganization would be the canonical homeostatic pathway, in which signaling dependent on calcium entry through L-type calcium channels (Ibata et al., 2008; Thiagarajan et al., 2005) acts on downstream targets including GluA2 (Gainey et al., 2009; Goold and Nicoll, 2010), (but see Altimimi and Stellwagen, 2013).

The data from single-MAGUK manipulations has supported the hypothesis that MAGUKs function primarily as ‘slots’ for AMPARs that control their synaptic abundance (Schnell et al., 2002; Shi et al., 2001). Knockdown of multiple MAGUKs, however, causes reductions in both AMPAR- and NMDAR-mediated transmission (Elias et al., 2006), suggesting

MAGUKs play a more fundamental role at the synapse: acting as basic scaffolding molecules localizing both classes of glutamate receptors. In this study, we have used a chained-miRNA approach to reduce expression of PSD-93, PSD-95, and SAP102 using RNAi-mediated knockdown. These results provide the first direct study of simultaneous knockdown of the MAGUKs shown to be responsible for synaptic localization of glutamate receptors. We find that knockdown of the three MAGUKs causes large decreases in both AMPAR and NMDAR transmission, with each of the three MAGUKs playing an equal role. This deficit results purely from a reduction in the number of synapses containing glutamate receptors without any decrease in synaptic strength of the remaining functional synapses or spine density. Furthermore, we show that the all-or-none loss of AMPARs is a result of "winner-take-all" synaptic consolidation, a process that acts to normalize quantal size. Remarkably, this process, which has not previously been described, implies that individual synapses have an intrinsic set point.

Results

Pan-MAGUK knockdown reduces synaptic AMPAR and NMDAR-mediated currents

To test whether the MAGUKs are necessary for glutamatergic transmission, we created a construct containing the CAG hybrid promoter driving expression of GFP and chained microRNAs targeting the three synaptic MAGUKs: PSD-93, PSD-95, and SAP102 (hereafter called the MAGUK miRNA, Figure 1A). The fourth member of the MAGUK family, SAP97, has been found not to play a role in baseline transmission (Howard et al., 2010) and was therefore initially excluded. Previous experiments exploring the role of the MAGUK family have been unable to make direct comparisons between neurons lacking MAGUKs and wild-type cells and have therefore suffered from an inability to quantify the effects of acute MAGUK removal directly. Viral infection of the MAGUK miRNA, using sequences that have previously been

validated individually (Elias et al., 2006), substantially reduced protein levels of PSD-93, PSD-95, and SAP102 in dissociated hippocampal neurons (Figure 1B). To determine the functional consequences of MAGUK knockdown, we performed dual whole-cell recordings in rat hippocampal organotypic cultures. We biolistically transfected neurons with the MAGUK miRNA and visually identified transfected, GFP-expressing CA1 pyramidal neurons by morphology and location. We then stimulated Schaffer collaterals and performed simultaneous whole cell recording of evoked excitatory postsynaptic currents (EPSCs) from pairs of transfected and neighboring untransfected control neurons. Expression of the MAGUK miRNA caused large and equivalent reductions in both AMPAR and NMDAR transmission (Figure 1C), leaving only a small glutamatergic EPSC. Importantly, viral infection of slice cultures via microinjection followed by dual whole-cell recording produced equivalent results (Figure 2A-2C), validating our use of viral infection for our biochemical characterization (Figure 1B). A previous report using germline knockouts showed the MAGUKs have the ability to compensate for loss of several family members (Elias et al., 2006), and our knockdown strategy left open the possibility that SAP97, though it has no role in baseline function, might play a compensatory role. To determine whether SAP97 plays such a role, we transfected slice cultures from SAP97 knockout mice (Howard et al., 2010) with the MAGUK miRNA. This resulted in no further reduction in transmission (Figure 2D-2F), indicating that SAP97 does not play a compensatory role after loss of other MAGUKs. We therefore continued the study looking only at knockdown of PSD-93, PSD-95, and SAP102. Although our results demonstrate that MAGUKs are responsible for the large majority of synaptic glutamatergic current, it is difficult to ascertain the source of the remaining current. It could be due either to an incomplete removal of MAGUK protein or to a MAGUK-independent mechanism.

The reduction in both AMPAR and NMDAR transmission could be explained by changes in the three synaptic parameters: a presynaptic decrease in neurotransmitter release probability (P_r), a decrease in number of functional synapses (N), or a decrease in the postsynaptic response to glutamate, here likely due to a decrease in the number of glutamate receptors at each synapse (q). Several previous studies have found knockdown of PSD-95 causes solely a postsynaptic effect (Elias et al., 2006; Schluter et al., 2006), (but see Futai et al., 2007). To determine whether the removal of all three MAGUKs results in a pre-synaptic deficit, we measured the paired-pulse ratio, an indicator of neurotransmitter release probability, and found no change (Figure 1D). This result indicates that the decrease in fast glutamatergic transmission cannot be explained by changes in P_r and is due to either a decrease in the number of functional synapses, a decrease in the number of receptors per synapse post-synaptically, or a combination of the two effects.

All MAGUKs play roles in baseline glutamate receptor localization

Before further characterizing the general role of the MAGUK protein family, we first wanted to know the contribution of each member to baseline fast excitatory transmission. Previous experiments (Elias et al., 2006) have reported that PSD-93 and PSD-95 each account for half of AMPAR-mediated transmission, while SAP102, although it plays no basal role, plays a compensatory role if both PSD-93 and PSD-95 are lost. Knockdown of PSD-93 or PSD-95 has been reported to have either no (Elias et al., 2006) or minimal effect (Ehrlich et al., 2007) on NMDAR currents. These single-knockdown results combined with our data that the MAGUK miRNA has a significant effect on NMDAR currents indicate that the MAGUKs may exhibit redundancy with regard to NMDAR currents, by which synaptic NMDARs are lost in significant numbers only when multiple MAGUKs are lost. To determine the individual contribution of each MAGUK family member in our system, we used miRNA constructs targeting each single

MAGUK as described in (Figure 1A), with a CAG promoter driving GFP followed by miRNA against PSD-93, PSD-95 or SAP102 in its 3' UTR.

We find that knockdown of each MAGUK caused equivalent decreases in glutamatergic transmission. Removal of PSD-93, PSD-95, or SAP102 individually caused a decrease of about 50% in AMPAR and 25% in NMDAR transmission (Figure 3A-3C). Furthermore, the arithmetic addition of individual contributions of the MAGUKs to baseline AMPAR transmission (50% per MAGUK member, summing to an impossible 150%) results in an overestimate of the total contribution (Figure 3D). This suggests that the MAGUKs act cooperatively, such that removal of a small number of MAGUKs causes a disproportionately large reduction in AMPAR currents. Electron microscopy studies have shown that synapses with PSD diameter <180 nm do not contain AMPARs and represent 'silent synapses'(Takumi et al., 1999), suggesting that although small PSDs presumably contain MAGUKs, a primary component of the PSD (Chen et al., 2008; Sheng and Hoogenraad, 2007), PSDs with few MAGUKs cannot localize AMPARs. Therefore, as MAGUKs are lost, AMPAR transmission will decrease disproportionately as many small MAGUK-containing synapses fall under the size threshold required to contain AMPARs (Takumi et al., 1999).

Incremental removal of MAGUKs results in a small reduction in NMDAR current that is additive, in contrast to the cooperative effects on AMPARs, with the triple MAGUK miRNA resulting in a decrease that is approximately three times as large as any single miRNA (Figure 3D). These results suggest that the relationship between MAGUK and NMDAR binding is roughly linear, with decreases in MAGUK abundance resulting in equivalent decreases in NMDAR content at synapses. This is in agreement with electron microscopy data showing NMDAR content is independent of PSD size (Takumi et al., 1999), meaning PSD size reductions

do not cause reductions in NMDAR content. It is therefore likely that NMDAR EPSC reductions reflect loss of NMDAR-containing synapses. Additionally, we were surprised to find that knockdown of SAP102, which previously had been thought to be unnecessary for baseline transmission in organotypic rat slices (Elias et al., 2006), reduced both AMPAR and NMDAR currents, demonstrating a role for SAP102 in mediating baseline currents (Figure 3C).

Dependence of SAP102 Phenotype on method of RNAi delivery

What might account for the difference between our present results (Figure 3C), in which knockdown of SAP102 reduced both AMPAR and NMDAR currents, and previous published results which found no effect (Elias et al., 2006)? One possible technical explanation for this disagreement could be the method of RNAi delivery in organotypic slices. We noticed a striking pattern in previous experiments: delivery of PSD-95 shRNA via viral transduction (Elias et al., 2006; Schluter et al., 2006) did not decrease NMDAR current, while biolistic transfection of PSD-95 shRNA constructs (Ehrlich et al., 2007; Futai et al., 2007) caused a decrease in both AMPAR and NMDAR current. We reasoned that biolistic transfection might be more effective at knocking down endogenous protein, and we therefore explored whether the method of RNAi transfection might account for the difference.

Although we used the same targeting sequences as Elias et al. (Elias et al., 2006), our RNAi construct has several key differences, most notably conversion of shRNA to miRNA and the resulting use of a different targeting construct and stronger promoter. These differences might explain the discrepancy in phenotype. If, however, viral transduction with our SAP102 RNAi construct causes no deficit, it would suggest that the phenotype we see is specific to biolistic transfection and implicate the transfection method as the critical parameter. Although our biochemical results using virus in dissociated cultures (Figure 1B) show almost complete

loss of MAGUK protein, we do not believe that we can quantify this data and directly extrapolate it to slice culture, due to differences in the preparation and the transduction method, including potential differences in expression levels of the MAGUKs, differential expression of the CAG promoter, and differences in multiplicity of infection.

We therefore injected virus carrying our SAP102 knockdown construct into organotypic slice cultures and performed simultaneous whole-cell recordings. We found that, in contrast to the decrease seen following biolistic transfection, viral knockdown had no effect on AMPAR currents compared to controls, although there was a small but significant decrease in NMDAR current that differed significantly from the decrease seen following biolistic transfection (Figure 4A). We therefore conclude that the method of delivery controls the SAP102 phenotype. One possible explanation is the duration of knockdown; infection with lentivirus may take effect more slowly than biolistic transfection. One alternate explanation, however, is the possibility that high miRNA expression levels could reveal off-target effects that were not strong enough to be functionally relevant at lower expression levels but now cause reductions in glutamatergic transmission. To determine whether biolistic transfection of SAP102 RNAi could be having off-target effects, we tested the SAP102 RNAi in slices from SAP102 germline knockout mice. Since the SAP102 protein has been genetically removed from all cells in this experiment, any differences between transfected and untransfected neurons caused by SAP102 miRNA transfection must be attributed to off-target effects on other proteins. As a control, we first confirmed our RNAi worked as expected in wild-type mice, causing a phenotype indistinguishable from that in rat (Figure 4B). In SAP102 knockout mice, we found biolistic transfection of SAP102 RNAi caused no change in either AMPAR or NMDAR transmission compared to controls (Figure 4C-4D). We therefore conclude that our biolistic SAP102

knockdown phenotype in rat is due to a more efficient removal of SAP102 protein and not an off-target effect.

These results demonstrate that the method of RNAi transfection has important consequences for knockdown phenotypes and that biolistic transfection of RNAi results in more efficient removal of MAGUKs than viral transduction. Furthermore, they indicate that SAP102 contributes to baseline currents, which had not been previously observed and is now apparent due to a methodological improvement.

MAGUK knockdown causes loss of functional glutamatergic synapses

After finding that PSD-93, PSD-95 and SAP102 all play roles in baseline transmission, we returned to the initial finding that knockdown of all three proteins causes large reductions of both AMPAR and NMDAR-mediated currents (Figure 1C). These reductions could be due to a reduction in the number of functional synapses (N), a reduction in the number of glutamatergic receptors present at each synapse (q), or a mixture of the two. Determination of these quantal parameters requires analysis of glutamatergic transmission at individual synapses, usually done by miniature EPSC (mEPSC) analysis. We chose to measure evoked currents rather than mEPSCs, and picked two complementary techniques to split evoked currents into their constituent quantal events. Each technique offered an advantage over mEPSC analysis: Sr^{2+}-evoked asynchronous EPSCs (aEPSCs) allowed us to link the quantal responses as closely as possible to the evoked currents we analyze elsewhere in this study, and coefficient of variation (CV) analysis allowed us to circumvent the electrical noise limit inherent in mEPSC recordings which prevents observation of synapses containing few AMPARs.

To record aEPSCs, we replaced the Ca^{2+} normally present in the extracellular solution with equimolar Sr^{2+}. When Ca^{2+} is replaced with Sr^{2+}, synchronous transmitter release is replaced by asynchronous release which lasts for a few hundred milliseconds after the stimulus (Miledi, 1966; Oliet et al., 1996; Xu-Friedman and Regehr, 2000). These asynchronous EPSCs (aEPSCs) are quantal events that can be temporally isolated and are amenable to detailed analysis. Analysis of the frequency (Figure 5A) and amplitude (Figure 5B) of aEPSCs from simultaneously recorded neurons yields information about quantal content ($N * P_r$) and quantal size (q), respectively. aEPSC frequency decreased following MAGUK knockdown (Figure 5C) with no difference in average aEPSC amplitude (Figure 5D), indicating that following MAGUK knockdown, quantal content has decreased with no change in quantal size. We additionally found no irregularities in the shape of the cumulative distribution functions for aEPSC amplitude and inter-event interval (Figure 5E-5F), indicating changes are occurring at all synapses. A decrease in quantal content could be due to either a reduction in functional synapse number or probability of neurotransmitter release. Since MAGUK knockdown caused no change in the paired-pulse ratio (Figure 1D) the decrease in quantal content is due to a reduction in the number of functional synapses.

To complement our aEPSC data, we performed coefficient of variation analysis on our EPSCs recorded in Ca^{2+}. This method of analysis utilizes the inherent variability in synaptic responses over many trials, which is caused by stochastic neurotransmitter release. By comparing the normalized variance in responses from two neurons receiving the same stimulus, it is possible to determine relative quantal size and quantal content. Changes in quantal size precisely change both the mean EPSC and the variance such that the normalized ratio of $mean^2/variance$, also known as $(coefficient\ of\ variation)^{-2}$ or CV^{-2}, remains constant. In contrast, changes in

quantal content will cause proportional changes of equal magnitude in CV^{-2} (Bekkers and Stevens, 1990; Del Castillo and Katz, 1954; Gray et al., 2011; Malinow and Tsien, 1990). To demonstrate this principle in our preparation, we compared NMDAR EPSCs from control neurons before and after adding 1μM D-APV, a sub-saturating concentration that blocks approximately half of all NMDARs, causing a reduction of about 50% in NMDAR EPSC (Figure 6A). The effect of this reduction on the variance can be visualized graphically by plotting mean EPSC against CV^{-2}. Average responses on the 45^{o} line represent equivalent changes in EPSC and CV^{-2} and therefore pure changes in quantal content, while responses on the horizontal $y = 1$ line represent changes in EPSC amplitude without changes in variance, and therefore represent changes in quantal size. In the case of D-APV, the ratio CV^{-2} is unchanged as would be expected from uniform block of 50% of NMDARs at all synapses causing a reduction in quantal size (Figure 6B, re-plotted in Figure 5I). Analysis of evoked AMPAR (Figure 5G) and NMDAR (Figure 5H) currents following MAGUK knockdown in simultaneously recorded neurons showed equal reductions in CV^{-2} and mean EPSC (Figure 5I), suggesting that the decrease in mean EPSC was due to decreased quantal content, in agreement with our aEPSC data (Figure 5A-5F). We conclude that MAGUK knockdown results in a decrease in the number of functional synapses.

One finding that could explain a loss of functional synapses is a decrease in the number of dendritic spines, the cellular sites of excitatory synaptic contacts (Harris and Kater, 1994; Harris and Stevens, 1989). We therefore used confocal microscopy to compare spine density on the primary apical dendrites of control and MAGUK miRNA-expressing neurons. We found no difference in spine density between control and transfected neurons, suggesting that the MAGUKs play no role in spine formation (Figure 6C-6D). This dissociation of the normally

tight relationship between spines and functional synapses suggests that excitatory synaptic formation is mechanistically a two-step process consisting first of a spinogenic phase, in which the structural framework for a functional synapse is laid, and a subsequent synaptogenic phase, in which ionotropic receptors localize to the synapse using a MAGUK-dependent mechanism. To determine whether MAGUKs might play a role in spine maintenance and maturation, we characterized spine morphology using super-resolution structured illumination microscopy (SIM). We find that MAGUK knockdown has no effect on spine neck length or diameter, but does significantly reduce spine head diameter (Figure 6E-6H). Interestingly, this deficit in spine head diameter is mediated by a selective reduction in the number of spines with large heads, which presumably fail to mature in the absence of MAGUKs (Figure 6I-6J). These results suggest that MAGUK loss curtails spine maturation. We therefore conclude that spine growth and maturation must have an initial MAGUK-independent phase followed by a MAGUK-dependent growth phase, likely an activity-dependent process dependent on the presence of a functional synapse. Finally, it has been suggested that the MAGUKs form complexes with extrasynaptic glutamate receptors (Rao et al., 1998). To determine whether MAGUKs might have a functional role in trafficking of glutamate receptors to the neuronal surface, we recorded whole-cell AMPAR and NMDAR currents (Figure 6K-6N). We found no change, suggesting that the MAGUKs are not necessary for trafficking of glutamate receptors to the neuronal surface and instead are specifically necessary for synaptic localization of surface glutamate receptors.

MAGUK knockdown triggers synaptic consolidation

Loss of the MAGUKs causes reductions in AMPAR and NMDAR transmission (Figure 1C). The MAGUKs are a critical component of the post-synaptic density likely required for normal AMPAR transmission at all synapses. One simple prediction following loss of MAGUKs

would therefore be uniform loss of AMPARs from every synapse resulting in a reduction of quantal size with little change in functional synapse number. Further analysis of the AMPAR transmission reduction, however, has found that it is due primarily to a reduction in the number of AMPAR-containing synapses with no change in quantal size (Ehrlich et al., 2007, this work, Figure 5; Elias et al., 2006). We therefore focused on this unexpected result, hypothesizing that a compensatory mechanism must be acting to normalize quantal size, with the effect of converting the initial uniform removal of some AMPAR from every synapse into an all-or-none loss of synapses.

We further reasoned that since previous studies of compensatory mechanisms have found they can occur more slowly *in vivo* vs. in dissociated preparations (Hengen et al., 2013; Lambo and Turrigiano, 2013), consolidation might be more easily detected *in vivo*, while in slice cultures it might occur too quickly to easily detect. To test this hypothesis, we recorded from acute slices at two different intervals following *in vivo* lentiviral knockdown of MAGUKs. These time points have equivalent reductions in AMPAR transmission, suggesting equal MAGUK knockdown efficiency (Figure 7A-7C, dashed line and shaded box indicate mean ± SEM of organotypic culture miRNA). Injection of lentiviral MAGUK miRNA at P8 causes decreases in both quantal size and quantal content shown by CV analysis 8 days post-injection at P16 (Figure 7D) as well as reductions in mEPSC amplitude and frequency (Figure 7E – 7F). 27 days post-injection at P35 there is only a decrease in quantal content by CV analysis (Figure 7G), as well as a reduction in mEPSC frequency, but not amplitude (Figure 7H – 7I). This recovery of mEPSC amplitude over time *in vivo* suggests a homeostatic program is working to re-normalize quantal size in the remaining functional synapses. We conclude from these experiments that MAGUK knockdown initially causes a loss of some AMPARs from all synapses and a reduction

of AMPAR quantal size. This AMPAR reduction triggers a compensatory program that consolidates synapses, in which a substantial population of synapses lose all AMPARs, while the remaining synapses scale their AMPARs back to normal levels.

L-type Voltage-Gated Calcium Channels are required for synaptic consolidation

We reasoned that an active compensatory program would require a sensor of perturbed activity, and began by testing the involvement of the most well-characterized activity sensor: the L-type voltage-gated calcium channel (LTCC), a critical sensor of neuronal activity required for the activity of downstream homeostatic effector molecules. Homeostasis is induced by deviations in LTCC activity. Direct reduction in LTCC signaling via nifedipine application induces scaling up (Ibata et al., 2008; Thiagarajan et al., 2005; Wang et al., 2011), and increased excitation reduces synaptic currents via a mechanism requiring the LTCC (Goold and Nicoll, 2010). Together, these data indicate that the L-type channel is required bi-directionally to maintain quantal size. We reasoned that involvement of the L-type channel in consolidation would suggest an active process at work akin to homeostasis working to maintain quantal size, while intact consolidation in the absence LTCC signaling would imply the canonical homeostatic pathways were not involved. We biolistically transfected neurons with the MAGUK miRNA while blocking the activity of LTCCs in organotypic slice cultures by addition of nifedipine (20 μM) to the culture media. We found that knockdown of the MAGUKs in the presence of nifedipine caused large decreases in AMPAR and NMDAR EPSCs compared to neighboring neurons (Figure 8A). This decrease did not differ significantly from the reductions caused by the MAGUK miRNA in the absence of nifedipine (Figure 8B-8C, dashed line and shaded box indicate mean ± SEM of miRNA without nifedipine), indicating that LTCCs are not involved in mediating the effect of MAGUK knockdown and suggesting homeostatic processes do not

modulate the magnitude of baseline EPSC reduction. These results indicate that synaptic consolidation shifts AMPARs to normalize quantal size without a change in overall receptor number (model, Figure 10F). Finally, there was no change in the paired-pulse ratio, indicating that the addition of nifedipine did not change probability of release (Figure 8D).

CV^{-2} analysis demonstrates that in the presence of nifedipine, the reduction in AMPAR EPSCs caused by MAGUK miRNA is largely due to a reduction in quantal size (Figure 8E), in contrast to the reduction in quantal content caused by the MAGUK miRNA without nifedipine (Figure 5G). A small decrease in CV^{-2} remains, however, and indicates a small reduction in quantal content, possibly due to an across-the-board reduction in AMPAR content converting weak synapses to AMPAR-silent synapses. CV^{-2} analysis of NMDAR EPSCs shows a reduction in quantal content (Figure 8F) identical to that seen in the absence of nifedipine (Figure 5H), meaning that the all-or-none loss of NMDAR-containing synapses is not reliant on L-type channel signaling. MAGUK miRNA data without nifedipine (Figure 5G) has been re-plotted to aid in comparison (Figure 8G). These results suggest that the AMPARs, but not NMDARs, undergo consolidation dependent on signaling by LTCCs following MAGUK knockdown.

Previous data showing the all-or-none loss following MAGUK removal has been collected following knockdown of a single member of the MAGUK family (Ehrlich et al., 2007; Elias et al., 2006). We have found knockdown of the entire MAGUK family leads to consolidation, but to directly determine whether consolidation acts following the milder disruption caused by removal of a single MAGUK family member, we knocked down PSD-95 in the presence of nifedipine. We find that knockdown of only PSD-95 causes consolidation which is blocked by incubation in nifedipine, demonstrating that loss of a single MAGUK family member is sufficient to trigger consolidation (Figure 8H).

Since addition of nifedipine to the slice culture media affects both the transfected and neighboring neurons, we wanted to test whether consolidation could be rescued in a cell-autonomous manner. Our CV^{-2} analysis reports differences between transfected and control neurons, and could be influenced by nifedipine acting on these controls. To confirm that LTCCs were acting to effect consolidation in the transfected neuron, we made use of cell-autonomous rescue with the nifedipine-insensitive T1036Y L-type channel mutant (Dolmetsch et al., 2001; He et al., 1997), hereafter referred to as T1036Y. If L-type channels in the transfected neuron underlie consolidation, block of consolidation by nifedipine should be rescued by expression of T1036Y. We first confirmed surface expression of T1036Y by simultaneously measuring calcium currents in neurons biolistically transfected with T1036Y and neighboring untransfected neurons (Figure 9A), finding a large nifedipine-insensitive increase in current in neurons expressing T1036Y (Figure 9B-9D). Before determining whether expression of T1036Y can rescue the block of synaptic consolidation caused by nifedipine, we first co-expressed T1036Y with the MAGUK miRNA in the absence of drug, finding with CV^{-2} analysis that overexpression of T1036Y did not modulate the reduction in quantal content caused by MAGUK knockdown (Figure 9E). Co-expression of T1036Y and MAGUK miRNA in the presence of nifedipine rescued synaptic consolidation and resulted in a reduction in AMPAR quantal content (Figure 8F-8G). In all cases, there was no change in the magnitude of amplitude reduction in either AMPAR or NMDAR transmission compared to the MAGUK miRNA alone (Figure 9H – 9J) indicating that under these circumstances, nifedipine has no independent effect on synaptic transmission.

Together, these results indicate that signaling pathways triggered by calcium flux through LTCCs is necessary for synaptic consolidation following knockdown of the MAGUKs. The

involvement of LTCCs strongly suggests a two-step process by which MAGUK knockdown causes a reduction in quantal size, followed by a compensatory process resulting in a normalization of quantal size and reduction in quantal content. Furthermore, the manipulation of a signaling pathway via pharmacology without any additional structural perturbation indicates reorganization is an active, regulated process rather than a structural consequence of MAGUK protein loss.

Direct electrophysiolgical observation of consolidation

Although incubation of miRNA-transfected slice cultures in nifedipine allowed us to infer that synaptic consolidation via L-type signaling must occur, we next attempted to strengthen this finding by directly observing neurons undergoing consolidation. We hypothesized that consolidation would occur on the same time scale as multiplicative synaptic scaling, a well-characterized form of homeostasis dependent on L-type signaling which occurs over roughly 24 hours (Ibata et al., 2008; Turrigiano et al., 1998). As previous studies have shown the half-life of PSD-95 is approximately 36 hours (El-Husseini Ael et al., 2002), recording within a few days of transfection, as would be required if consolidation happened on the same time scale as synaptic scaling, would not allow sufficient time for degradation of the existing protein. Instead, we took advantage of the finding that nifedipine blocks consolidation and incubated organotypic slices in nifedipine for 6 days, as done to test the involvement of L-type channels (Figure 8A-8H), which allows time for MAGUK protein degradation while blocking consolidation. Following 6 days in nifedipine, during which consolidation did not occur, slices were removed from nifedipine and recordings were done to assess the degree of consolidation on each subsequent day.

We found consolidation to be a linear process resulting in complete consolidation by 4 days following nifedipine washout (Figure 8I-7K; intermediate time points in Figure 8K-8L). We additionally recorded from slices incubated in nifedipine with no washout to determine whether some consolidation might occur during this longer incubation despite the presence of nifedipine. We found no consolidation occurred in the presence of nifedipine (Figure 8M). These experiments establish a time course for consolidation. Additionally, they demonstrate that consolidation can occur long after the loss of MAGUKs, further dissociating it from the initial EPSC reduction and showing that it is a separate compensatory process.

CaM kinase kinase is required for consolidation of synapses

We next attempted to identify targets of signaling through L-type channels during consolidation. Previous work has determined protein synthesis is necessary for certain forms of homeostatic plasticity, and has specifically identified CaM Kinase 4 (CaMK4) as a transcriptional regulator that plays a role downstream of the L-type calcium channel (Goold and Nicoll, 2010; Ibata et al., 2008). Additionally, the relatively long period required for full consolidation suggests changes in protein synthesis may be required. The upstream CaMK4 regulator CaMKK (Soderling, 1999; Wayman et al., 2008) is an attractive target for testing whether CaMK4-mediated transcriptional regulation is necessary for consolidation, since both pharmacological inhibition and cell-autonomous rescue of inhibition via a drug-insensitive recombinant protein are possible. Inhibition of CaMKK by STO-609 (3μM) (Tokumitsu et al., 2002) in slices transfected with the MAGUK miRNA hampered consolidation, resulting in a reduction in quantal size (Figure 10A-10B). This deficit in consolidation was rescued by expression of CaMKK L233F, which is insensitive to STO-609 (Tokumitsu et al., 2003). Co-expression of MAGUK miRNA and CaMKK L233F in the presence of STO-609 resulted in

consolidation indistinguishable from MAGUK miRNA alone, indicating that the deficit in consolidation is due to block of CaMKK signaling in the transfected neuron rather than a non-cell autonomous result of incubation in STO-609 (Figure 10C-10D). In agreement with previous work, CaMKK has no role in maintaining baseline transmission (Goold and Nicoll, 2010). Critically, incubation with STO-609, with or without co-expression of CaMKK L233F, had no effect on the reduction in AMPAR and NMDAR EPSCs caused by MAGUK knockdown (Figure 10E-10G).

These results indicate that signaling through the L-type calcium channel activates CaMKK. CaMK4, the major downstream target of CaMKK, plays a role in transcriptional regulation, most notably through the transcription factor CREB (Bito et al., 1997). We therefore conclude that, in agreement with the previously described role for CaMKK (Goold and Nicoll, 2010; Ibata et al., 2008), calcium influx through L-type channels leads to consolidation via changes in protein synthesis in a CaMKK/CaMK4-dependent manner. It is not possible, however, to directly test the necessity of translation in our system due to the relatively long time required for consolidation to occur.

GluA2 is required for consolidation of synapses following MAGUK knockdown

The GluA2 AMPAR subunit has previously been implicated as an effector molecule in the homeostatic response to perturbations in cell activity levels (Gainey et al., 2009; Goold and Nicoll, 2010), (but see Altimimi and Stellwagen, 2013), which in hippocampal neurons is expressed as a modulation of both quantal content and quantal size (Goold and Nicoll, 2010; Thiagarajan et al., 2002). It is therefore a promising candidate for involvement in quantal size re-normalization. To test whether the GluA2 subunit is involved, we knocked down the MAGUKs in organotypic slice cultures from GluA2 knockout animals (Jia et al., 1996) and assessed

whether loss of GluA2 blocked the putative homeostatic consolidation of synapses. We would expect block of synapse consolidation to be expressed as a decrease in quantal size relative to control neurons. We found that coefficient of variation analysis (Figure 11A-11C) and analysis of Sr^{2+}-evoked asynchronous EPSCs (aEPSCs) (Figure 11D-11E) both revealed a decrease in quantal size. As seen with L-type channel block, a small decrease in quantal content remains ($p < 0.05$). Much of the observed reduction in aEPSC frequency (Figure 11D) is likely due to low-amplitude aEPSCs occurring below the noise threshold. In contrast, MAGUK knockdown in neurons from wild-type organotypic rat cultures causes no decrease in quantal size as measured by aEPSCs (Figure 5C-5D) or coefficient of variation analysis (Figure 5G-5I). Importantly, the relative decrease in EPSC amplitude is unchanged (Figure 12) compared to that seen in wild-type organotypic rat cultures. We therefore conclude that synaptic consolidation uses machinery from the well-characterized homeostatic pathways, and the GluA2 AMPAR subunit is necessary for synaptic consolidation following MAGUK knockdown.

Discussion

We find that the MAGUK family is of paramount importance in the localization of both AMPARs and NMDARs at excitatory glutamatergic synapses, as is demonstrated by the loss of most glutamatergic current following knockdown of PSD-93, PSD-95, and SAP102. We used a combination of approaches to characterize the role of MAGUKs in excitatory transmission. Analysis of spine density and surface glutamatergic currents indicate a specific role for MAGUKs in synaptic glutamate receptor localization separate from spine formation or receptor surface trafficking. Further characterization of the knockdown of all three MAGUKs reveals that the deficit in glutamatergic current is mediated by a postsynaptic reduction in the number of functional synapses. We go on to show that this reduction in synapse number is caused by a

compensatory consolidation of synapses following MAGUK loss by a mechanism dependent on L-type calcium channels, CaMKK, and GluA2, implicating a homeostasis-like pathway. Notably, the consolidation does not result in multiplicative synaptic scaling, demonstrating that the canonical homeostatic pathway likely plays additional roles. These findings extend previous work by demonstrating that MAGUKs, in addition to their previously reported role acting as 'slots' for AMPARs, are a core component of the post-synaptic density with an equal role in regulating both types of glutamate receptors. Furthermore, we describe a compensatory pathway that utilizes the canonical homeostatic pathway and functions to oppose deviations in quantal size. This process implies that individual synapses have an intrinsic set point.

The role of MAGUKs at the post-synaptic density

Our results suggest the MAGUKs play a specific functional role: localizing glutamate receptors to the post-synaptic density. We find no deficit in either surface spine density (Figure 6C-6D) or receptor trafficking (Figure 6K-6N), in agreement with previous results (Elias et al., 2008), (but see Ehrlich et al., 2007). The MAUGK family has been suggested to act as a 'slot protein' for AMPARs at the PSD, controlling the number of AMPARs present at synapses. This role, however, which has been characterized by single-MAGUK knockdown, does not preclude additional functions, and electron microscopy data showing that loss of PSD-95 causes disruption of the electron-dense PSD (Chen et al., 2008) suggests that beyond localizing synaptic glutamate receptors, MAGUKs are also responsible for localization of scaffolding and signaling proteins in the PSD. Furthermore, the initial biochemical characterization of MAGUK function found a direct interaction with NMDARs, not AMPARs (Kornau et al., 1995). Here, we find that knockdown of the three MAGUK family members together causes approximately an 80% reduction in both AMPAR and NMDAR synaptic responses (Figure 1C). Although it is tempting

to speculate that the remaining current is mediated by MAGUKs that have not been removed, it is worth noting that a previous study using a combination of knockout mice and RNAi-mediated knockdown to remove MAGUKs found a quantitatively similar reduction in AMPAR currents (Elias et al., 2006), opening the possibility that the remaining receptors may not require MAGUKs for localization.

Transfection methods and the role of SAP102

The reduction in baseline glutamatergic currents caused by SAP102 knockdown (Figure 4C) was unexpected, given the lack of effect reported previously (Elias et al., 2006). In fact, the reduction was indistinguishable from that caused by knockdown of PSD-93 or PSD-95, which have been thought to play more central roles at the synapse (but see Kruger et al., 2013). Our findings show the difference in results is due to the method of transfection: biolistic transfection by gold particles coated with many copies of DNA plasmid is more effective than lentiviral transfection, presumably due to higher copy number following biolistic transfection (Figure 4). The method of transfection also likely explains another area of disagreement: the reduction in NMDAR-mediated current following knockdown of PSD-93 or PSD-95. Groups using viral transduction of neurons have reported no change in NMDAR-mediated currents following PSD-95 knockdown (Elias et al., 2006; Schluter et al., 2006), while other groups using biolistics have shown a modest decrease in NMDAR-mediated current, likely due to more effective knockdown by biolistics (Ehrlich et al., 2007; Futai et al., 2007). Given these conflicting results, we would caution against direct quantitative comparison of data obtained with different transfection methods. The lack of difference in AMPAR current reduction between these two methods would suggest that the loss of additional MAGUK primarily affects NMDARs, which are located at the center of the PSD (Chen et al., 2008). One simple mechanistic possibility would be that loss of

the MAGUKs causes a shrinking of the post-synaptic density that has a larger effect on the AMPARs, which are located at the periphery of the PSD. Removal of a substantial percentage of the MAGUKs, on the other hand, would greatly disrupt the PSD such that neither AMPARs nor NMDARs are retained at the synapse.

The role of MAGUKs in synaptogenesis

One unresolved question in the study of synaptic development is the role and assembly order of proteins at the nascent synapse. Another group (Ehrlich et al., 2007) has found that knockdown of PSD-95 causes a loss of NMDAR current and a decrease in spine density, which they interpret as a role for MAGUKs in the initial formation of spines. In our hands, however, we find no decrease in spine density, suggesting that the MAGUKs do not play a role in the initial formation of spines, but are critical for filling the PSD with glutamate receptors. While the reasons for the differing results are unclear, several key differences in experimental approach exist. We believe that knockdown of the entire MAGUK family and observation of the resulting phenotype at a time point at which protein has been maximally removed provides the best chance for accurate assessment of the role of the MAGUK family. Our data demonstrates that synaptogenesis is mechanistically a two-step process, with an initial spinogenic step controlled by structural proteins such as neuroligin, whose loss causes a decrease in spine density (Chih et al., 2005; Shipman et al., 2011), and a second synaptogenic step dependent on MAGUKs that fills the spine with proteins that are necessary for a functional synapse. As we have not removed SAP97 during our anatomical experiments, however, we cannot rule out a specific role for SAP97 in spine formation but not synaptogenesis. One implication of this hypothesis is that spinogenic proteins cannot fully depend on MAGUKs for their localization. Proteins like Kalirin-7, which are thought to interact with PDZ-containing proteins and have been implicated

in spine formation (Penzes et al., 2001), must have alternate mechanisms of localizing to the nascent spine. Furthermore, in agreement with previous results from mice lacking glutamate receptors (Lu et al., 2013), our data demonstrates that dendritic spines are maintained despite lacking functional glutamatergic synapses. Interestingly, we see a decrease in large-diameter spine heads with no decrease in quantal size. We speculate that these large-diameter spines may represent spines containing multiple PSDs, and their reduction reflects loss of an entire PSD, which would be reflected physiologically as a decrease in synapse number.

Synaptic consolidation following MAGUK loss

The decrease in quantal size following MAGUK knockdown in the GluA2 knockout and in slices treated with nifedipine or STO-609 suggests that the all-or-none synapse loss seen in untreated slices is the result of a two-step process: a loss of AMPARs from all functional synapses resulting in a quantal size decrease, followed by a compensatory consolidation of synapses which increases quantal size back to baseline. Consolidation has the effect of preventing changes in quantal size, and may be active throughout the life of the organism. Indeed, quantal size does not increase measurably over the life of the organism (Hsia et al., 1998), despite developmental increases in the amount of available synaptic protein (Sans et al., 2000). Rather, quantal content increases with quantal size held constant, a phenomenon comparable to the consolidation observed in this study.

Consolidation requires LTCC activity, while nifedipine-induced scaling is induced by its absence. We believe this difference underlies the two separate effects of their shared pathway: consolidation maintains quantal size, while nifedipine-induced scaling increases it (Thiagarajan et al., 2005). Consolidation utilizes intact LTCC signaling, which maintains quantal size at baseline levels, to counteract the reduction in quantal size and bring synapses back to baseline

quantal size. In contrast, nifedipine-induced scaling increases quantal size by disrupting the LTCC-dependent signal that maintains quantal size. Furthermore, MAGUK knockdown reduces the scaffolding proteins available before consolidation. This reduction means only a subset of synapses can be scaled up. Returning this subset to baseline quantal size comes at the cost of complete functional loss of other synapses, likely as scaffolding proteins consolidate at the 'winning' synapses. While it is not clear what factors determine the winning synapses, only a subset of synapses maintain NMDARs (Figure 5G). Perhaps NMDAR-containing synapses would be favored in this competition.

How is consolidation maintained as an all-or-none effect? An active signal delivered via tonic LTCC activity to consolidated synapses maintains baseline quantal size and counteracts the signal of the losing, functionally empty synapses to 'scale up'. It cannot be that empty synapses lack the capacity to add glutamate receptors in this context, since neurons introduced to nifedipine after consolidation has occurred lose the tonic LTCC signal and no longer maintain consolidated synapses (Figure 9). Therefore, active LTCC signaling maintains the 'winner' of winner-take-all consolidation. In the absence of LTCC activity, no winner is generated or maintained and no imbalance in quantal size appears. Instead, AMPA receptors are distributed evenly and all synapses have relatively equal, reduced, quantal sizes.

We have found that L-type channels, CaMKK, and the GluA2 subunit are required for consolidation, in line with previous evidence that they are required for homeostatic plasticity. The previously-identified roles of the L-type channel and CaMKK in transcription leave two possibilities for the role of GluA2. Either GluA2-containing receptors are an essential co-regulator, with LTCCs, of CaMKK-dependent transcription, or GluA2-containing receptors themselves are selectively modulated during the execution of homeostasis. In either case,

proteins which selectively bind to GluA2, but not GluA1, such as GRIP, PICK1, and NSF (Bredt and Nicoll, 2003; Song and Huganir, 2002), are likely to underlie the selective reliance on GluA2, either by transducing a synaptic signal, or acting to change the abundance of GluA2 at the synapse.

Notably, the consolidation of synapses changes only the distribution of synaptic AMPARs, not their absolute number, as opposed to multiplicative synaptic scaling, which causes an overall increase in the absolute number of synaptic AMPARs in response to decreased activity. This process is therefore closely related but distinct from multiplicative synaptic scaling. The longer duration required for consolidation, 96 hours vs. 24 hours for multiplicative scaling, further differentiates it. Indeed, although previous work (Sun and Turrigiano, 2011) has found activity-dependent synaptic scaling to be dependent on MAGUKs, they observe an all-or-none loss of synapses following MAGUK knockdown, suggesting that, in agreement with our findings, the three synaptic MAGUKs are not necessary for synapse consolidation. The difference between synaptic consolidation and homeostasis suggests that in MAGUK-knockdown neurons, the machinery for determining 'default' quantal size is intact even though the ability to change that set point via multiplicative scaling has been abolished, potentially due to the reduction in MAGUKs.

Following nifedipine washout, synapses in MAGUK miRNA-transfected neurons precisely return their quantal size to that of control neurons despite the overall decrease in excitatory input. This implies that synapses may function as autonomous homeostatic elements independent of neuronal-level homeostasis. While many lines of evidence show neuronal-level homeostasis in response to changes in firing rate, the mechanisms of synapse-level homeostasis are still being explored (reivewed in Lee et al., 2014). The canonical homeostatic pathway, most

well-studied in the context of neuron-level manipulations, is likely responsible for activating an array of related processes beyond neuron-level multiplicative scaling in response to activity perturbation. For example, the GluA2 subunit is necessary for proper distance-dependent scaling, a process which sets 'default' quantal size, likely in a synapse-specific manner, and is an example of non-multiplicative scaling (Shipman et al., 2013).

One open question is whether the consolidation process acting through LTCCs, CaMKK, and GluA2 directly redistributes PSD area with subsequent effects on AMPAR distribution, or if the consolidation of AMPARs happens without an associated redistribution of the PSD proteins. The answer to this question will likely follow from a resolution to the broader question of how synaptic size is controlled. One possibility would be that signaling molecules carefully control the number of AMPARs present at each synapse independent of PSD area, and without direct manipulation of these molecules, quantal size will remain constant. The finding that scaling down results in an increase in the rate of AMPAR unbinding from the synapse suggests that signaling may be acutely modulating synaptic AMPAR retention (Tatavarty et al., 2013), and would imply that a consolidation of AMPARs without redistribution of PSD proteins might be likely. Alternatively, quantal size may simply be secondary to spine / PSD size. In this case, PSD protein redistribution would be a prerequisite for AMPAR consolidation. In support of this model, several lines of evidence have shown that the number of AMPARs, PSD size, and spine head volume are all strongly correlated (Arellano et al., 2007; Harris and Stevens, 1989; Matsuzaki et al., 2001; Takumi et al., 1999). This data alone would leave open the possibility that active signaling at larger spines might increase the density (and therefore the overall number) of AMPARs, but importantly, there is no significant correlation between AMPAR density and PSD size (Nusser et al., 1998), suggesting that increases in AMPAR density cannot

explain the increase in the number of AMPARs at larger spines. Beyond the association between baseline AMPAR content and spine / PSD size, changes in AMPAR content are correlated with anatomical changes: increases in quantal size following LTP are associated with parallel increases in spine size, (Matsuzaki et al., 2004) while application of TTX causes increases in both quantal size (Turrigiano et al., 1998) and PSD area (MacGillavry et al., 2013). Together, these findings suggest anatomical growth as a universal mechanism underlying addition of AMPARs to synapses. Further exploration is needed to elucidate the signaling pathways and causal relationships involved in control of quantal size.

Synaptic consolidation explains the all-or-none loss of synapses seen following single-MAGUK knockdown, as well as knockdown of the MAGUK family. Beyond the MAGUK family, removal of two other PSD scaffolding proteins, GKAP (Shin et al., 2012) and Shank1 (Hung et al., 2008), causes a loss of AMPAR-containing synapses without changes in spine number or quantal size, indicating an all-or-none loss of functional synapses. These molecules, along with the MAGUKs, are also thought to be present at all synapses, suggesting that the synaptic consolidation we see here may be a general response by neurons to changes in abundance of scaffolding molecules and may explain the all-or-none functional synaptic loss seen following removal of seemingly-ubiquitous proteins.

Notably, our manipulations only block synaptic consolidation of AMPARs: in all cases NMDARs are lost in an all-or-none fashion. While it is possible that NMDARs are less dependent than AMPARs on cytoplasmic scaffolding molecules, the absolute reduction in AMPA and NMDA transmission caused by MAGUK loss is quantitatively very similar, suggesting that both receptor types are equally dependent on MAGUKs for synaptic localization. Instead, it is possible that NMDAR number is regulated by a separate mechanism. In support of

the latter idea, a previous study (Goold and Nicoll, 2010) has found that protein synthesis and GluA2 are necessary for homeostatic changes in AMPAR but not NMDAR transmission, indicating the phenomena are separable. Furthermore, NMDAR content does not correlate with PSD size as AMPAR content does; instead, synapses contain similar numbers of NMDARs independent of PSD size (Takumi et al., 1999). It is therefore likely that graded NMDAR loss does not occur, but instead that all-or-none NMDAR loss occurs only when MAGUK loss at individual synapses results in a PSD too small to support a functional synapse.

These results clarify our understanding of the MAGUK family and reveal a compensatory pathway that activates in response to reductions in available MAGUK scaffolding protein. We demonstrate here the feasibility of knockdown of a protein family by simultaneously removing PSD-93, PSD-95, and SAP102. We additionally show a role for all three MAGUKs in mediating baseline transmission and show that a consolidation pathway locally normalizes synaptic strength while causing complete loss of a subset of functional synapses. Further exploration of this pathway will improve our understanding of the regulation of synaptic strength and may give insight into the remarkable finding that synaptic strength remains constant throughout development, even as synapse number and protein abundance change dramatically. Finally, given the ability of the MAGUKs to heterodimerize (Kim et al., 1996), we have created a reagent in the MAGUK miRNA that, when combined with overexpression of recombinant protein, provides the opportunity to perform detailed structure-function analyses of individual MAGUK family members on a background lacking endogenous MAGUKs.

Figure 1: Pan-MAGUK knockdown reduces synaptic AMPAR and NMDAR-mediated currents. (A) CAG hybrid promoter drives EGFP with a synthetic 3' UTR containing miRNA hairpins against PSD-93, PSD-95, and SAP102. (B) Infection of dissociated hippocampal neurons with lentivirus expressing the MAGUK miRNA construct results in reductions in the amount of PSD-95, PSD-93, and SAP102 protein without any change in the loading control actin. (C) Scatter plots showing reductions in AMPAR and NMDAR EPSCs in MAGUK miRNA-transfected neurons compared to untransfected controls (AMPAR, 20.84 ± 4.03% control, $p < 0.005$, $n = 41$; NMDAR, 33.59 ± 8.22% control, $p < 0.005$, $n = 41$). Scatter plots of EPSCs show single pairs (open circles). Bar graphs show mean ratio ± SEM. AMPAR scale bars represent 25 ms, 25 pA; NMDAR scale bars represent 100 ms, 25 pA. (D) No change in paired-pulse ratio (PPR), defined as second EPSC over first EPSC (Ctrl 1.75 ± 0.07 , Expt 1.59 ± 0.06; $p > 0.05$, $n= 17$). Scale bars represent 25 pA, 50 ms.

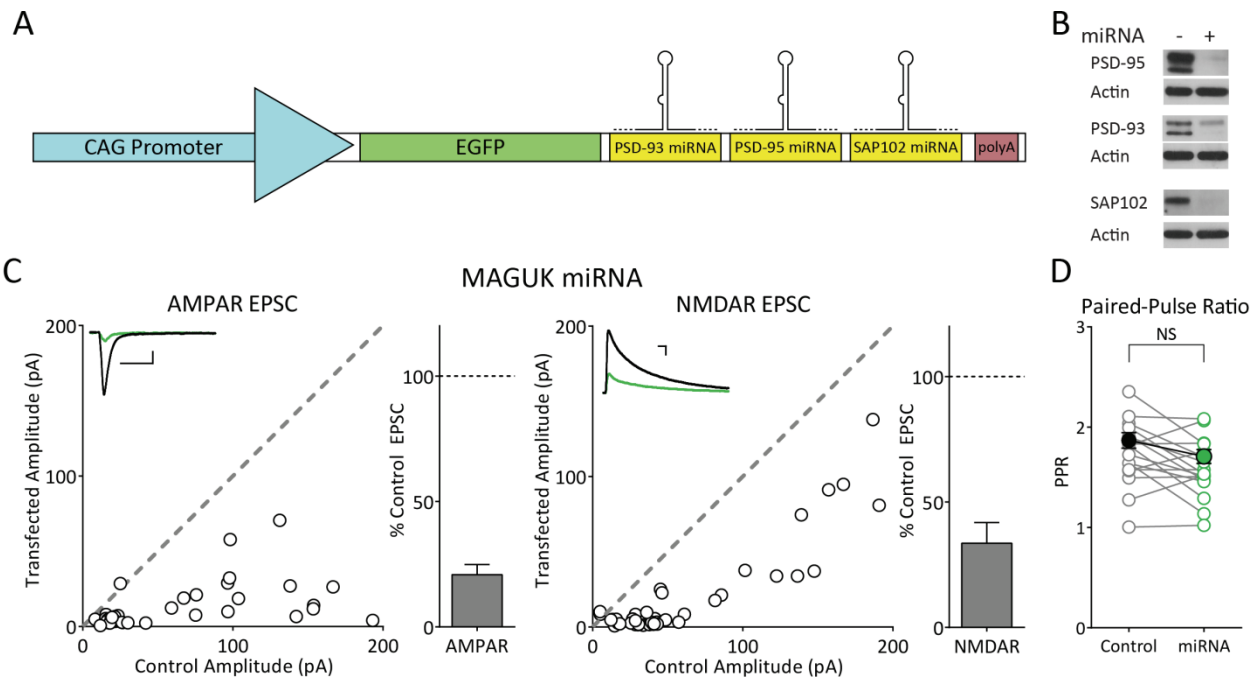
A
CAG Promoter
EGFP
PSD-93 miRNA
PSD-95 miRNA
SAP102 miRNA
polyA
B
miRNA - +
PSD-95
Actin
PSD-93
Actin
SAP102
Actin
C
MAGUK miRNA
AMPAR EPSC
NMDAR EPSC
Transfected Amplitude (pA)
Control Amplitude (pA)
% Control EPSC
AMPAR
NMDAR
D
Paired-Pulse Ratio
NS
PPR
Control
miRNA

Figure 2: MAGUK miRNA viral infection, and transfection in SAP97 conditional knockouts. (A) Viral MAGUK miRNA infection in organotypic cultures causes reductions in AMPAR and NMDAR EPSCs (AMPAR 24.59 ± 3.60%, n = 14; NMDAR 45.82 ± 13.94%, n = 16; $p < 0.05$ for both). (B-C) Viral MAGUK miRNA transfection does not change relative reduction in EPSCs compared to biolistic transfection of rat organotypic cultures. (AMPAR biolistics vs. virus $p > 0.05$; NMDAR biolistics vs. virus $p > 0.05$). (D) MAGUK miRNA transfection of wild-type mice causes reductions in AMPAR and NMDAR EPSCs (AMPAR 27.64 ± 7.07%, n = 5; NMDAR 54.41 ± 16.07%, n = 5; $p < 0.05$ for both). (E-F) MAGUK miRNA transfection in SAP97 conditional knockout does not increase relative reduction in EPSCs over reduction seen in miRNA transfection of rat organotypic cultures (WT vs. SAP97, $p > 0.05$ for both). (G) MAGUK miRNA transfection of SAP97 conditional knockout mice causes reductions in AMPAR and NMDAR EPSCs (AMPAR 32.28 ± 4.35%, n = 9; NMDAR 56.47 ± 9.22 %, n = 9; $p < 0.05$ for both). Scale bars represent 25pA, 50ms.

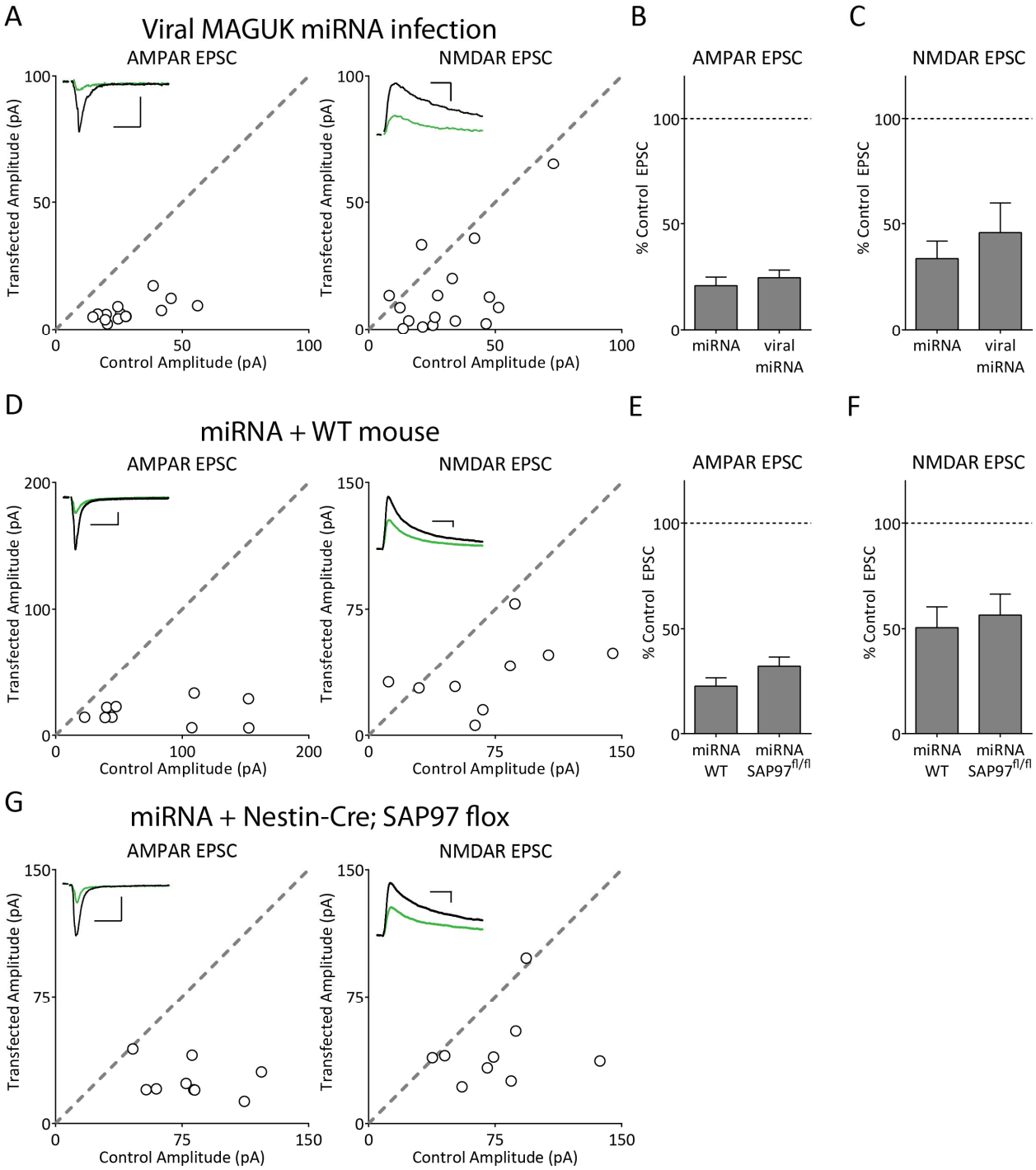
A
Viral MAGUK miRNA infection
AMPAR EPSC
NMDAR EPSC
Transfected Amplitude (pA)
Control Amplitude (pA)
B
AMPAR EPSC
% Control EPSC
miRNA
viral miRNA
C
NMDAR EPSC
D
miRNA + WT mouse
E
F
G
miRNA + Nestin-Cre; SAP97 flox
miRNA WT
miRNA SAP97fl/fl

Figure 3: All MAGUKs play roles in baseline glutamate receptor localization. Open circles represent amplitudes for single pairs. (A) PSD-93 knockdown causes decrease of AMPAR-mediated current (49.23 ± 8.34% control, $p < 0.005$, $n = 17$) and NMDAR-mediated current (71.34 ± 11.44% control, $p < 0.05$, $n = 17$). (B) PSD-95 knockdown causes decrease of AMPAR-mediated current (45.38 ± 7.457% control, $p < 0.005$, $n = 34$) and NMDAR-mediated current (75.38 ± 11.37% control, $p < 0.05$, $n = 31$). (C) SAP102 knockdown causes decrease of AMPAR-mediated current (54.83 ± 12.45% control, $p < 0.05$, $n = 13$) and NMDAR-mediated current (63.74 ± 20.07% control, $p < 0.01$, $n = 11$). (D) Summary graphs of mean ± SEM EPSC amplitudes, expressed as a percentage of control EPSC values. Scale bars represent 25 pA, 50 ms.

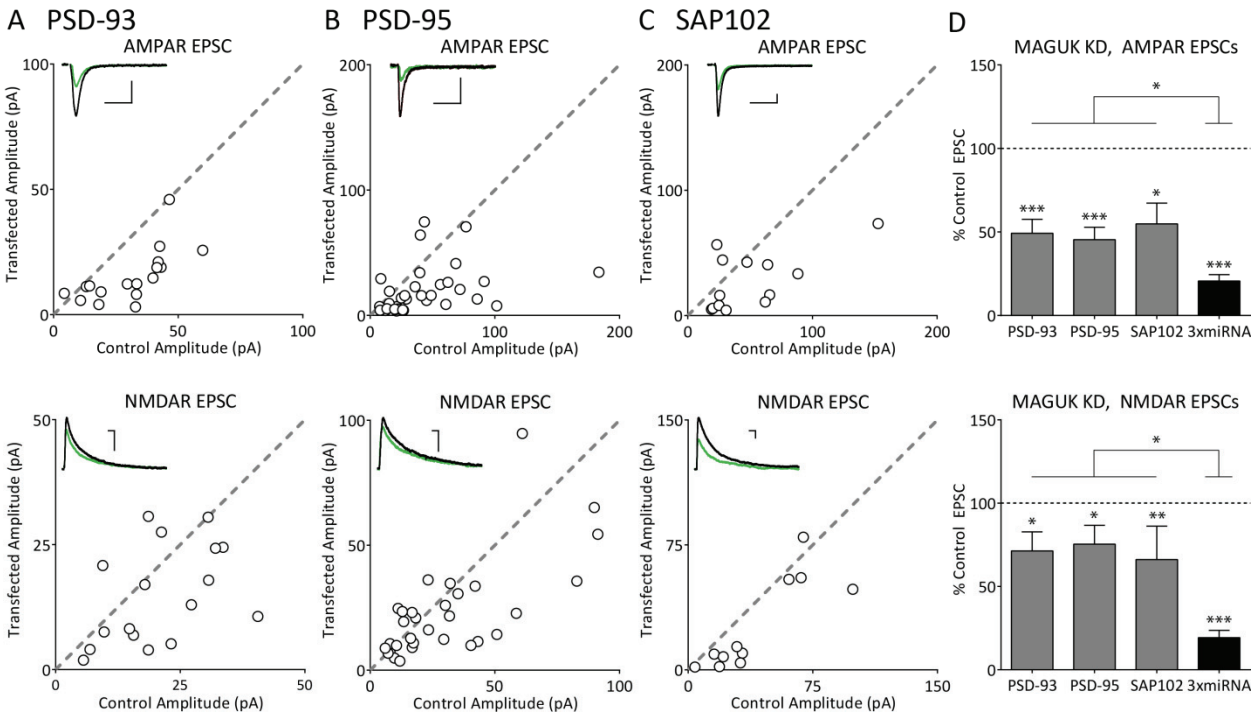
A PSD-93
AMPAR EPSC
Transfected Amplitude (pA)
Control Amplitude (pA)
B PSD-95
AMPAR EPSC
Transfected Amplitude (pA)
Control Amplitude (pA)
C SAP102
AMPAR EPSC
Transfected Amplitude (pA)
Control Amplitude (pA)
D
MAGUK KD, AMPAR EPSCs
% Control EPSC
PSD-93
PSD-95
SAP102
3xmiRNA
NMDAR EPSC
Transfected Amplitude (pA)
Control Amplitude (pA)
NMDAR EPSC
Transfected Amplitude (pA)
Control Amplitude (pA)
NMDAR EPSC
Transfected Amplitude (pA)
Control Amplitude (pA)
MAGUK KD, NMDAR EPSCs
% Control EPSC
PSD-93
PSD-95
SAP102
3xmiRNA

Figure 4: Dependence of SAP102 phenotype on method of RNAi delivery. Open circles represent amplitudes for single pairs. (A) SAP102 knockdown by viral transduction does not decrease AMPAR currents (88.95 ± 8.87% control, $p > 0.05$, n = 16) and compared to biolistic knockdown (54.83 ± 12.45% control) results in statistically larger AMPAR currents (biolistics vs. virus $p < 0.05$, n = 13 biolistics; n = 16 virus). SAP102 knockdown by viral transduction slightly decreases NMDAR currents (83.03 ± 11.04% control, $p < 0.05$, n = 15) and compared to biolistic knockdown (63.74 ± 20.07% control) results in statistically larger NMDAR currents (biolistics vs. virus $p < 0.01$, n = 11 biolistics; n = 15 virus). (B) Biolistic knockdown of SAP102 in wild-type mice causes a decrease of AMPAR-mediated current (52.03 ± 7.06% control, $p < 0.01$, n = 13). Biolistic knockdown of SAP102 in wild-type mice causes a decrease of NMDAR-mediated current (65.58 ± 9.49% control, $p < 0.05$, n = 13). (C) Biolistic knockdown of SAP102 in SAP102 knockout mice results in no change in AMPAR-mediated currents (102.70 ± 20.06% control, $p > 0.05$, n = 15) or NMDAR-mediated currents (90.16 ± 15.22% control, $p > 0.05$, n = 14). (D) Knockdown of SAP102 in wild-type mice causes a statistically significant decrease in AMPAR-mediated current compared to knockdown in SAP102 knockout mice (wild-type vs. KO $p < 0.05$, n = 13 WT, n = 15 KO). Knockdown of SAP102 in wild-type mice causes a statistically significant decrease in NMDAR current compared to controls, but not compared to knockdown in SAP102 knockout mice, although there is a trend towards significance (wild-type vs. KO $p > 0.05$, n = 13 WT, n = 14 KO). Scale bars represent 25 pA, 50 ms.

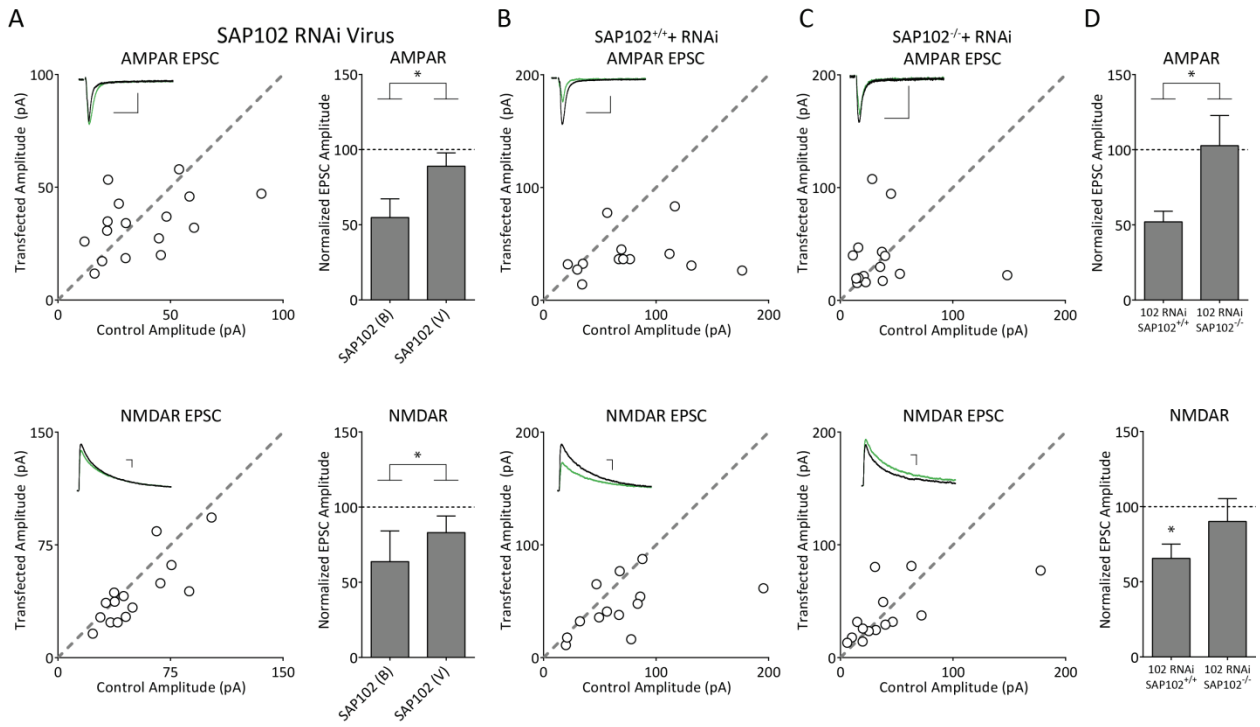
A
SAP102 RNAi Virus
AMPAR EPSC
Transfected Amplitude (pA)
Control Amplitude (pA)
AMPAR
Normalized EPSC Amplitude
SAP102 (B)
SAP102 (V)
B
SAP102+/+ + RNAi
AMPAR EPSC
C
SAP102-/- + RNAi
AMPAR EPSC
D
AMPAR
102 RNAi SAP102+/+
102 RNAi SAP102-/-
NMDAR EPSC
NMDAR

Figure 5: MAGUK knockdown causes loss of functional glutamatergic synapses. (A) Representative sample traces of asynchronous EPSCs (aEPSCs) recorded in the presence of Sr^{2+} in neurons expressing MAGUK miRNA or control neurons. 50 ms following stimulation (grey box) was excluded from analysis. Scale bars represent 50 ms, 15 pA. (B) Representative average aEPSC traces showing no change in average amplitude. Black trace is control; green trace is experimental. Scale bars represent 20 ms, 4 pA. (C) aEPSC frequency in neurons expressing MAGUK miRNA. Plot shows single pairs (open circles) and mean ± SEM (filled circles). aEPSC frequency is significantly reduced ($p < 0.05$) in neurons expressing MAGUK miRNA. (D) aEPSC amplitude in neurons expressing MAGUK miRNA. Plot as in (C). There is no change in amplitude between control and MAGUK miRNA neurons ($p = 0.15$, $n = 13$). (E-F) Cumulative distribution plots of aEPSC frequency and amplitude. Control shown in black, experimental in green. Cumulative distribution functions show no irregularities. (G-H) Coefficient of variation analysis of simultaneously recorded pairs of control/miRNA neurons. CV^{-2} graphed against ratio of mean amplitude within each pair. Results along the horizontal y = 1 line are consistent with change in quantal size (q), results along grey dashed identity (45^{o}) line is consistent with change in quantal content ($N \times P_r$). Analysis of AMPAR and NMDAR responses suggests decrease is due to reduction in quantal content. Small solid and dashed lines indicate linear regression line and 95% confidence intervals, respectively. (I) Summary of coefficient of variation analysis. Both AMPAR and NMDAR average fall on the identity line ($p < 0.05$ vs horizontal line), while average response after D-APV falls on horizontal y = 1 line ($p > 0.05$).

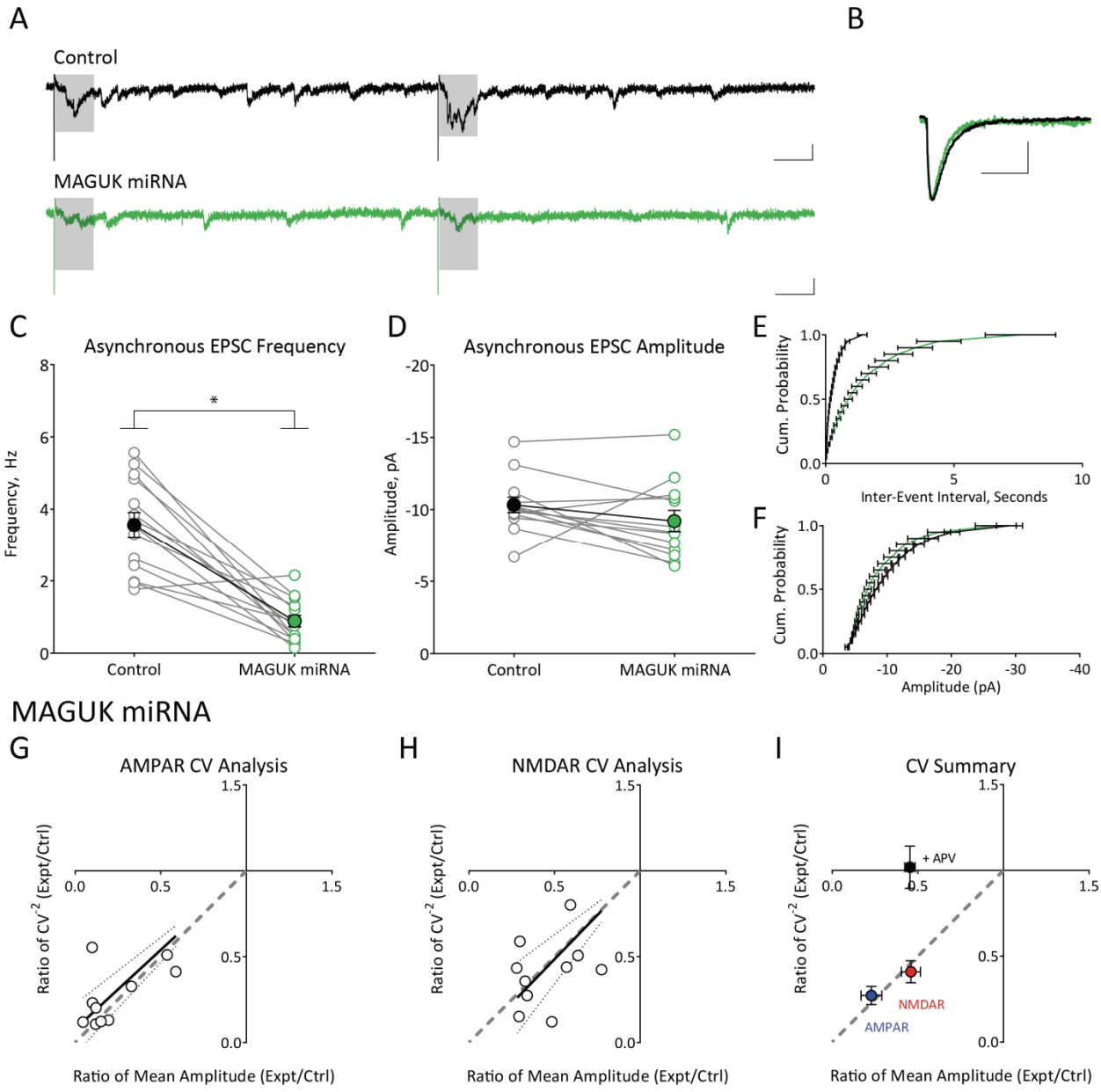
A
Control
MAGUK miRNA
B
C
Asynchronous EPSC Frequency
Frequency, Hz
Control
MAGUK miRNA
D
Asynchronous EPSC Amplitude
Amplitude, pA
Control
MAGUK miRNA
E
Cum. Probability
Inter-Event Interval, Seconds
F
Cum. Probability
Amplitude (pA)
MAGUK miRNA
G
AMPAR CV Analysis
Ratio of CV-2 (Expt/Ctrl)
Ratio of Mean Amplitude (Expt/Ctrl)
H
NMDAR CV Analysis
Ratio of CV-2 (Expt/Ctrl)
Ratio of Mean Amplitude (Expt/Ctrl)
I
CV Summary
+ APV
NMDAR
AMPAR
Ratio of CV-2 (Expt/Ctrl)
Ratio of Mean Amplitude (Expt/Ctrl)

Figure 6: MAGUK knockdown does not affect spine density or surface glutamate receptors. (A) Application of 1μM D-APV causes a reduction of NMDAR EPSC (44.91 ± 5.66%; n = 9; $p < 0.05$). Open circles represent single neurons before/after APV wash-in. Scale bars represent 100 ms, 50pA. (B) Coefficient of variation analysis pre/post APV application in individual neurons. CV^{-2} graphed against ratio of mean amplitude within each pair. Results along the horizontal y = 1 line are consistent with change in quantal size (q), results along identity (45^o) line is consistent with change in quantal content (N x P_r). No change in CV^{-2} ($p > 0.05$ compared to horizontal line) consistent with decrease in quantal size. Small solid and dashed lines indicate linear regression line and 95% confidence intervals, respectively. (C-D) Spine density on primary apical dendrite is unchanged following MAGUK knockdown (n = 21 GFP, n = 11 MAGUK miRNA; $p > 0.05$). Scale bar represents 10 μm. (E) Sample images of primary apical dendrite from neurons expressing GFP and GFP + miRNA imaged using super-resolution structured illumination microscopy (SIM). For all morphological analysis, n = 7 neurons, 148 control spines; n = 8 neurons, 103 miRNA spines. (F) Neck length is unchanged by MAGUK knockdown (GFP, mean ± SEM length = 700.0 ± 28.16nm; miRNA, length = 730.5 ± 33.60nm; $p > 0.05$). Data is displayed as a box-and-whiskers plot showing median, interquartile and range. (G) Neck diameter is unchanged by MAGUK knockdown (GFP, diameter = 231.3 ± 6.25nm; miRNA, diameter = 230.5 ± 9.29nm; $p > 0.05$). (H) Spine head diameter is reduced by MAGUK knockdown (GFP, diameter = 878.1 ± 34.2nm; miRNA, diameter = 673.7 ± 23.35nm; $p < 0.05$). (I) Distribution of spine head diamaters. (J) Normalized distribution of spine head diameters, each distribution normalized to largest bin, showing selective loss of large-diameter spine heads. (K-L) Whole-cell currents in response to fast application of AMPA or NMDA show that

MAGUKs play no role in AMPAR or (M-N) NMDAR surface localization ($p > 0.05$). Scale bars represent 5 sec, 200 pA.

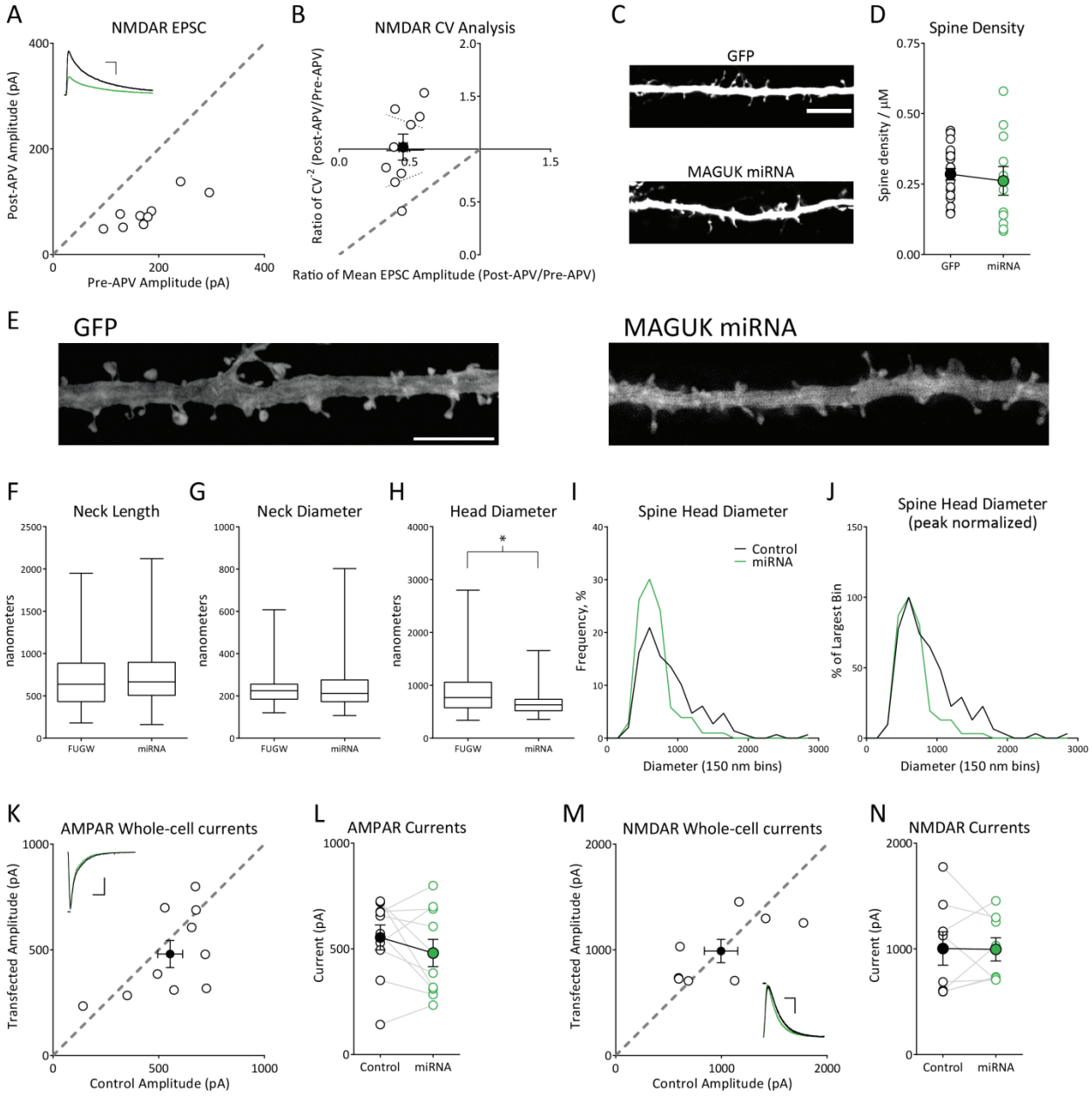
A
NMDAR EPSC
Post-APV Amplitude (pA)
Pre-APV Amplitude (pA)
B
NMDAR CV Analysis
Ratio of CV-2 (Post-APV/Pre-APV)
Ratio of Mean EPSC Amplitude (Post-APV/Pre-APV)
C
GFP
MAGUK miRNA
D
Spine Density
Spine density / µM
GFP
miRNA
E
GFP
MAGUK miRNA
F
Neck Length
nanometers
FUGW
miRNA
G
Neck Diameter
nanometers
FUGW
miRNA
H
Head Diameter
*
nanometers
FUGW
miRNA
I
Spine Head Diameter
Control
miRNA
Frequency, %
Diameter (150 nm bins)
J
Spine Head Diameter
(peak normalized)
% of Largest Bin
Diameter (150 nm bins)
K
AMPAR Whole-cell currents
Transfected Amplitude (pA)
Control Amplitude (pA)
L
AMPAR Currents
Current (pA)
Control
miRNA
M
NMDAR Whole-cell currents
Transfected Amplitude (pA)
Control Amplitude (pA)
N
NMDAR Currents
Current (pA)
Control
miRNA

Figure 7: MAGUK knockdown in vivo triggers synaptic consolidation. (A) MAGUK knockdown by viral infection at P8 *in vivo* causes a decrease in AMPAR EPSCs compared to neighboring uninfected neurons (24.49 ± 5.74%, n = $p < 0.05$) as recorded in acute slices from P16 rats. (B) MAGUK knockdown by viral infection at P8 *in vivo* causes a decrease in AMPAR EPSCs (30.42 ± 5.80%, n = $p < 0.05$) as recorded in acute slices from P35 rats. (C) The absolute magnitude of reduction in AMPAR EPSCs following P8 viral infection does not differ significantly ($p > 0.05$) in rats sacrificed at P16 or P35. Dashed line and shaded area represent mean ± SEM of MAGUK miRNA in organotypic cultures (Figure 1C). (D) mEPSC frequency is significantly reduced (control 0.18 ± 0.04 Hz; miRNA 0.01 ± 0.02 Hz, n = 9, $p < 0.05$) in neurons infected with MAGUK miRNA *in vivo* at P8 and recorded at P16. (E) mEPSC amplitude is significantly reduced (control -11.59 ± 1.36 pA; miRNA -8.87 ± 0.07 pA, n = 9, $p < 0.05$) in neurons infected with MAGUK miRNA at P8 and recorded at P16. (F) Coefficient of variation analysis of simultaneously recorded pairs of control/miRNA neurons infected at P8 and recorded at P16. CV^{-2} graphed against ratio of mean amplitude within each pair. Results along the horizontal y = 1 line are consistent with change in quantal size (q), results along identity (45^{o}) line is consistent with change in quantal content (N x P_r). Analysis of AMPAR responses suggests decrease is due to reductions in both quantal content and quantal size. Small solid and dashed lines indicate linear regression line and 95% confidence intervals, respectively. (G) mEPSC frequency is significantly reduced (control 0.36 ± 0.13 Hz; miRNA 0.12 ± 0.03 Hz, n = 10, $p < 0.05$) in neurons infected with MAGUK miRNA at P8 and recorded at P35. (H) mEPSC amplitude is not reduced in neurons infected with MAGUK miRNA (control -11.07 ± 0.60 pA; miRNA -9.90 ± 0.52 pA, n = 10, $p > 0.05$) at P8 and recorded at P35. (I) Coefficient of variation analysis of simultaneously recorded pairs of control/miRNA neurons infected at P8 and recorded

at P35. CV^{-2} graphed against ratio of mean amplitude within each pair. Results along the horizontal y = 1 line are consistent with change in quantal size (q), results along identity (45^{o}) line is consistent with change in quantal content (N x P_r). Analysis of AMPAR responses suggests decrease is due to reduction in quantal content. Small solid and dashed lines indicate linear regression line and 95% confidence intervals, respectively.

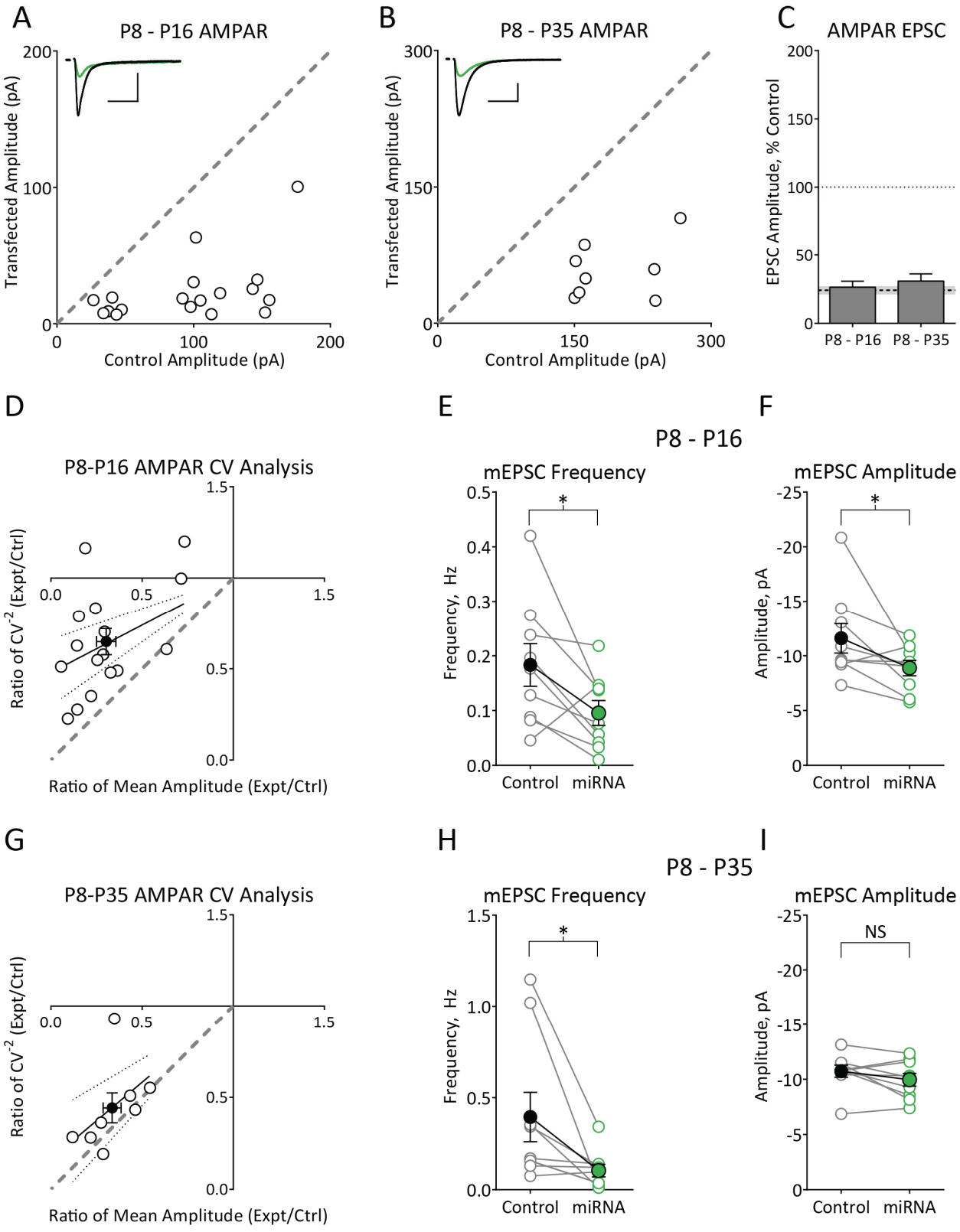
A
P8 - P16 AMPAR
Transfected Amplitude (pA)
Control Amplitude (pA)
B
P8 - P35 AMPAR
Transfected Amplitude (pA)
Control Amplitude (pA)
C
AMPAR EPSC
EPSC Amplitude, % Control
P8 - P16
P8 - P35
D
P8-P16 AMPAR CV Analysis
Ratio of CV-2 (Expt/Ctrl)
Ratio of Mean Amplitude (Expt/Ctrl)
E
P8 - P16
mEPSC Frequency
Frequency, Hz
Control
miRNA
F
mEPSC Amplitude
Amplitude, pA
Control
miRNA
G
P8-P35 AMPAR CV Analysis
Ratio of CV-2 (Expt/Ctrl)
Ratio of Mean Amplitude (Expt/Ctrl)
H
P8 - P35
mEPSC Frequency
Frequency, Hz
Control
miRNA
I
mEPSC Amplitude
NS
Amplitude, pA
Control
miRNA

Figure 8: L-Type Calcium Channels are required for synaptic consolidation. (A) MAGUK miRNA transfection in the presence of 20 μM nifedipine causes significant reductions in both AMPAR and NMDAR EPSCs compared to neighboring untransfected neurons (AMPAR 20.17 ± 3.24%; NMDAR 21.35 ± 4.17%; n = 10 and $p < 0.05$ for both). (B-C) Summary data showing no additional change in AMPAR or NMDAR EPSCs in MAGUK miNRA-expressing neurons with nifedipine compared to MAGUK miRNA alone ($p > 0.05$ for both). Dashed line and shaded area show mean ± SEM of normalized synaptic responses for MAGUK miRNA without nifedipine. (D) No change in paired-pulse ratio (PPR), defined as second EPSC over first EPSC (Ctrl 1.63 ± 0.11, Expt 1.72 ± 0.17; $p > 0.05$, n= 9). (E-F) Coefficient of variation analysis of simultaneously recorded pairs of control/miRNA neurons. CV^{-2} graphed against ratio of mean amplitude within each pair. Results along the horizontal line are consistent with change in quantal size (q), results along identity (45^{o}) line are consistent with change in quantal content (N x P_r). Decrease in AMPAR EPSC is due to reduction in quantal size. Decrease in NMDAR EPSC is due to reduction in quantal content. Small solid and dashed lines indicate linear regression line and 95% confidence intervals, respectively. (G) Summary of coefficient of variation analysis. AMPAR average falls near the horizontal line ($p < 0.05$ compared to horizontal line) and NMDAR average falls on the identity line. Data from MAGUK miRNA without nifedipine incubation (Figure 5G) are re-plotted to aid comparison. (H) Coefficient of variation analysis of simultaneously recorded pairs of control/PSD-95 miRNA neurons (black circle) shows the reduction in AMPAR EPSC is due to reductions in quantal content. Reduction in AMPAR EPSC following PSD-95 knockdown and nifedipine incubation (green circle) is due to reductions in quantal size. (I-J) coefficient of variation analysis of simultaneously recorded pairs of control/miRNA neurons either 24 hours (I) or 96 hours (J) after nifedipine washout. 24 hours

after washout, the decrease in AMPAR EPSC is due to reductions in quantal content and quantal size. 96 hours after nifedipine washout, the decrease in AMPAR EPSC is due to pure reduction in quantal content. (K) Summary graph showing slope of CV dataset regression line vs. hours post-nifedipine washout. As a control, nifedipine was not washed out of some slices (dashed line and black square).

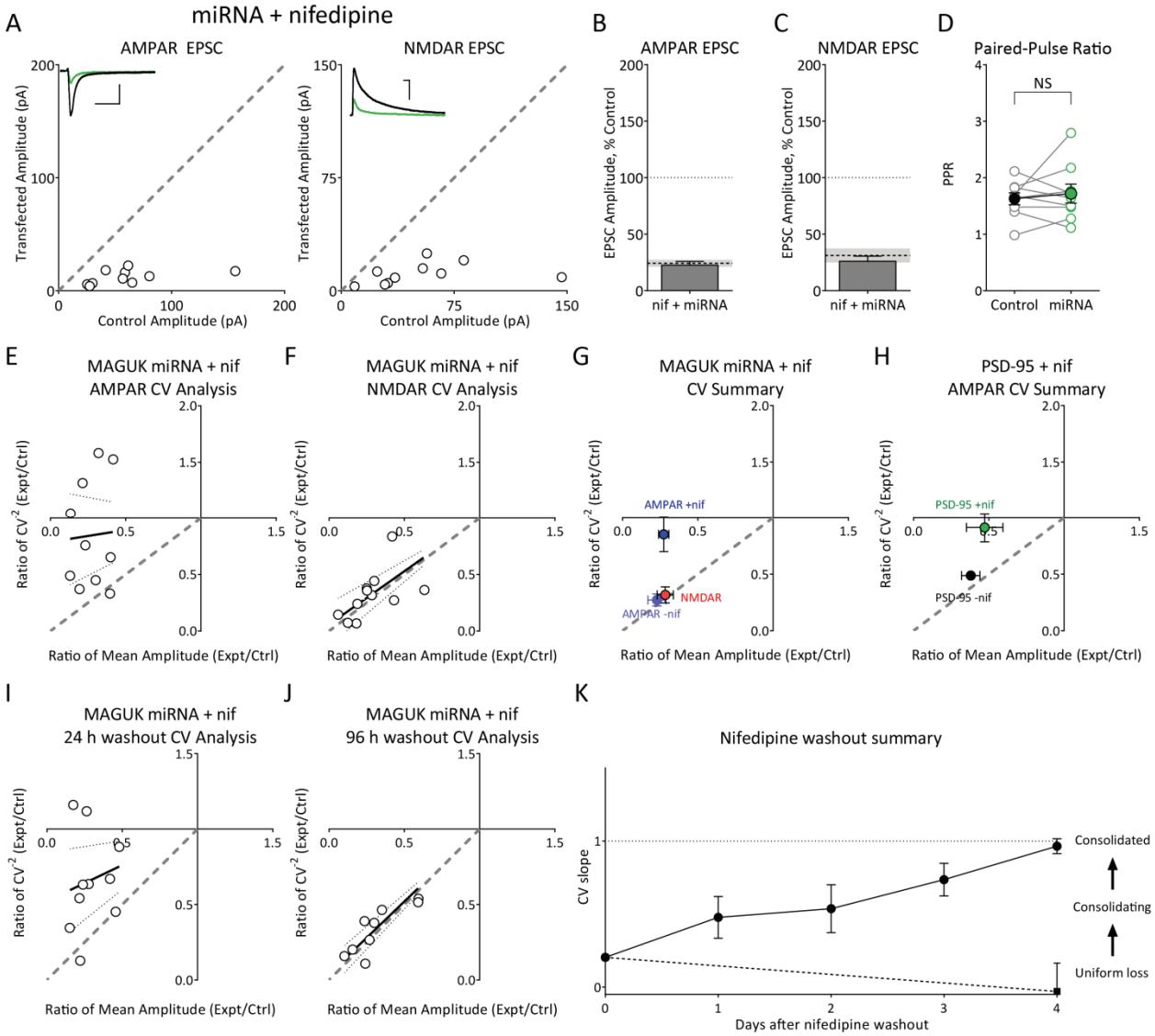
A
miRNA + nifedipine
AMPAR EPSC
NMDAR EPSC
Transfected Amplitude (pA)
Control Amplitude (pA)
B
AMPAR EPSC
EPSC Amplitude, % Control
nif + miRNA
C
NMDAR EPSC
EPSC Amplitude, % Control
nif + miRNA
D
Paired-Pulse Ratio
NS
PPR
Control
miRNA
E
MAGUK miRNA + nif
AMPAR CV Analysis
F
MAGUK miRNA + nif
NMDAR CV Analysis
G
MAGUK miRNA + nif
CV Summary
AMPAR +nif
NMDAR
AMPAR -nif
H
PSD-95 + nif
AMPAR CV Summary
PSD-95 +nif
PSD-95 -nif
Ratio of CV-2 (Expt/Ctrl)
Ratio of Mean Amplitude (Expt/Ctrl)
I
MAGUK miRNA + nif
24 h washout CV Analysis
J
MAGUK miRNA + nif
96 h washout CV Analysis
K
Nifedipine washout summary
CV slope
Days after nifedipine washout
Consolidated
Consolidating
Uniform loss

Figure 9: T1036Y mutant α1c calcium channel rescues synaptic consolidation. (A) Sample calcium currents. Currents were evoked by 500ms step from -50mV to 0mV. (B) Increase in calcium currents following expression of T1036Y mutant calcium channel (Control 283.28 pA, T1036Y 821.30 pA, $n = 7$, $p < 0.05$). Scale bars represent 500 pA, 100 ms. (C) Increase in calcium currents following expression of T1036Y mutant channel is unaffected by nifedipine (Control 186.89 pA, T1036Y 740.93 pA, $n = 4$, $p < 0.05$). (D) Nifedipine-sensitive current is unaffected by expression of T0136Y channel (Control 105.37 pA, T1036Y 157.34 pA, $n = 4$, $p > 0.05$). (E) Coefficient of variation analysis of simultaneously recorded pairs of control/miRNA + T1036Y neurons in the absence of nifedipine. Reductions in AMPAR and NMDAR EPSC are due to reductions in quantal content. Small solid and dashed lines indicate linear regression line and 95% confidence intervals, respectively. (F) Coefficient of variation analysis of simultaneously recorded pairs of control/miRNA + T1036Y neurons incubated in 20 μM nifedipine. Reductions in AMPAR and NMDAR EPSCs are due to reductions in quantal content. (G) Summary of coefficient of variation analysis. AMPAR average indicates changes in quantal size and quantal content. Data from MAGUK miRNA plus nifedipine incubation (Figure 5E) is re-plotted to aid comparison. (H) MAGUK miRNA co-transfected with T1036Y calcium channel subunit causes reductions in both AMPAR and NMDAR EPSC (AMPAR 37.3 ± 7.5%, $n = 12$; NMDAR 33.1 ± 8.0%, $n = 11$; $p < 0.05$ for both). (I) MAGUK miRNA co-transfected with T1036Y calcium channel subunit in the presence of nifedipine causes reductions in both AMPAR and NMDAR EPSC (AMPAR 31.8 ± 5.8%; NMDAR 27.8 ± 6.1%; $n = 11$, $p < 0.05$ for both). (J) Summary data showing no additional change in AMPAR or NMDAR EPSCs in MAGUK miNRA-expressing neurons co-expressing T1036Y ± 20 μM nifedipine compared to MAGUK miRNA alone ($p > 0.05$ for all). Dashed line and shaded area show mean ± SEM of

normalized synaptic responses for MAGUK miRNA alone. (K-L) Coefficient of variation analysis of simultaneously recorded pairs of control/miRNA neurons recorded either 48 hours (K) or 72 hours (L) after nifedipine washout. CV^{-2} graphed against ratio of mean amplitude within each pair. Results along the horizontal y = 1 line are consistent with change in quantal size (q), results along identity (45^{o}) line is consistent with change in quantal content (N x P_r). Analysis of AMPAR responses in both cases suggests decrease is due to reductions in both quantal content and quantal size. Small solid and dashed lines indicate linear regression line and 95% confidence intervals, respectively. (M) Coefficient of variation analysis of simultaneously recorded pairs of control/miRNA neurons after incubation in nifedipine for 10 days. Analysis of AMPAR responses suggests decrease is due to reductions in quantal size. Small solid and dashed lines indicate linear regression line and 95% confidence intervals, respectively. (N) Coefficient of variation analysis of simultaneously recorded pairs of control/miRNA neurons following nifedipine incubation from DIV 7-11. Analysis of AMPAR responses suggests EPSC decrease is due to reductions in quantal size and quantal content. Small solid and dashed lines indicate linear regression line and 95% confidence intervals, respectively. (O) Coefficient of variation data from (N) re-plotted against data from MAGUK miRNA without drugs (Figure 5; -nif) and MAGUK miRNA incubated in nifedipine (Figure 5; +nif 1-11DIV) to aid comparison. Wash-in of nifedipine results in intermediate phenotype and partial reversal of consolidation. Scale bars in (A) represent 250 pA, 100 ms; scale bars in (H-I) represent 25 pA, 50 ms.

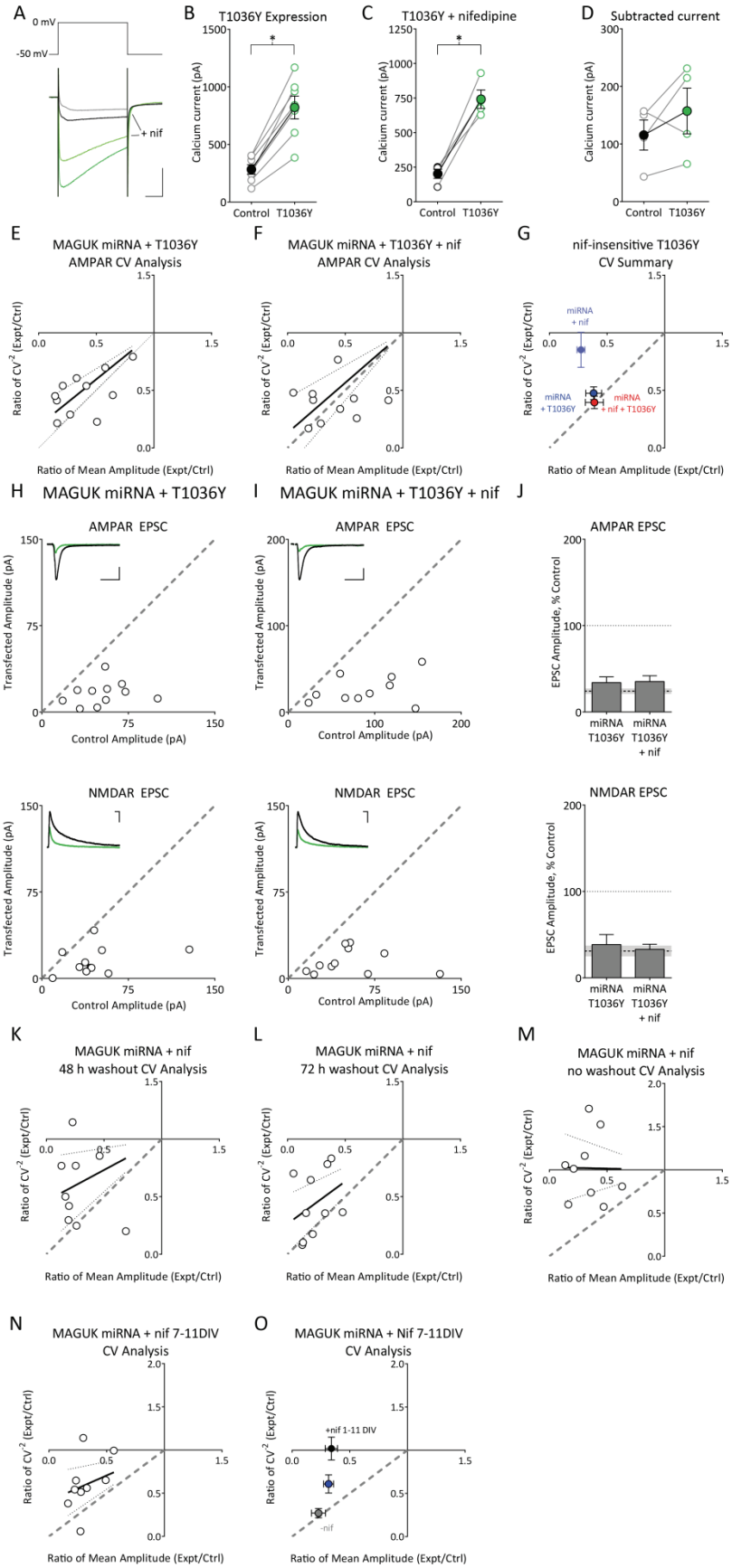
A
0 mV
-50 mV
+ nif
B
T1036Y Expression
Calcium current (pA)
Control T1036Y
C
T1036Y + nifedipine
Calcium current (pA)
Control T1036Y
D
Subtracted current
Calcium current (pA)
Control T1036Y
E
MAGUK miRNA + T1036Y
AMPAR CV Analysis
Ratio of CV-2 (Expt/Ctrl)
Ratio of Mean Amplitude (Expt/Ctrl)
F
MAGUK miRNA + T1036Y + nif
AMPAR CV Analysis
Ratio of CV-2 (Expt/Ctrl)
Ratio of Mean Amplitude (Expt/Ctrl)
G
nif-insensitive T1036Y
CV Summary
miRNA + nif
miRNA + T1036Y
miRNA + nif + T1036Y
Ratio of CV-2 (Expt/Ctrl)
Ratio of Mean Amplitude (Expt/Ctrl)
H
MAGUK miRNA + T1036Y
AMPAR EPSC
Transfected Amplitude (pA)
Control Amplitude (pA)
I
MAGUK miRNA + T1036Y + nif
AMPAR EPSC
Transfected Amplitude (pA)
Control Amplitude (pA)
J
AMPAR EPSC
EPSC Amplitude, % Control
miRNA T1036Y
miRNA T1036Y + nif
NMDAR EPSC
Transfected Amplitude (pA)
Control Amplitude (pA)
NMDAR EPSC
Transfected Amplitude (pA)
Control Amplitude (pA)
NMDAR EPSC
EPSC Amplitude, % Control
miRNA T1036Y
miRNA T1036Y + nif
K
MAGUK miRNA + nif
48 h washout CV Analysis
Ratio of CV-2 (Expt/Ctrl)
Ratio of Mean Amplitude (Expt/Ctrl)
L
MAGUK miRNA + nif
72 h washout CV Analysis
Ratio of CV-2 (Expt/Ctrl)
Ratio of Mean Amplitude (Expt/Ctrl)
M
MAGUK miRNA + nif
no washout CV Analysis
Ratio of CV-2 (Expt/Ctrl)
Ratio of Mean Amplitude (Expt/Ctrl)
N
MAGUK miRNA + nif 7-11DIV
CV Analysis
Ratio of CV-2 (Expt/Ctrl)
Ratio of Mean Amplitude (Expt/Ctrl)
O
MAGUK miRNA + Nif 7-11DIV
CV Analysis
+nif 1-11 DIV
-nif
Ratio of CV-2 (Expt/Ctrl)
Ratio of Mean Amplitude (Expt/Ctrl)

Figure 10: CaM kinase kinase (CaMKK) is required for synaptic consolidation. (A) Coefficient of variation analysis of simultaneously recorded pairs of control/miRNA neurons in slices incubated with 3μM STO-609. The decrease in AMPAR EPSCs is due to reduction in quantal size and quantal content. Small solid and dashed lines indicate linear regression line and 95% confidence intervals, respectively. (B) Summary of coefficient of variation analysis. Data from MAGUK miRNA alone (Figure 5G), and plus nifedipine incubation (Figure 5E) are re-plotted to aid comparison. (C) Coefficient of variation analysis of simultaneously recorded pairs of control/miRNA + CaMKK L233F neurons in slices incubated in STO-609. The decrease in AMPAR EPSC is due to reduction in quantal content. (D) Summary of coefficient of variation analysis. Data from MAGUK miRNA alone (Figure 5G), and plus nifedipine incubation (Figure 5E) are re-plotted to aid comparison. (E) MAGUK miRNA transfected in the presence of 3μM STO-609 causes reductions in both AMPAR and NMDAR EPSC (AMPAR 31.93 ± 6.66%, n = 12; NMDAR 46.98.1 ± 13.14%, n = 12; $p < 0.05$ for both). (F) MAGUK miRNA co-transfected with STO-609 insensitive CaMKK L233F in the presence of STO-609 causes reductions in both AMPAR and NMDAR EPSC (AMPAR 22.31 ± 4.32%, n = 9; NMDAR 22.86 ± 3.14%, n = 6; $p < 0.05$ for both). (G) Summary data showing no additional change in AMPAR EPSC reduction due to incubation in STO-609 and co-expression of CaMKK L233F. ($p > 0.05$ for all).

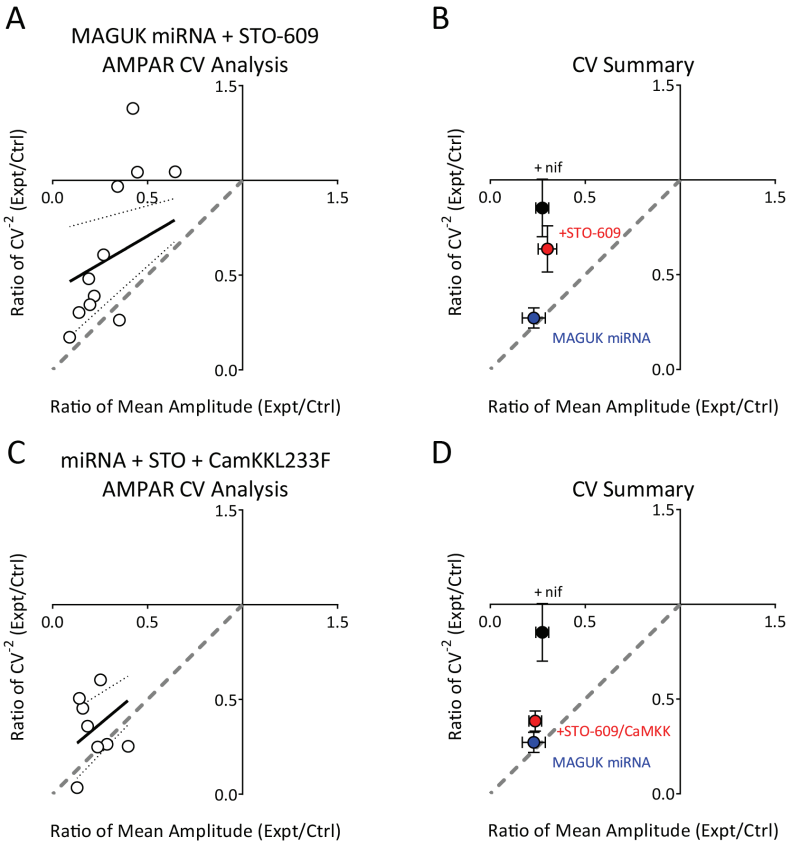
A
MAGUK miRNA + STO-609
AMPAR CV Analysis
Ratio of CV-2 (Expt/Ctrl)
Ratio of Mean Amplitude (Expt/Ctrl)
B
CV Summary
+ nif
+STO-609
MAGUK miRNA
C
miRNA + STO + CamKKL233F
AMPAR CV Analysis
D
CV Summary
+ nif
+STO-609/CaMKK
MAGUK miRNA

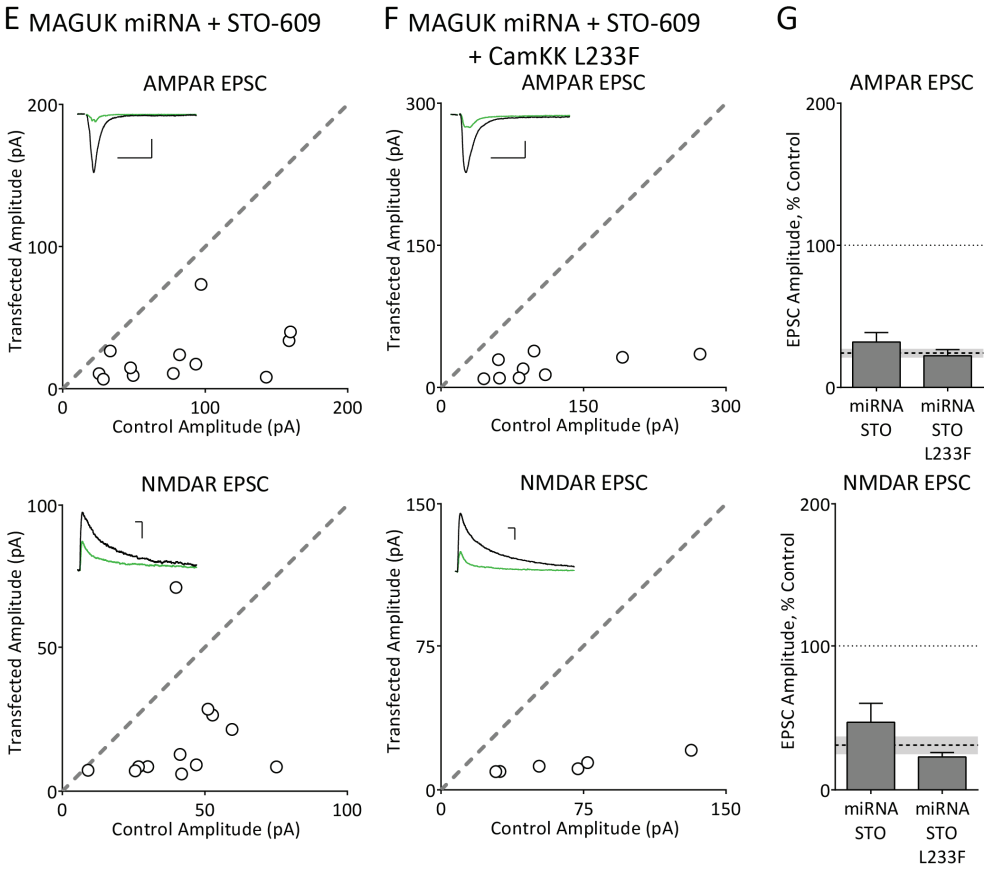
E MAGUK miRNA + STO-609
F MAGUK miRNA + STO-609
+ CamKK L233F
G
AMPAR EPSC
NMDAR EPSC
Transfected Amplitude (pA)
Control Amplitude (pA)
EPSC Amplitude, % Control
miRNA STO
miRNA STO L233F

Figure 11: GluA2 AMPAR subunit is required for synaptic consolidation. (A-B) Coefficient of variation analysis of simultaneously recorded pairs of control/miRNA neurons in GluA2$^{-/-}$ slices. The decrease in AMPAR EPSC is due to reduction in quantal size and quantal content ($p < 0.01$ compared to horizontal line). The decrease in NMDAR EPSC is due to reduction in quantal content. (C) Summary of coefficient of variation analysis. Data from MAGUK miRNA (Figure 5G) are re-plotted to aid comparison. (D-E) Sr^{2+}-evoked aEPSC amplitude and frequency are reduced in neurons from GluA2$^{-/-}$ slices shot with MAGUK miRNA compared to neighboring GluA2$^{-/--}$ neurons ($p<0.05$). (F) Model of synaptic consolidation. MAGUK loss initially causes reductions in number of AMPARs present at individual synapses. Over time, compensatory processes normalize the number of AMPARs present at the few remaining synapses, at the cost of complete loss of other synapses. The glutamate receptors lost from synapses are re-distributed on the plasma membrane at extrasynaptic sites and have been omitted for clarity. The total number of surface-localized receptors remains unchanged.

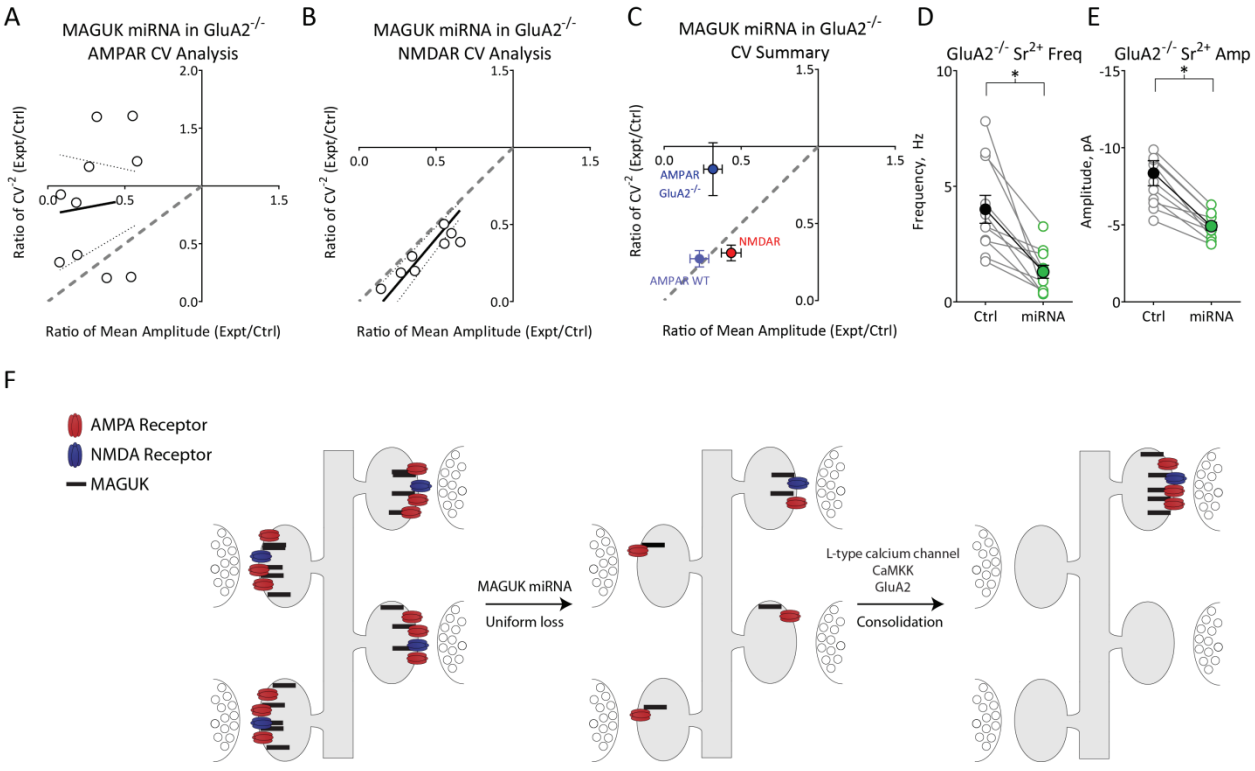
A
MAGUK miRNA in GluA2-/-
AMPAR CV Analysis
Ratio of CV-2 (Expt/Ctrl)
Ratio of Mean Amplitude (Expt/Ctrl)
B
MAGUK miRNA in GluA2-/-
NMDAR CV Analysis
Ratio of CV-2 (Expt/Ctrl)
Ratio of Mean Amplitude (Expt/Ctrl)
C
MAGUK miRNA in GluA2-/-
CV Summary
AMPAR GluA2-/-
NMDAR
AMPAR WT
Ratio of CV-2 (Expt/Ctrl)
Ratio of Mean Amplitude (Expt/Ctrl)
D
GluA2-/- Sr2+ Freq
Frequency, Hz
Ctrl
miRNA
E
GluA2-/- Sr2+ Amp
Amplitude, pA
Ctrl
miRNA

F

AMPA Receptor
NMDA Receptor
MAGUK
MAGUK miRNA
Uniform loss
L-type calcium channel
CaMKK
GluA2
Consolidation

Figure 12: Baseline currents following MAGUK miRNA transfection in GluA2-/- slices. (A) Biolistic transfection of MAGUK miRNA in GluA2$^{-/-}$ slices causes significant reduction in AMPAR and NMDAR EPSC (AMPAR 21.17 ± 3.43%, n = 10; NMDAR 52.32 ± 13.13%, n = 8; $p < 0.05$ for both). (B) AMPAR EPSC reduction due to MAGUK miRNA transfection in GluA2$^{-/-}$ slices is indistinguishable from that seen in wild-type rat slices ($p > 0.05$). Dashed line and shaded area show mean ± SEM of normalized synaptic responses for MAGUK miRNA alone. (C) NMDAR EPSC reduction due to MAGUK miRNA transfection in GluA2$^{-/-}$ slices is indistinguishable from that seen in wild-type mouse slices ($p > 0.05$). Dashed line and shaded area show mean ± SEM of normalized synaptic responses for MAGUK miRNA alone. Scale bars represent 25 pA, 50 ms.

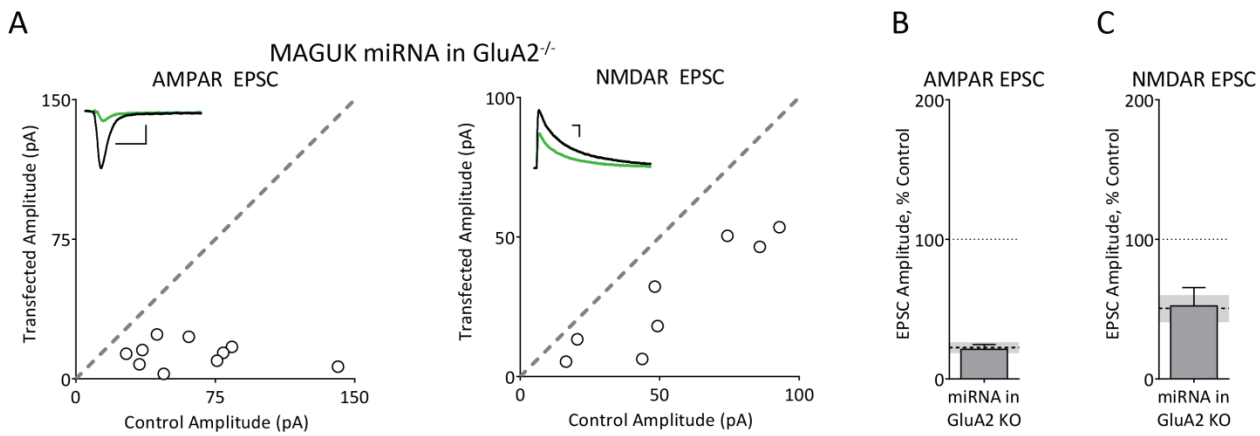
A
MAGUK miRNA in GluA2-/-
AMPAR EPSC
NMDAR EPSC
Transfected Amplitude (pA)
Control Amplitude (pA)
150
75
0
100
50
B
C
EPSC Amplitude, % Control
200
miRNA in
GluA2 KO

CHAPTER 4: Diversity of function within the MAGUK family

Introduction

The enrichment of glutamate receptors at central nervous system synapses is necessary for excitatory neurotransmission. Furthermore, fine control of the location and number of glutamate receptors allows for more complex activity such as information storage. In the mammalian hippocampus, a structure required for formation of new memories, information storage involves synaptic insertion of a particular class of glutamate receptors, called AMPA receptors, which mediate most fast, excitatory neurotransmission in the brain. Insertion of receptors strengthens connections between neurons, which provides for the storage of new information. Although there are many physiological triggers for the increase in synaptic AMPARs, the underlying mechanisms are complex and difficult to isolate, and are not fully understood.

Overexpression of AMPA receptors causes no increase in the number of surface or synaptic AMPARs, meaning the AMPARs themselves play no instructive role in their synaptic trafficking and are not rate-limiting (Kessels et al., 2009). Furthermore, any receptors present in an extrasynaptic surface reserve pool can localize to synapses given the proper stimulus (Granger et al., 2013). In contrast, the family of cytoplasmic scaffolding proteins, the MAGUKs, that bind the AMPARs at synapses appear to play an instructive role. RNAi-mediated knockdown of MAGUKs reduces AMPAR-mediated transmission (Elias et al., 2006), while overexpression of PSD-93, PSD-95, or SAP102, the three members of the MAGUK family, increases it (Elias et al., 2006; Schnell et al., 2002). Together, these results indicate that the number of MAGUKs present at the synapse determines the number of AMPARs.

Although overexpression of any MAGUK family member increases the number of synaptic AMPARs, clear differences between the family members exist. Previous studies in slice culture have focused on differences between PSD-93/PSD-95 and SAP102 (Elias et al., 2008; Schnell et al., 2002). During development, SAP102 is expressed early and is supplanted by PSD-93/PSD-95, the two MAGUKs expressed highly in adult (Elias et al., 2008; Sans et al., 2000). Therefore, differences between juvenile and adult MAGUKs may drive differences in learning rules over development. PSD-93 and PSD-95 are the MAGUKs that play major roles in adulthood, and may each play slightly different roles. Animals lacking functional PSD-95 and therefore expressing only PSD-93 and SAP102 are unable to undergo long-term depression (LTD) by standard procedures (Migaud et al., 1998). In contrast, knockout of PSD-93, isolating synapses containing only PSD-95 and SAP102, has no effect on LTD (Carlisle et al., 2008), suggesting that the two MAGUKs may play different roles during plasticity – AMPARs anchored by PSD-95 may be removed from the synapse, while AMPARs connected to PSD-93 may not.

We were interested in determining whether PSD-93 and PSD-95 might exhibit differential function with regard to baseline AMPAR synaptic localization and homeostatic plasticity. To determine whether PSD-93 and PSD-95 play functionally distinct roles, we co-expressed PSD-93 or PSD-95 with the MAGUK miRNA, preventing heterodimerization between endogenous and recombinant MAGUKs. We find that PSD-95 can localize synaptic AMPARs in the presence or absence of endogenous MAGUKs, but PSD-93 requires endogenous MAGUKs to localize glutamate receptors to synapses. This difference in function is conferred by the extreme N-terminal of the MAGUK; swapping the PSD-93 and PSD-95 N-terminal domains enables PSD-93 to localize glutamate receptors to synapses and prevents PSD-95 from doing so.

These results suggest that a balance of PSD-93 and PSD-95 may influence synaptic glutamate receptor localization. In agreement with this line of thinking, we find that although overexpression of PSD-95 increases synaptic AMPAR EPSCs regardless of activity state, PSD-93 overexpression in the presence of gabazine does not increase synaptic AMPAR localization, indicating PSD-93 but not PSD-95 is sensitive to the homeostatic scaling machinery in this context.

Results

PSD-93 requires interaction with endogenous MAGUKs for function

We set out to first determine the extent of heterogeneity within the MAGUK family in the MAGUK overexpression model of potentiation. To do this, we overexpressed PSD-93 and PSD-95, finding that overexpression of PSD-95 (Figure 13A) or PSD-93 (Figure 13B) both selectively increase AMPAR EPSCs with no change in NMDAR EPSCs, in agreement with previous results (Elias et al., 2006). These overexpression results, however, are complicated by possible heterodimerization within the MAGUK family (Kim et al., 1996). To remove the caveat of heterodimerization and isolate the function of the overexpressed protein, we next knocked down the endogenous synaptic MAGUKs, SAP102, PSD-93, and PSD-95, using the MAGUK miRNA (Figure 1), while overexpressing either PSD-93 or PSD-95. PSD-95 overexpression on the MAGUK miRNA background increased AMPAR EPSCs to the same degree as overexpression alone, and additionally caused a non-significant increase in NMDAR EPSCs (Figure 13C, 13E). Interestingly, when co-expressed with the MAGUK miRNA, PSD-93 did not increase AMPAR or NMDAR EPSCs (Figure 13D, 13F), although it is able to counteract the decrease induced by the MAGUK miRNA and return EPSCs to baseline.

These results demonstrate an interesting difference between PSD-93 and PSD-95 – namely a PSD-93 dependence on endogenous MAGUKs. Although the finding that recombinant PSD-93 requires endogenous MAGUKs is interesting, it is critical to determine whether the endogenous PSD-93 has the same requirement. To test these results with endogenous protein, we simultaneously knocked down either PSD-93 and SAP102 (Figure 14A) or PSD-95 and SAP102 (Figure 14B), and compared them to the simultaneous knockdown of all three MAGUKs. We find that knockdown of PSD-95 and SAP102 does not differ significantly from removal of all three MAGUKs, suggesting the remaining PSD-93 plays little role (Figure 14C). Importantly, knockdown of PSD-93 alone results in an AMPAR EPSC decrease of roughly 50%, equivalent to that caused by PSD-95 knockdown (Figure 14C), demonstrating that endogenous PSD-93 and PSD-95 play equal roles in these neurons, and that we are not simply manipulating a protein with no endogenous function.

Loss of endogenous MAGUKs hampers regulation of synaptic strength

The AMPAR EPSC increase caused by PSD-95 overexpression has been reported to act primarily through an increase in the number of synapses containing AMPARs. We carried out CV analysis and find that in agreement with previous data, PSD-95 overexpression increases quantal content (Figure 15A). These findings have been interpreted previously as an unsilencing of synapses, since AMPAR-containing synapses increase with no change in spine number of NMDAR-containing synapses. Importantly, these findings suggest that a regulatory mechanism blunts addition of AMPARs to existing synapses, as although PSD-95 overexpression induces a small increase in mEPSC amplitude, the majority of the increase is in mEPSC frequency (El-Husseini et al., 2000; Stein et al., 2003), indicating that widespread addition of AMPARs to all synapses does not occur. This regulation is reminiscent of the tight control over the number of

NMDARs at synapses. Although many manipulations, including LTP and manipulation of the MAGUKs, are able to change the number of AMPARs at synapses, it is difficult to change the number of NMDARs, suggesting active control. Although PSD-95 overexpression, with or without the MAGUK miRNA caused AMPAR EPSC increases that appeared identical in magnitude, suggesting that control of AMPAR quantal size might remain intact, we were intrigued by the increase in NMDAR EPSC following expression of PSD-95 and the MAGUK miRNA (Figure 13C), which suggested that knockdown of the MAGUKs may have destroyed the tight control of receptors per synapse that is normally present.

To determine whether transient loss of the MAGUKs might allow increases in AMPAR quantal size, we performed CV analysis on neurons co-expressing PSD-95 and the MAGUK miRNA. We find that in contrast to overexpression of PSD-95, which results in primarily an increase in quantal content, co-expression of PSD-95 with the MAGUK miRNA causes an increase in quantal size with no appreciable change in quantal content (Figure 15B). These results suggest that on a background lacking endogenous MAGUKs, PSD-95 overexpression, rather than increasing the number of AMPAR-containing synapses, brings more AMPARs to existing synapses.

Since overexpression of PSD-95 with knockdown of all three MAGUKs results in a quantal size increase, we were next interested in whether a single member of the MAGUK family was responsible for regulating quantal size. We therefore overexpressed PSD-95 and knocked down either SAP102, or PSD-93 and PSD-95, with the goal of determining whether knockdown of these proteins recapitulated the PSD-95 + MAGUK miRNA effect, an increase in quantal size. We find that both manipulations resulted in an increase in quantal content similar to overexpression of PSD-95 alone (Figure 15C-15D), indicating that no single MAGUK is

responsible for quantal size regulation. Instead, it is possible either that quantal size is maintained by redundant interactions between a sensor and multiple MAGUKs, or by a general property of the PSD that is only disrupted through loss of all MAGUKs.

Overexpression of PSD-93, like PSD-95, causes an increase in quantal content (Figure 15E). Although PSD-93 co-expression with the MAGUK miRNA does not cause, on average, an increase in AMPAR EPSC, we can split the dataset into two groups: individual neurons with AMPAR EPSCs that are larger than controls, and those with smaller AMPAR EPSCs. Looking only at neurons with larger AMPAR EPSCs to determine the basis of this increase, we find an increase in quantal size (Figure 15G). In contrast, CV analysis shows that neurons exhibiting a decrease in AMPAR EPSC compared to a neighboring control have a reduction in quantal size, in line with data suggesting that synaptic strength is conserved following MAGUK loss (Figure 5).

Since synaptic strength is not correctly regulated following MAGUK knockdown and overexpression of PSD-93 or PSD-95, we were next interested if dendritic spine density might also be dysregulated. We performed confocal imaging of dendritic spines to determine whether MAGUK knockdown, or co-expression of PSD-93/PSD-95, might change spine density. We find that co-expression of PSD-95 and the MAGUK miRNA reduces spine density by approximately 50%, indicating that dysregulation of synaptic strength is coupled to spine loss (Figure 16B). These data suggest that PSD-95 overexpression in the absence of other MAGUKs increases quantal size and causes loss of a subset of spines. Co-expression of PSD-93 and MAGUK miRNA, which has little increase in AMPAR EPSCs, does not cause spine loss, suggesting loss of spines could be a homeostatic process triggered by increased spiking downstream of increased AMPAR EPSCs (Goold and Nicoll, 2010). We therefore incubated transfected neurons with

NBQX to block activity, finding that incubation of neurons with NBQX prevents the loss of spines (Figure 16B), consistent with a homeostatic process. It is also possible that an activity-dependent competitive process induced by the abundance of PSD-95 destabilizes synapses and allows an increase AMPAR quantal size at the cost of loss of a subset of spines,

PSD-93 interacts with all endogenous MAGUKs

Since no specific MAGUK is required for synapse stabilization and control of quantal size, we next wanted to determine whether any specific MAGUK is required for PSD-93 to enhance AMPAR EPSCs. We find that, in agreement with the data from the knockdown experiments (Figure 15), PSD-93 overexpression plus knockdown of any single MAGUK family member increases AMPAR EPSCs similarly to overexpression of PSD-93 alone (Figure 17). Additionally, double knockdown of PSD-93 and SAP102 does not prevent the AMPAR EPSC increase. Only removal of PSD-95 and SAP102 is able to block the AMPAR EPSC enhancement mediated by PSD-93 overexpression, although there is a small increase, potentially due to incomplete knockdown of PSD-95/SAP102 by RNAi. These results were somewhat surprising to us, since PSD-93 has been linked directly to PSD-95 via heterodimerization (Kim et al., 1996), but not to SAP102. To more rigorously test the hypothesis that PSD-93 relies only on PSD-95, we overexpressed PSD-93 in the PSD-95 knockout mouse, finding that PSD-93 potentiation of AMPAR EPSCs is identical in the presence or absence of PSD-95 (Figure 18).

These results suggest that PSD-93 requires either PSD-95 or SAP102 for full function. No direct interaction between PSD-93 and SAP102 has been proposed, suggesting that the PSD-93 requirement for other MAGUKs might be not due to direct interaction such as heterodimerization, but due to a general functional difference between PSD-93 and the rest of the

MAGUK family. PSD-93 homomers may efficiently localize AMPARs to synapses only under specific conditions.

N-terminal of PSD-95 mediates differential function

We were next interested in the structural basis for the functional differences between PSD-93 and PSD-95. We therefore co-expressed chimeric PSD-93 and PSD-95 proteins with the MAGUK miRNA to determine which sequences of PSD-95 might be sufficient to mediate its ability to enhance AMPAR EPSCs. Through a series of chimeric proteins, we isolated the minimal region responsible for enhancement of AMPAR EPSCs (Figure 19). Surprisingly, this region was not in the PDZ domains, but in the N-terminal of the protein. Replacement of the first 31 amino acids of PSD-95 with those from PSD-93, plus an insertion present only in PSD-93, was sufficient to block the enhancement of AMPAR EPSCs following co-expression of PSD-95Δ(1-31) with the MAGUK miRNA (Figure 19A). Similarly, replacement of the first 29 amino acids of PSD-93 with those from PSD-95 was sufficient to rescue the enhancement of AMPAR EPSCs, meaning co-expression of PSD-93Δ(1-29) and the MAGUK miRNA enhanced AMPAR EPSCs to the same degree as overexpression of PSD-93 (Figure 19B). There are several motifs present in the N-terminal that vary between PSD-93 and PSD-95: the palmitoylated cysteines, the PEST motif, and the unknown insertion between amino acids 29 and 30 in PSD-93. It is not clear whether these motifs, or an uncharacterized region in the N-terminal that differs between PSD-93 and PSD-95, might underlie this striking difference.

Discussion

We find that PSD-93 and PSD-95 have several functional differences. First, recombinant PSD-93 relies on endogenous MAGUKs to localize AMPARs, a finding supported by the data

that additional knockdown of PSD-93 on a PSD-95/SAP102 knockdown background has little effect. In contrast, recombinant PSD-95 is capable of localizing AMPARs in the absence of endogenous MAGUKs. We find that the endogenous MAGUKs play equal roles in supporting recombinant PSD-93. This ability is mediated by the N-terminal of PSD-95, which is necessary for PSD-95 to localize AMPARs in the absence of endogenous MAGUKs, and is sufficient to transfer this ability to PSD-93. An additional area of functional difference is the interaction of MAGUKs with homeostatic mechanisms – the increase in AMPAR EPSCs caused by PSD-93 overexpression is blocked by homeostatic mechanisms induced by increased activity, while the AMPAR EPSC increase caused by PSD-95 overexpression is not. Finally, we find that the endogenous MAGUKs are critical for regulating quantal size. Removal of endogenous MAGUKs allows further MAGUK overexpression to increase quantal size, whereas MAGUK overexpression in the presence of endogenous MAGUKs has little effect on quantal size. This increase in quantal size can lead to activity-dependent spine loss, potentially by a homeostatic mechanism.

Synapse stability mediated by endogenous MAGUKs

We demonstrate a pure increase in quantal size following MAGUK overexpression and knockdown of endogenous MAGUKs. This quantal size increase stands in contrast to the increase in quantal content induced by MAGUK overexpression alone. These data suggest that endogenous MAGUKs play a synapse-specific role controlling quantal size, meaning that an intact scaffold of endogenous MAGUKs prevents rapid changes in quantal size at individual synapses. These data are in agreement with two-photon imaging data demonstrating that during glutamate uncaging-induced potentiation, the existing PSD-95 scaffold is destabilized and transiently lost. PSD-95 mutations that block this transient loss inhibit uncaging induced

potentiation (Steiner et al., 2008). Therefore, one model for synaptic plasticity would be that MAGUKs, or proteins bound to them, encode a synapse-specific quantal size set point. Further research is required to determine this signal, but one intriguing possibility is that the size of the PSD determines the number of AMPARs at the synapse, in line with electron microscopy data demonstrating PSD size and AMPAR number are highly correlated (Takumi et al., 1999).

Figure 13: PSD-93 requires interactions endogenous MAGUKs to increase AMPAR EPSCs. (A) PSD-95 overexpression increases AMPAR EPSCs but not NMDAR EPSCs compared to untransfected controls (AMPAR, 348.37 ± 43.85% control, $p < 0.01$, $n = 9$; NMDAR 100.56 ± 13.39% control, $p > 0.05$, $n = 7$). (B) PSD-93 overexpression increases AMPAR EPSCs but not NMDAR EPSCs compared to untransfected controls (AMPAR, 191.85 ± 27.69% control, $p < 0.01$, $n = 19$; NMDAR 94.40 ± 16.80% control, $p > 0.05$, $n = 16$). (C) PSD-95 co-expression with MAGUK miRNA enhances AMPAR but not NMDAR EPSCs. (AMPAR, 446.45 ± 84.61% control, $p < 0.01$, $n = 14$; NMDAR 154.16 ± 26.42% control, $p > 0.05$, $n = 13$) (D) PSD-93 co-expression with MAGUK miRNA does not enhance AMPAR or NMDAR EPSCs. (AMPAR, 112.18 ± 17.43% control, $p > 0.05$, $n = 25$; NMDAR 94.40 ± 16.80% control, $p < 0.05$, $n = 23$) (E) PSD-95 overexpression is identical with or without endogenous MAGUKs. (PSD-95 OE vs. PSD-95 OE + MAGUK miRNA; AMPAR $p > 0.05$; NMDAR $p > 0.05$) (F) PSD-93 overexpression causes significantly increased AMPAR EPSCs in the presence of endogenous MAGUKs (PSD-93 OE vs. PSD-93 OE + MAGUK miRNA; AMPAR $p < 0.05$; NMDAR $p > 0.05$).

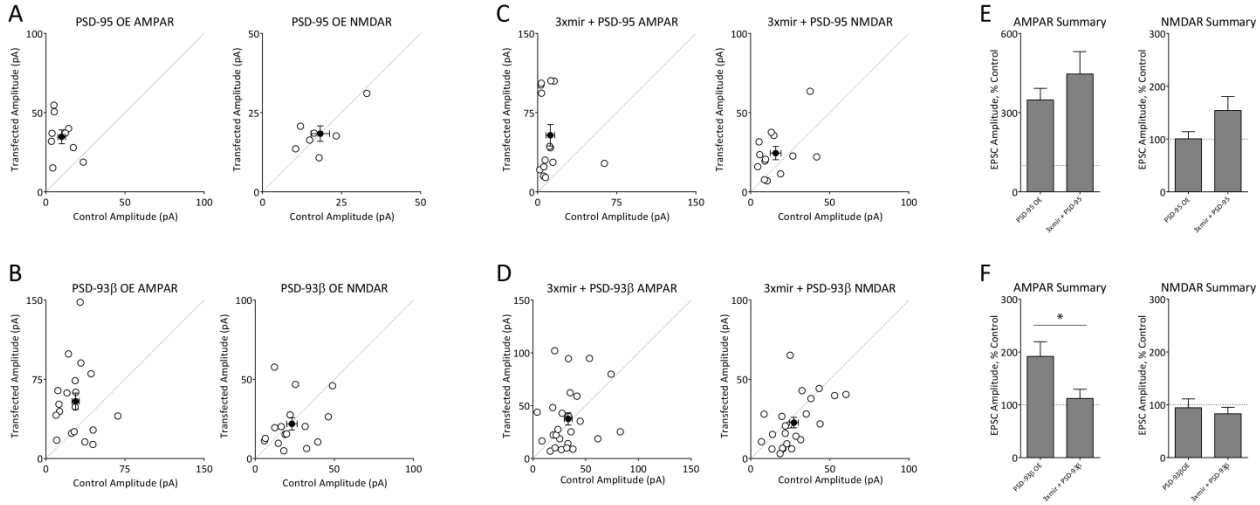
A
PSD-95 OE AMPAR
PSD-95 OE NMDAR
B
PSD-93β OE AMPAR
PSD-93β OE NMDAR
C
3xmir + PSD-95 AMPAR
3xmir + PSD-95 NMDAR
D
3xmir + PSD-93β AMPAR
3xmir + PSD-93β NMDAR
E
AMPAR Summary
NMDAR Summary
F
AMPAR Summary
NMDAR Summary
Transfected Amplitude (pA)
Control Amplitude (pA)
EPSC Amplitude, % Control
*

Figure 14: Endogenous PSD-93 plays no role in the absence of PSD-95 and SAP102. (A) Simultaneous knockdown of PSD-93 and SAP102 reduces AMPAR and NMDAR EPSCs. (AMPAR 61.39 ± 10.45% control, $p < 0.05$, $n = 18$; NMDAR, 63.84 ± 8.90% control, $p < 0.05$, $n = 15$) (B) Simultaneous knockdown of PSD-95 and SAP102 reduces AMPAR and NMDAR EPSCs. (AMPAR 22.49 ± 3.62% control, $p < 0.001$, $n = 19$; NMDAR, 29.59 ± 5.20% control, $p < 0.001$, $n = 15$) (C) PSD-95/SAP102 knockdown is identical to knockdown of PSD-93/PSD-95/SAP102. (AMPAR 22.49 ± 3.62% vs. 20.64 ± 3.82%, $p > 0.05$; NMDAR 29.59 ± 5.20% vs. 19.29 ± 4.33%, $p > 0.05$). PSD-93/SAP102 knockdown is significantly different from PSD-93/PSD-95/SAP102 knockdown. (AMPAR 61.39 ± 10.45% vs. 20.64 ± 3.82%, $p < 0.001$; NMDAR 63.84 ±8.89% vs. 19.29 ± 4.33%, $p < 0.001$). Data for PSD-93, PSD-95, and PSD-93/PSD-95/SAP102 knockdown re-plotted from Figure 3 for ease of comparison.

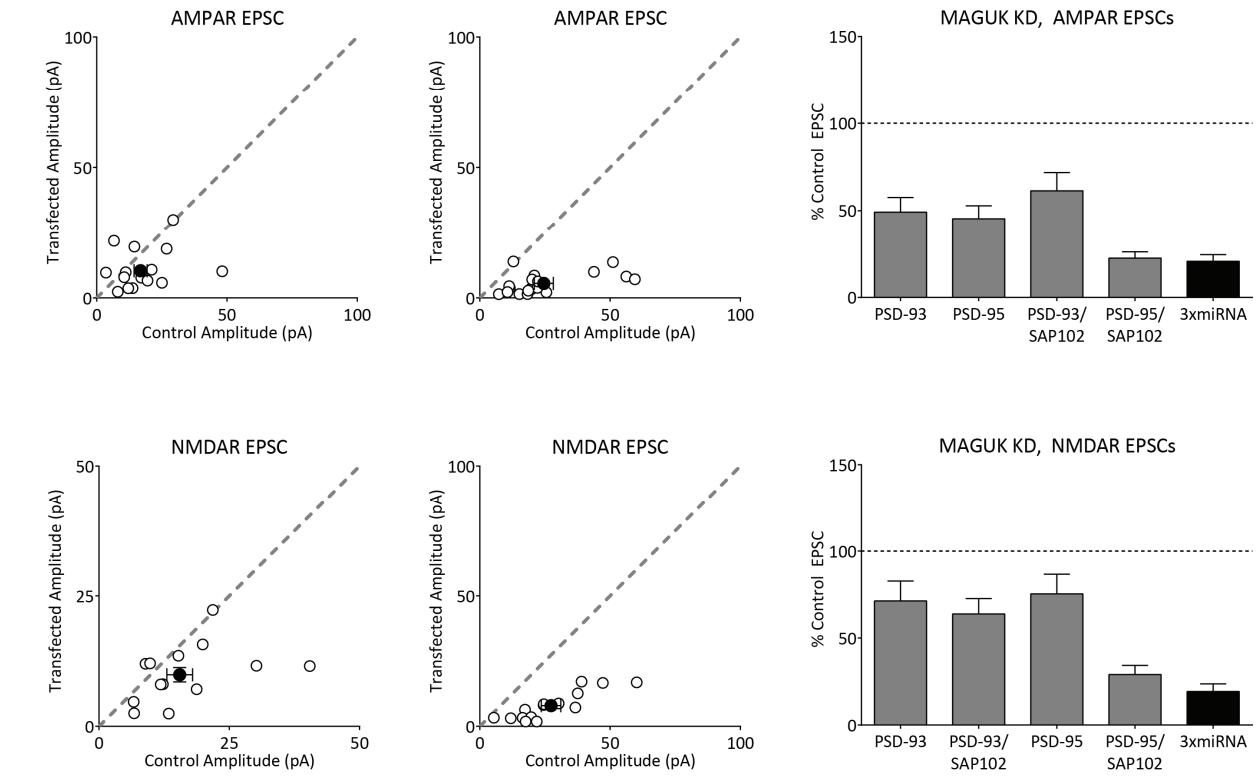
A PSD-93/SAP102
B PSD-95/SAP102
C
AMPAR EPSC
Transfected Amplitude (pA)
Control Amplitude (pA)
MAGUK KD, AMPAR EPSCs
% Control EPSC
PSD-93
PSD-95
PSD-93/ SAP102
PSD-95/ SAP102
3xmiRNA
NMDAR EPSC
MAGUK KD, NMDAR EPSCs

Figure 15: Loss of endogenous MAGUKs results in quantal size increases following MAGUK overexpression. (A) CV Analysis of PSD-95 overexpression indicates increase in AMPAR EPSCs is due primarily to an increase in quantal content. (B) (A) CV Analysis of PSD-95 overexpression plus MAGUK miRNA indicates increase in AMPAR EPSCs is due primarily to an increase in quantal size. (C) CV Analysis of PSD-95 overexpression plus PSD-93/PSD-95 miRNA indicates increase in AMPAR EPSCs is due primarily to an increase in quantal content. (D) CV Analysis of PSD-95 overexpression plus SAP102 miRNA indicates increase in AMPAR EPSCs is due primarily to an increase in quantal content. (E) CV Analysis of PSD-93 overexpression indicates increase in AMPAR EPSCs is due primarily to an increase in quantal content. (F) PSD-93 overexpression plus MAGUK miRNA shows no change in average AMPAR EPSC. (G) CV analysis of neurons overexpressing PSD-93 plus MAGUK miRNA with increased AMPAR EPSCs shows increase is due to increased quantal size. (H) CV analysis of neurons overexpressing PSD-93 plus MAGUK miRNA with decreased AMPAR EPSCs shows decrease is due to reduction in quantal content.

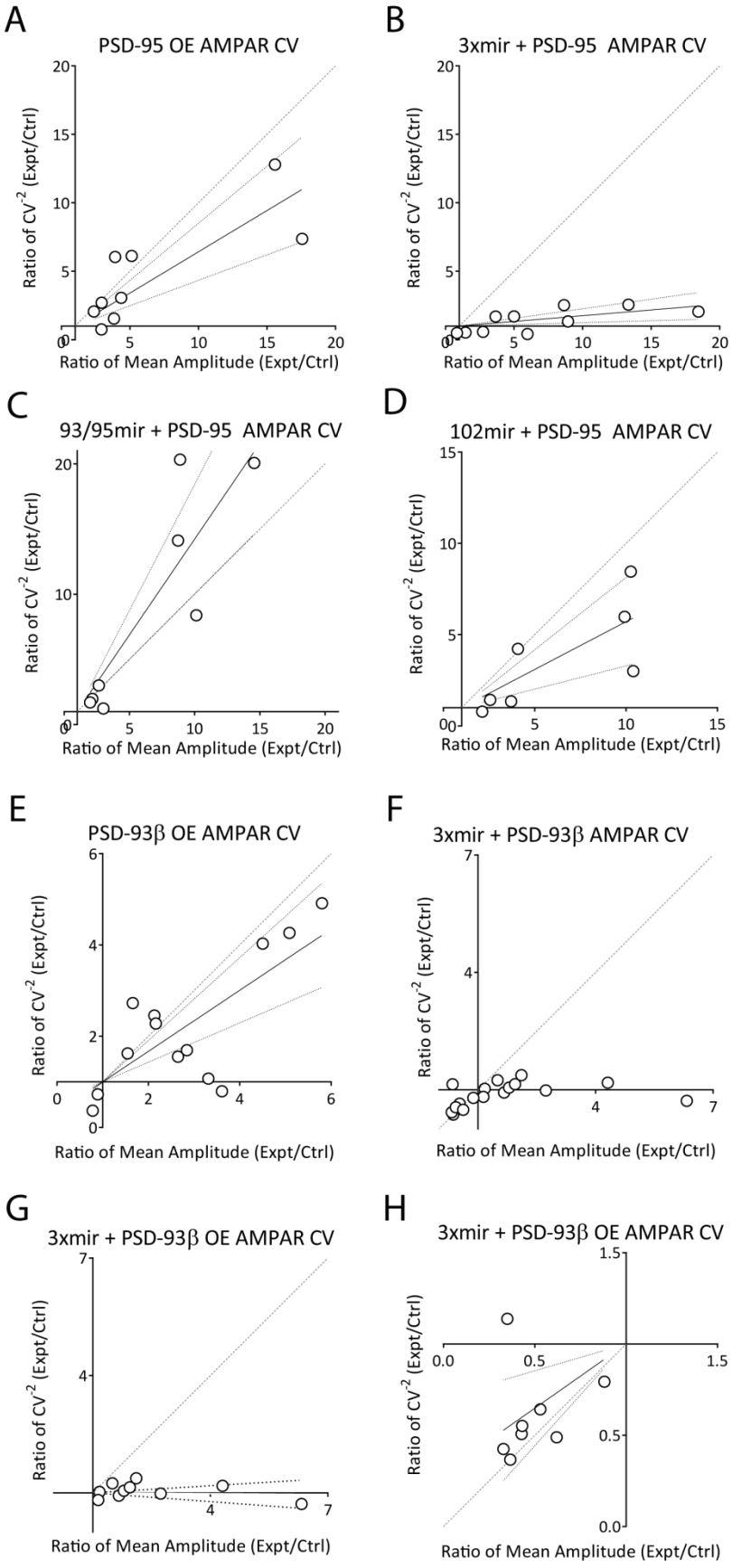
A
PSD-95 OE AMPAR CV
Ratio of CV-2 (Expt/Ctrl)
Ratio of Mean Amplitude (Expt/Ctrl)
B
3xmir + PSD-95 AMPAR CV
Ratio of CV-2 (Expt/Ctrl)
Ratio of Mean Amplitude (Expt/Ctrl)
C
93/95mir + PSD-95 AMPAR CV
Ratio of CV-2 (Expt/Ctrl)
Ratio of Mean Amplitude (Expt/Ctrl)
D
102mir + PSD-95 AMPAR CV
Ratio of CV-2 (Expt/Ctrl)
Ratio of Mean Amplitude (Expt/Ctrl)
E
PSD-93β OE AMPAR CV
Ratio of CV-2 (Expt/Ctrl)
Ratio of Mean Amplitude (Expt/Ctrl)
F
3xmir + PSD-93β AMPAR CV
Ratio of CV-2 (Expt/Ctrl)
Ratio of Mean Amplitude (Expt/Ctrl)
G
3xmir + PSD-93β OE AMPAR CV
Ratio of CV-2 (Expt/Ctrl)
Ratio of Mean Amplitude (Expt/Ctrl)
H
3xmir + PSD-93β OE AMPAR CV
Ratio of CV-2 (Expt/Ctrl)
Ratio of Mean Amplitude (Expt/Ctrl)

Figure 16: Synapse destabilization leads to spine loss. (A) Sample confocal images of dendrites. Slices were transfected for 6 days before imaging. See Methods for complete description of data collection and analysis protocol. (B) Co-expression of MAGUK miRNA + PSD-95, but not MAGUK miRNA + PSD-93, reduces spine density. This reduction in spine density is activity-dependent and is blocked by incubation with NBQX.

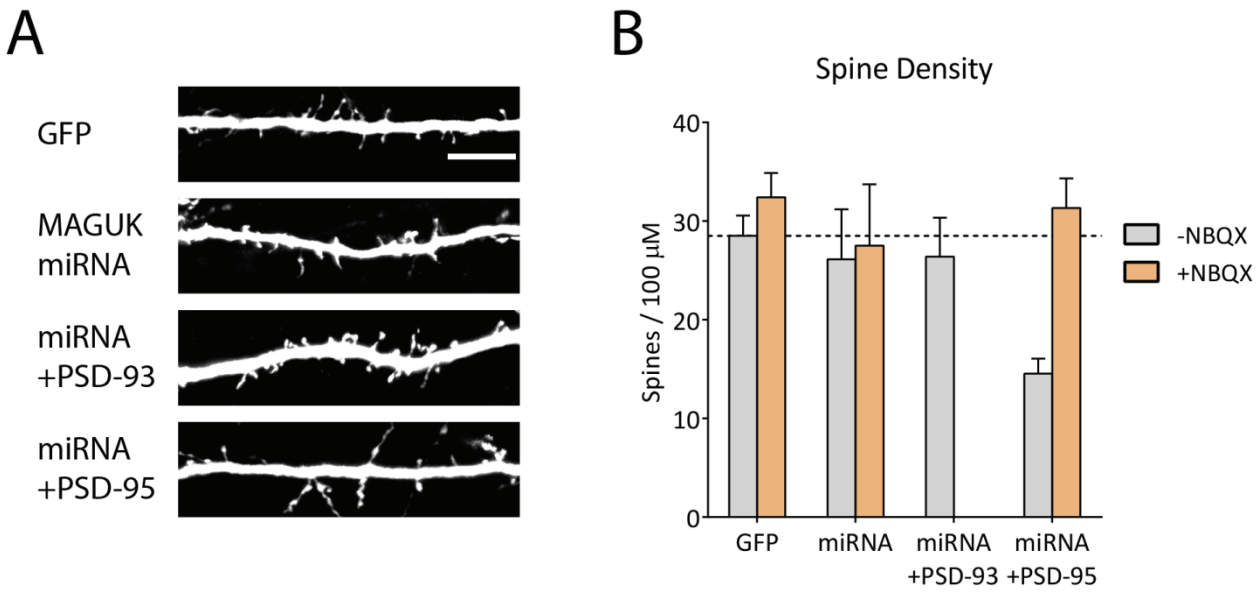
A
GFP
MAGUK
miRNA
miRNA
+PSD-93
miRNA
+PSD-95
B
Spine Density
Spines / 100 µM
40
30
20
10
0
GFP
miRNA
miRNA
+PSD-93
miRNA
+PSD-95
-NBQX
+NBQX

Figure 17: PSD-93 interacts with endogenous PSD-95 and SAP102. (A) PSD-93 overexpression with PSD-95 miRNA increases AMPAR EPSCs (181.85 ± 34.05 % control, $p < 0.01$, $n = 12$). (B) PSD-93 overexpression with SAP102 miRNA increases AMPAR EPSCs (179.23± 30.41% control, $p < 0.05$, $n = 17$). (C) PSD-93 overexpression with PSD-95/SAP102 miRNA does not increase AMPAR EPSCs (109.33 ± 39.47% control, $p > 0.05$, $n = 8$). (D) Summary plot of PSD-93 overexpression with miRNA targeting MAGUKs. No single MAGUK mediates increase in AMPAR EPSCs after PSD-93 overexpression. Knockdown of PSD-95 and SAP102 is required to prevent increase in AMPAR EPSCs.

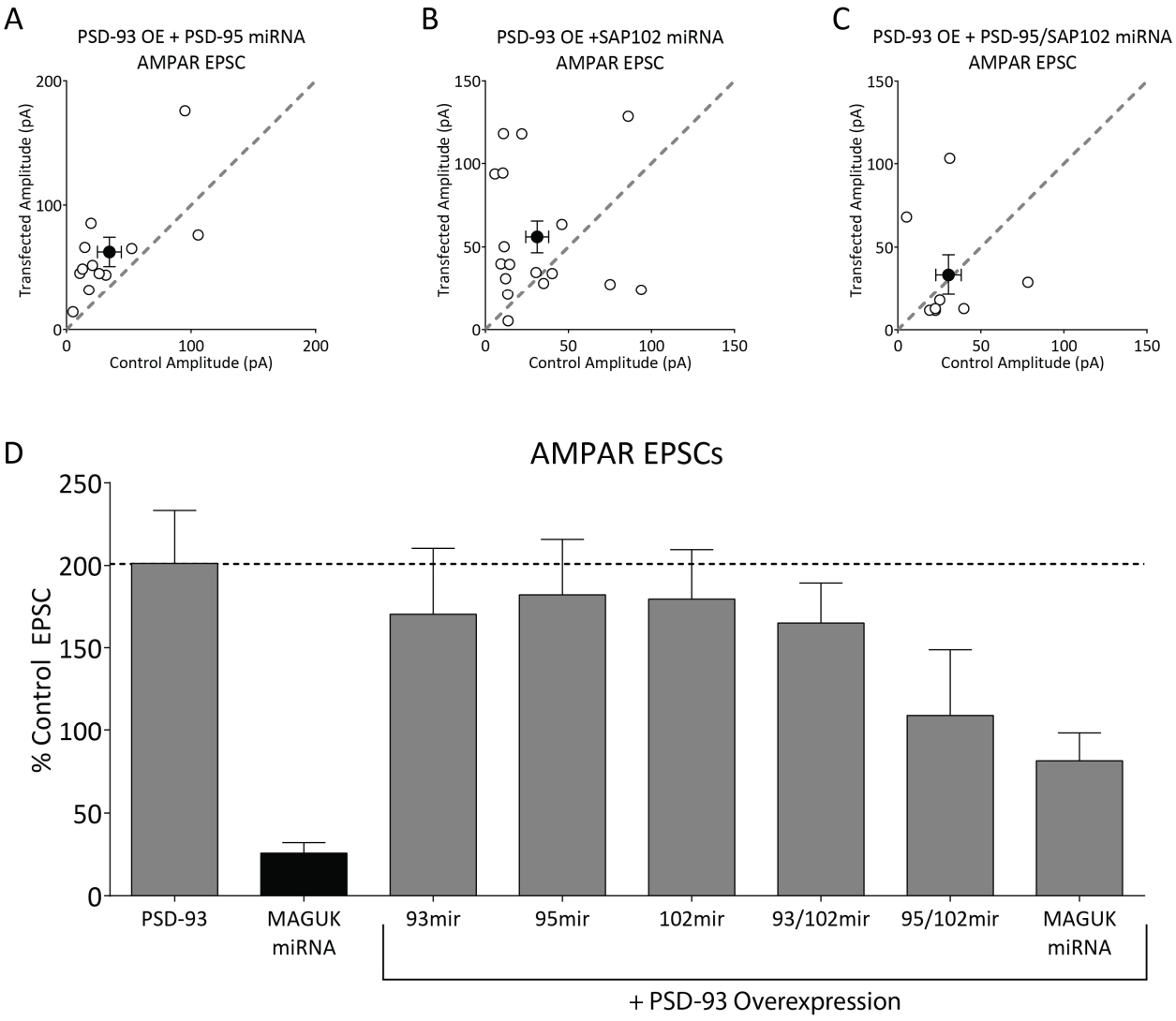
A
PSD-93 OE + PSD-95 miRNA
AMPAR EPSC
Transfected Amplitude (pA)
Control Amplitude (pA)
B
PSD-93 OE +SAP102 miRNA
AMPAR EPSC
Transfected Amplitude (pA)
Control Amplitude (pA)
C
PSD-93 OE + PSD-95/SAP102 miRNA
AMPAR EPSC
Transfected Amplitude (pA)
Control Amplitude (pA)
D
AMPAR EPSCs
% Control EPSC
PSD-93
MAGUK miRNA
93mir
95mir
102mir
93/102mir
95/102mir
MAGUK miRNA
+ PSD-93 Overexpression

Figure 18: PSD-93 Overexpression increases AMPAR EPSCs in PSD-95 KO. (A) PSD-93 overexpression in slices from the PSD-95 KO mouse increases AMPAR EPSCs (184.34 ± 22.85% control, $p < 0.01$, $n = 10$). (B) PSD-93 overexpression in slices from the PSD-95 KO mouse does not change NMDAR EPSCs (101.37 ± 13.45% control, $p > 0.05$, $n = 10$). (C-D) No difference between AMPAR of NMDAR EPSCs after PSD-93 overexpression in wild-type rat slices vs. PSD-95 KO mouse slices ($p > 0.05$, rat vs. mouse).

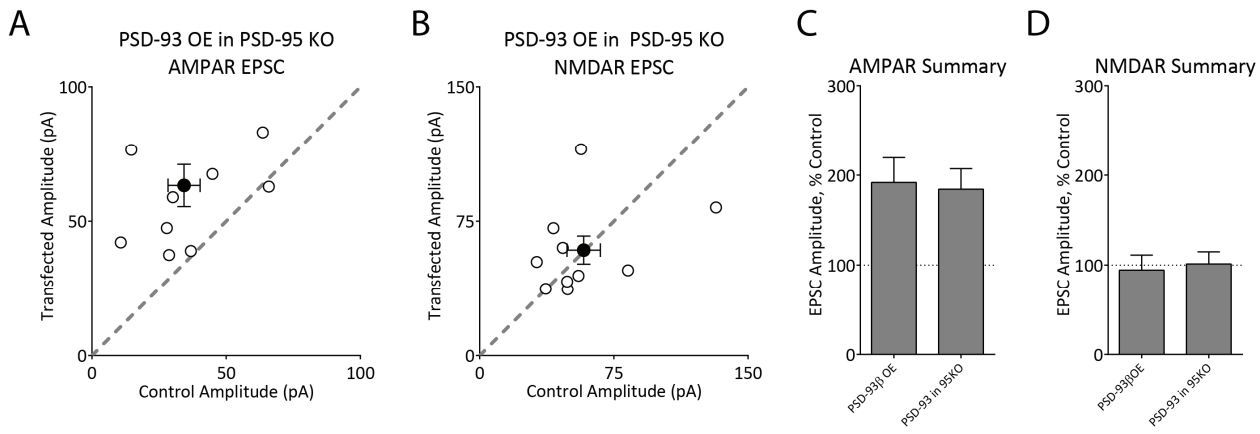
A
PSD-93 OE in PSD-95 KO
AMPAR EPSC
Transfected Amplitude (pA)
Control Amplitude (pA)
0
50
100
B
PSD-93 OE in PSD-95 KO
NMDAR EPSC
Transfected Amplitude (pA)
Control Amplitude (pA)
0
75
150
C
AMPAR Summary
EPSC Amplitude, % Control
0
100
200
300
PSD-93β OE
PSD-93 in 95KO
D
NMDAR Summary
EPSC Amplitude, % Control
0
100
200
300
PSD-93β OE
PSD-93 in 95KO

Figure 19: MAGUK N-terminal underlies differential function. (A) Co-expression of PSD-95Δ(1-31) with MAGUK miRNA does not increase AMPAR EPSCs. (AMPAR 110.67 ± 38.24% control, $p > 0.05$, $n = 8$; NMDAR 89.74 ± 34.38% control, $p > 0.05$, $n = 10$). (B) Co-expression of PSD-93Δ(1-29) increases AMPAR EPSCs. (AMPAR 194.38 ± 49.86% control, $p < 0.05$, $n = 14$; NMDAR 122.26 ± 20.02% control, $p > 0.05$, $n = 14$). (C) Schematic of critical N-terminal swaps, PSD-95 in red, PSD-93 in blue. (D) Sequence of PSD-93 and PSD-95 N-terminal. Known interactions are labeled: palmitoylated cysteines, ubiquitinated PEST domain, small insertion of unknown function and homology in PSD-93. (E) PSD-93Δ(1-29) plus MAGUK miRNA increases AMPAR EPSC indistinguishably from overexpression of full-length PSD-93. (F) PSD-95Δ(1-31) does not increase AMPAR EPSCs when co-expressed with the MAGUK miRNA, similarly to PSD-95 and in contrast to overexpression of full length PSD-95.

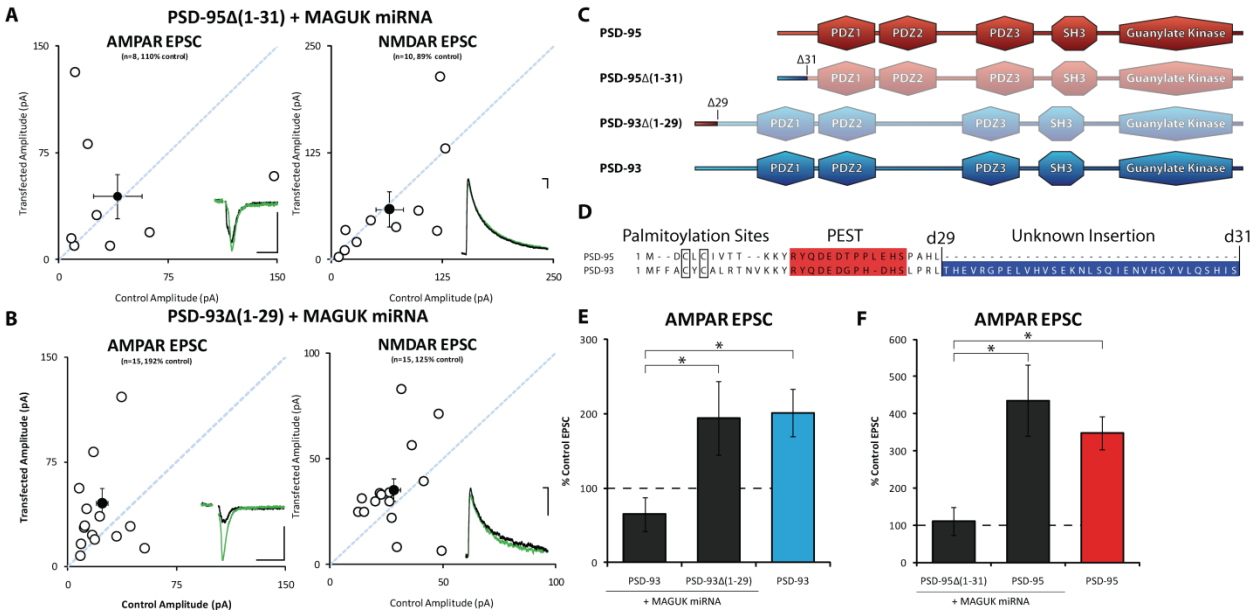
A
PSD-95Δ(1-31) + MAGUK miRNA
AMPAR EPSC
(n=8, 110% control)
NMDAR EPSC
(n=10, 89% control)
Transfected Amplitude (pA)
Control Amplitude (pA)
B
PSD-93Δ(1-29) + MAGUK miRNA
AMPAR EPSC
(n=15, 192% control)
NMDAR EPSC
(n=15, 125% control)
C
PSD-95
PSD-95Δ(1-31)
PSD-93Δ(1-29)
PSD-93
Δ31
Δ29
PDZ1
PDZ2
PDZ3
SH3
Guanylate Kinase
D
Palmitoylation Sites
PEST
d29
Unknown Insertion
d31
PSD-95
PSD-93
E
AMPAR EPSC
% Control EPSC
PSD-93
PSD-93Δ(1-29)
PSD-93
+ MAGUK miRNA
F
AMPAR EPSC
% Control EPSC
PSD-95Δ(1-31)
PSD-95
PSD-95
+ MAGUK miRNA

CHAPTER 5: A developmentally-constrained synaptogenic role for MAGUKs

Introduction

Formation and maintenance of glutamatergic synapses in the central nervous system is critical for proper information processing by the brain. Proper formation of the post-synaptic side of the synapse requires two mechanistically distinct, sequential processes: First, the creation of the anatomical foundation of a mature excitatory chemical synapse by spine formation and trans-synaptic cell adhesion contacts, and second, the filling of the nascent spine with glutamate receptors and their associated signaling and scaffolding proteins. These processes are generally thought to utilize the same underlying mechanisms as synapse maintenance, in that the same proteins – neuroligins, MAGUKs, CaMKII – have been implicated in both processes and are present at both nascent and mature synapses. The major family of cytoplasmic scaffolding proteins implicated in both synaptic formation and maintenance is the membrane-associated guanylyl kinase (MAGUK) family, consisting of three functional members: PSD-93, PSD-95, and SAP102.

The MAGUKs are cytoplasmic synaptic scaffolding molecules which are highly expressed in the hippocampus beginning at the time of early excitatory synaptogenesis. Their central position at the PSD and high abundance as a fraction of total PSD protein naturally led to the suggestion that they are a necessary part of an organized post-synaptic density. SAP102 is expressed by the second postnatal day (Sans et al., 2000), while PSD-93 and PSD-95 are expressed soon after, by the second postnatal week (Elias et al., 2008; Sans et al., 2000). Germline removal of both PSD-93 and PSD-95 causes a reduction in animal weight and decrease in hippocampal AMPAR transmission by three to five weeks after birth, indicating that these proteins are necessary for proper development early in the animal's life. Similarly, RNAi-mediated knockdown of SAP102 early in development by *in utero* electroporation causes

reductions in both AMPAR and NMDAR transmission, indicating its importance in correct synaptic assembly early. Interestingly, SAP102, though it appears fully redundant once PSD-93 and PSD-95 are expressed, remains expressed in the brain at high levels. Manipulation of the MAGUKs in organotypic slice cultures, a reduced system, has shown that they play a critical role mediating AMPAR and NMDAR transmission at excitatory synapses in a manner that suggests they are a key molecule involved at the developing synapse in a synaptogenic manner. Much less is known, however, about whether the phenotype in the germline knockout is dependent on synaptogenesis, which would primarily occur early in development, or synaptic maintenance, which would occur later in development.

The previous results from the PSD-93/PSD-95 double KO suggest that the MAGUKs play a key role in the hippocampus during development and adulthood. Furthermore, numerous studies in immature and reduced systems have implicated the MAGUKs as critical scaffolding proteins that are central to the continued existence of a synapse. None of these experiments, however, directly address whether MAGUKs are necessary for proper synaptic function in adult animals. In this study, we use viral injection of a chained miRNA to knock down the three synaptic MAGUKs, PSD-93, PSD-95, and SAP102, specifically in adult animals. We find that, surprisingly, removal of the MAGUKs has little effect on either AMPAR- or NMDAR-mediated transmission in adult animals. Injection of this virus in perinatal animals causes a large reduction in both AMPAR and NMDAR transmission, in accordance with previous results from organotypic slice culture, and we show that this deficit is maintained into adulthood, indicating that the adult phenotype of the constitutive MAGUK knockout is likely due to removal of the protein from the juvenile. We additionally show that overexpression of PSD-95, which enhances transmission fourfold in

juveniles, has very little effect in adults, supporting the notion that the MAGUKs have a vastly diminished role in these animals.

Results

MAGUKs knockdown has little effect on synaptic transmission at mature CA1 synapses

To directly test the necessity of MAGUKs for proper excitatory transmission in the adult hippocampus, we stereotaxically injected lentivirus expressing a GFP marker and miRNA targeting all three MAGUKs (Levy et al., 2015) into area CA1 of P30 – P34 rats (Figure 20A). The MAGUKs have been implicated as scaffolding molecules critical to the existence of an organized post-synaptic density. We then took acute hippocampal slices from these animals seven to ten days later and performed dual whole-cell recordings while stimulating Schaffer Collateral inputs to directly compare excitatory transmission in visually-identified virally transduced neurons to that in neighboring uninfected control cells.

We found that viral knockdown of the MAGUKs has no effect in adult CA1 neurons. In GFP+ transduced neurons, neither AMPAR nor NMDAR-mediated transmission differs significantly from that in control neurons (Figure 20A – 20B). A viral incubation length of 7 days, as we have done here, has been shown previously in slice cultures to cause a robust decrease in AMPAR and NMDAR transmission (Levy et al., 2015). One possible difference between cultures and animals could be an increase in the half-life of the MAGUK protein. In cultured neurons, the half-life of PSD-95 has been reported to be ~36 hours (El-Husseini Ael et al., 2002), in agreement with the idea that slice cultures have high rates of synapse turnover. In the intact brain, the half-life of PSD-95 has been reported to be roughly 14 days (Price et al., 2010), although this figure does not account for potential stability differences between brain regions. The longer PSD-95 half-life could be due to increased synaptic stability in the adult

animal compared to slice cultures, which have high rates of synapse turnover. This increased synaptic stability could lead to reduced turnover of MAGUK protein. We attempted to control for this by expressing the miRNAs longer, for 2 weeks. In this case, we see a small but significant effect on AMPAR, but not NMDAR currents (Figure 20C-20D). Additionally, this effect is much smaller than that reported previously in slice culture.

In an attempt to further determine whether the knockdown of MAGUKs is age-dependent, we injected the MAGUK miRNA virus into dentate gyrus, a region previously shown to resemble an immature CA1 (Shipman and Nicoll, 2012) to determine whether a non-specific issue, such as a global increase in MAGUK half-life, might be preventing effective MAGUK knockdown in adult rat brain. We stereotaxically injected virus into dentate gyrus and recorded seven to ten days later as in (Figure 20E – 20F) while stimulating perforant path axons. In contrast to our recordings in CA1, we found that MAGUK knockdown in dentate caused a reduction in both AMPAR and NMDAR that was similar in magnitude to what has previously been reported in slice culture. (Figure 1C – 1D). Furthermore, the decrease in AMPAR transmission was significantly greater than that following long viral incubation in CA1 neurons (Figure 20G – 20H). We therefore conclude that knockdown of the MAGUKs has little effect in excitatory transmission in area CA1 in the postadolescent rat, although it has a major effect in dentate gyrus. One possibility is the turnover of the MAGUK protein is slower in CA1, potentially due to greater stability. We note that previous results have found no decrease in AMPAR transmission after knockdown of the neuroligins in adult CA1 (Shipman and Nicoll, 2012).

MAGUKs are necessary for AMPAR transmission in juvenile animals

Our results in adult hippocampus indicate that the MAGUK knockdown does not have an effect at P35 in CA1. Interestingly, however, knockdown in dentate gyrus, which has been described as similar to an immature CA1, causes a large decrease in AMPAR EPSC. We therefore tested whether MAGUKs play a role in immature CA1. To do this, we stereotaxically injected the MAGUK miRNA virus into P8 animals and waited 8 days, until P16. We then made acute slices and performed dual whole-cell recordings. We found that knockdown of the MAGUKs in younger animals caused a 75% reduction in AMPAR-mediated transmission (Figure 21A) without any change in NMDAR transmission (Figure 21B). Furthermore, we see a small but significant increase in the paired-pulse ratio (Figure 21C), indicating a mild decrease in the probability of release. Interestingly, the decrease in probability of release does not lead to a reduction in NMDAR currents, indicating either that the P_r change has elicited a compensatory response, or the change is specific to synapses containing AMPARs (non-silent synapses). A change in non-silent synapses could suggest specific changes at those synapses, which may initially require a larger PSD and might be more sensitive to loss of MAGUKs, or a bias in the AMPARs that are lost following MAGUK knockdown, indicating AMPARs at higher- P_r synapses may be preferentially lost, leaving only lower-P_r synapses.

We therefore conclude that the MAGUK contribution to synaptic transmission is age-dependent in CA1, with synaptic transmission early in life acutely dependent on MAGUK transcription, but with synapses becoming resistant to acute decreases in MAGUK transcription later in life, potentially due to an increase in MAGUK protein half-life. Furthermore, the mechanism of reduction in transmission, a decrease in both quantal content and size, is distinct from that previously reported in slice cultures (Figure 7). The reduction in synapse number seen in slice cultures is the result of a homeostatic process that conserves quantal size when faced

with a reduction in MAGUK scaffolding molecules. It is possible that *in vivo*, this process is slower and therefore recording at 8 days after MAGUK knockdown allows us to observe the consolidation process in action.

Removal of MAGUKs *in utero* results in AMPAR and NMDAR decreases

The decrease only in AMPAR mediated transmission following MAGUK knockdown at P8 differs from the phenotype observed in organotypic slice cultures from P8 animals, where MAGUK knockdown causes decreases in both AMPAR and NMDAR currents. One possible explanation for this difference is that the process of making slice cultures has altered the normal course of neuronal development. Slicing the hippocampus results in the loss of many synapses, which are then re-formed (Muller et al., 1993). In contrast, acute P8 slices have a larger number of intact synaptic connections. To control for these differences and remove MAGUKs *in vivo* before synapses are made, we decided to use *in utero* electroporation to transfect the progenitors of hippocampal pyramidal neurons with the MAGUK miRNA. This would knock down the MAGUKs in neuronal progenitors, before synapses had been formed, and indeed, before the creation of the postmitotic neuron.

We electroporated E15.5 – E16 rats with the MAGUK miRNA and waited until P16, roughly the same time point as used in the P8 injections, to record excitatory currents. We found that in contrast to the results obtained from P8 injections, we saw reductions in both AMPAR and NMDAR currents (Figure 21D – 21E), suggesting that neurons are more sensitive to MAGUK loss early in development, before synapses have been made. We additionally saw a small but significant increase in paired-pulse ratio (Figure 21F), indicating a small decrease in probability of release, consistent with the results seen at P8. While it is possible that the decrease

in probability of release underlies the decrease in NMDAR current, it is important to note that this decrease exists at P8 with no measurable decrease in NMDAR current.

Mature animals are not influenced by increases in MAGUK content

Our RNAi-mediated knockdown experiments demonstrate the MAGUKs are acutely necessary for proper synaptic localization of glutamate receptors in young, but not old animals. In a set of complementary experiments, we wanted to know if increases in MAGUK content, previously reported to increase synaptic AMPAR transmission in slice cultures and young animals (Ehrlich and Malinow, 2004; Schnell et al., 2002), are sufficient to increase AMPAR transmission in older animals. Overexpression studies of PSD-95 have found that overexpression increases AMPAR mEPSC frequency and amplitude without any change in probability of release or NMDAR currents, suggesting a post-synaptic effect (Ehrlich and Malinow, 2004; Stein et al., 2003) (but see Futai et al., 2007). These findings have been interpreted to mean that overexpression of PSD-95 unsilences AMPAR-lacking synapses, increasing average mEPSC amplitude either by localizing above-average numbers of AMPARs to PSD-95-unsilenced synapses or by increasing mEPSC frequency and amplitude in a manner that recapitulates LTP, in which synapses are unsilenced and average mEPSC amplitude at existing AMPAR-containing synapses is increased. We were therefore interested if overexpression of PSD-95 in postadolescent animals, in which few silent synapses are postulated to exist, is sufficient to increase AMPAR transmission. As LTP, but not synapse unsilencing, is a robust mechanism for AMPAR potentiation at this time point, we expect an increase in AMPAR transmission to indicate PSD-95 overexpression recapitulates LTP, while a lack of increase might suggest it plays a more prominent role in developmental synapse unsilencing, which is a critical aspect of LTP in younger animals.

We made lentivirus expressing a PSD-95::GFP fusion protein and first injected it into organotypic slice cultures made from P8 animals, followed by simultaneous recording of synaptic currents from paired neurons. We found that overexpression of PSD-95::GFP caused a roughly fourfold increase in AMPAR transmission without any change in NMDAR currents, consistent with previous reports of PSD-95 overexpression from slice cultures (Figure 22A). We next stereotaxically injected the PSD-95::GFP-expressing lentivirus into area CA1 of P8 animals as before and recorded at P18-P20. We found that transduced neurons had a roughly fourfold selective increase in AMPAR transmission, in agreement with our slice culture results (Figure 22B). These results indicate that our virally-expressed PSD-95 functionally integrates into synapses in a similar manner in slice cultures and young CA1 synapses. We then injected lentivirus into P34 animals and recorded from paired neurons. We found that the PSD-95::GFP protein, though it was localized to synapses as determined by the presence of GFP puncta in dendritic spines, was unable to enhance AMPAR transmission to the same degree as seen previously in younger animals and slice cultures. We found a modest (130%) but significant increase in AMPAR transmission compared to control neurons, in contrast to the fourfold increase seen previously (Figure 22C). We therefore conclude that PSD-95 overexpression in postadolescent animals does not substantially increase AMPAR transmission, in agreement with the hypothesis that PSD-95 is involved primarily in the unsilencing and strengthening of nascent synapses.

To test this hypothesis further, we overexpressed PSD-95 via *in utero* electroporation followed by recording in postadolescent animals at P37 – P39, a time point at which fewer silent synapses are thought to exist. If PSD-95 primarily accelerates the conversion of silent synapses to synapses containing AMPARs without increasing overall synapse number or quantal size, we

would predict that overexpression through development and recording at a time point at which silent synapses have been converted to AMPAR-containing synapses in control neurons would not dramatically enhance AMPAR currents compared to these controls. If, however, strengthening of synapses following PSD-95 overexpression functions to stabilize synapses that otherwise would be lost or causes formation of new synapses, it might lead to a permanent increase in synapse number and AMPAR transmission in postadolescent animals. Previous experiments have shown that *in utero* overexpression of PSD-95 followed by recording at P15 – P17 cause an increase in AMPAR transmission (Elias et al., 2008) in agreement with our experiments finding increased AMPAR transmission in P18-P20 animals injected at P8. At P37 – P39, we found that overexpressing PSD-95 during development via *in utero* electroporation caused a small but significant increase in AMPAR transmission with no change in NMDAR transmission (Figure 22D). This increase in AMPAR transmission was identical to that seen with overexpression in postadolescent animals and was significantly less than the large increase seen in juvenile animals (Figure 22E). We therefore conclude that MAGUK overexpression accelerates the natural developmental time course of synapse unsilencing, possibly by promoting synapse unsilencing, without increasing synapse stability or causing *de novo* formation of synapses. Increased expression of PSD-95, either by overexpression of recombinant protein or by the natural increase in expression of the endogenous protein during development (Sans et al., 2000) accelerates the natural unsilencing of synapses, but PSD-95 overexpression alone is not sufficient to increase the number of AMPAR-containing synapses above the physiological complement present in the adult.

Early loss of MAGUKs has lasting effect

We next wanted to explore why MAGUKs appear to be required for AMPAR localization in younger but not older animals. If synapse formation and maintenance are fully independent of MAGUKs in older animals, we might expect that the reduction in glutamatergic currents in younger animals could be transient, as MAGUK-independent synapse formation in older animals will 'wipe out' the early deficit. If, however, MAGUKs are still necessary in some way for synapse formation, either directly as an scaffolding protein, or indirectly, for example if MAGUK-independent mechanisms can only modulate existing MAGUK-dependent excitatory synapses, we would expect that in older animals glutamatergic current is still reduced as a result of a synapse formation deficit. To test this, we injected virus at P8 and recorded neurons at P35 – P40, the same age as the other recordings done in postadolescent animals.

We found that AMPAR transmission in older animals did not recover, but rather was identical to our recordings from P16 done from neurons transduced at P8, reduced by ~75% (Figure 23A). There is an additional deficit in NMDAR-mediated transmission, potentially a secondary effect due to long-term depression of AMPAR transmission. We also recorded from neurons electroporated at E17.5 with MAGUK miRNA and recorded at P35 (Figure 23B). Interestingly, these neurons had a deficit in AMPAR transmission without a decrease in NMDAR transmission, showing that the NMDAR decrease found at P16 is transient. It is not clear why P8 injections and E17.5 electroporations produce effects that are inconsistent at this aged time point.

These results indicate that knockdown of the MAGUKs in young animals causes lasting reduction of AMPAR transmission, through P35-P40 (Figure 23C-D). This is in contrast to knockdown in adults, which has no effect. Early loss of the MAGUKs therefore prevents synapse formation, leading to a lasting decrease at a time point at which their acute loss has no effect.

The increased stability of the proteins in adult animals means that MAGUKs must be removed before adulthood for an acute phenotype to be seen. These results additionally are in agreement with data demonstrating that genetic removal of multiple MAGUKs via conventional mouse KOs causes reductions in AMPAR transmission (Elias et al., 2006).

Discussion

This study provides a detailed analysis of the role of MAGUKs *in vivo* during the first two months of development. Our findings demonstrate that the MAGUKS play a critical role during synapse formation early in development. In postadolescent animals, acute knockdown of MAGUKs has no effect. This change may reflect an increased stability of MAGUKs or of synapses themselves. We find that removal of MAGUKs *in utero* leads to large reductions in both AMPAR and NMDAR transmission, in contrast to removal via viral transduction in postadolescent animals, which causes only minimal changes. Furthermore, overexpression of MAGUKs demonstrates that early in development, an increase in the MAGUK protein present in the neuron is sufficient to cause a large increase in AMPAR transmission equivalent to that seen in slice culture, while in older animals only a small increase is seen. This large increase early in development represents an occlusion of the developmental increase in AMPAR transmission, since overexpression throughout development causes only a small increase in AMPAR transmission. Together, these results suggest that MAGUKs function to add glutamatergic synapses to nascent spines during development. Finally, long-term knockdown of MAGUK protein from birth through adolescence causes a large decrease in AMPAR transmission, indicating that although MAGUK knockdown in postadolescent animals has no effect, there is no independent pathway for synapse maintenance in postadolescent animals.

Synapse maintenance in postadolescent animals

In postadolescent animals, the MAGUKs are still present the synapse at high levels and are incorporated into the PSD. This does not necessarily indicate they play a critical functional role; SAP102, which is expressed highly in the juvenile, continues to be expressed throughout the life of the animal though it has no known physiological role in adulthood. While knockdown of the MAGUKs has no acute effect on baseline transmission, potentially due to increased stability of either synapses or MAGUKs, we cannot eliminate the possibility that it perturbs another facet of glutamatergic transmission, such as plasticity or homeostasis. Additionally, as demonstrated by our longer incubation with the MAGUK miRNA, a small deficit in baseline transmission emerges only after a longer miRNA incubation time, possibly due to the increased half-life of the MAGUK protein *in vivo.*

What might mediate the differences between synapses in juveniles and post-adolescent animals? Mature synapses may be very stable. There are PDZ domain-containing proteins expressed in CA1 that have been poorly characterized in adult animals, such as MAGI2, which has been shown to bind directly to TARPs in biochemical assays. Furthermore, the mature synapse could not rely on any single protein family for maintenance. Rather, many of the proteins known to bind TARPs and NMDARs, such as the MAGUKs, NLGNs, MAGIs, and NSF/SNAP could function in a fully redundant manner to maintain baseline transmission at mature synapses. Stable AMPAR baseline transmission, however, is insufficient for robust learning. Each of the protein families expressed in adults could have unique roles in different facets of NMDAR trafficking, LTP, LTD, and homeostatic plasticity.

Regional and temporal specificity of MAGUKs

Our experiments with older animals demonstrated that in dentate gyrus, in contrast to CA1, neurons are sensitive to acute MAGUK knockdown. Our data suggest that in this respect, the

dentate gyrus appears similar to an immature CA1. One possibility is that dentate gyrus synapses in older animals are rapidly forming and remodeling in a MAGUK-dependent process, while CA3-CA1 Schaffer collateral synapses are relatively stable and this stabilization of the PSD greatly diminishes protein turnover. In younger animals, synapses in area CA1 are rapidly forming and maturing through P25 – P30 as measured by increases in spine density (Kirov et al., 2004; Martinez-Tellez et al., 2009; Norrholm and Ouimet, 2000), which correlates well with our data indicating a role for MAGUKs before P25 but not after P35. Finally, our data in which MAGUKs are knocked down through the period at which baseline transmission is MAGUK independent suggests that two different processes are at work in young and old animals. If MAGUK-independent synapse formation were happening in older animals, we would expect to see a recovery of synaptic transmission as the animal began forming synapses in a MAGUK-independent manner. Instead, the animal is only able to support the small number of synapses left after MAGUK knockdown blocks the majority of synapse formation. Alternatively, it is possible that there is a MAGUK-dependent critical period early in hippocampal development, followed by a MAGUK-independent period that does not contain meaningful levels of synapse formation. Our data from long-term MAGUK knockdown are in agreement with previous data from germline MAGUK PSD-93/PSD-95 knockout animals, in which recordings in adult animals show reductions in AMPAR transmission. The germline knockouts are most similar to our long-term MAGUK knockdown, in which animals are lacking MAGUKs throughout development. Therefore, in germline KO animals as in our long-term knockdown, the AMPAR deficit seen in adult animals is a result of a juvenile phenotype that has been uncorrected as the animal ages.

A hippocampal critical period

One intriguing implication of this data is the existence of a MAGUK-dependent hippocampal critical period, in which instability of MAGUKs and synapses allows for a more plastic CA1. This possibility is supported by data demonstrating the existence of critical periods with heightened spine turnover in young animals in other forebrain regions, for example the elevated spine turnover that occurs before P45 in forebrain neurons and is dependent on Nogo Receptor 1 (Akbik et al., 2013). Interestingly, the dependence on MAGUKs appears to differ in CA1 and dentate gyrus, suggesting that dentate retains higher plasticity through maturity. While the mechanistic reasons for this difference remain unclear, one potential rationale for its existence could be the requirement of adult dentate, but not adult CA1, to efficiently integrate adult-born neurons into dentate circuits.

Furthermore, we have found little evidence for MAGUK involvement in mature circuits, although it is quite likely that the high stability of MAGUKs prevents efficient knockdown. From these data, we can only conclude that knockdown of the MAGUK protein does not affect CA1 neurons as quickly in adults as in juveniles. These results suggest an intriguing increase in MAGUK stability specific to older animals, to CA1 but not dentate gyrus neurons.

Figure 20: Limits of RNAi-mediated knockdown of MAGUKs in CA1 in vivo. (A-B) Knockdown of MAGUKs for 1 week at P30 does not reduce AMPAR or NMDAR EPSCs. (AMPAR 108.87 ± 9.69% control, $p > 0.05$, n = 26; NMDAR 128.50 ± 14.14% control, $p > 0.05$, n = 21). (C-D) 2-week incubation of MAGUK miRNA reduces AMPAR EPSCs (AMPAR 71.31 ± 11.92% control, $p < 0.05$, n = 10; NMDAR 129.70 ± 19.58% control, $p > 0.05$, n = 10). (E-F) Knockdown of MAGUKs in DG for 1 week at P30 reduces AMPAR and NMDAR EPSCs. (AMPAR 18.21 ± 3.46% control, $p < 0.001$, n = 13; NMDAR 50.88 ± 9.04% control, $p < 0.01$, n = 8). (G-H) AMPAR and NMDAR EPSCs are significantly decreased in DG vs. CA1 datasets ($p < 0.05$ for all). CA1 long incubation AMPAR EPSCs are significantly decreased compared to CA1 short incubation ($p < 0.05$). Open circles indicate individual data points, filled circles indicate dataset mean ± SEM.

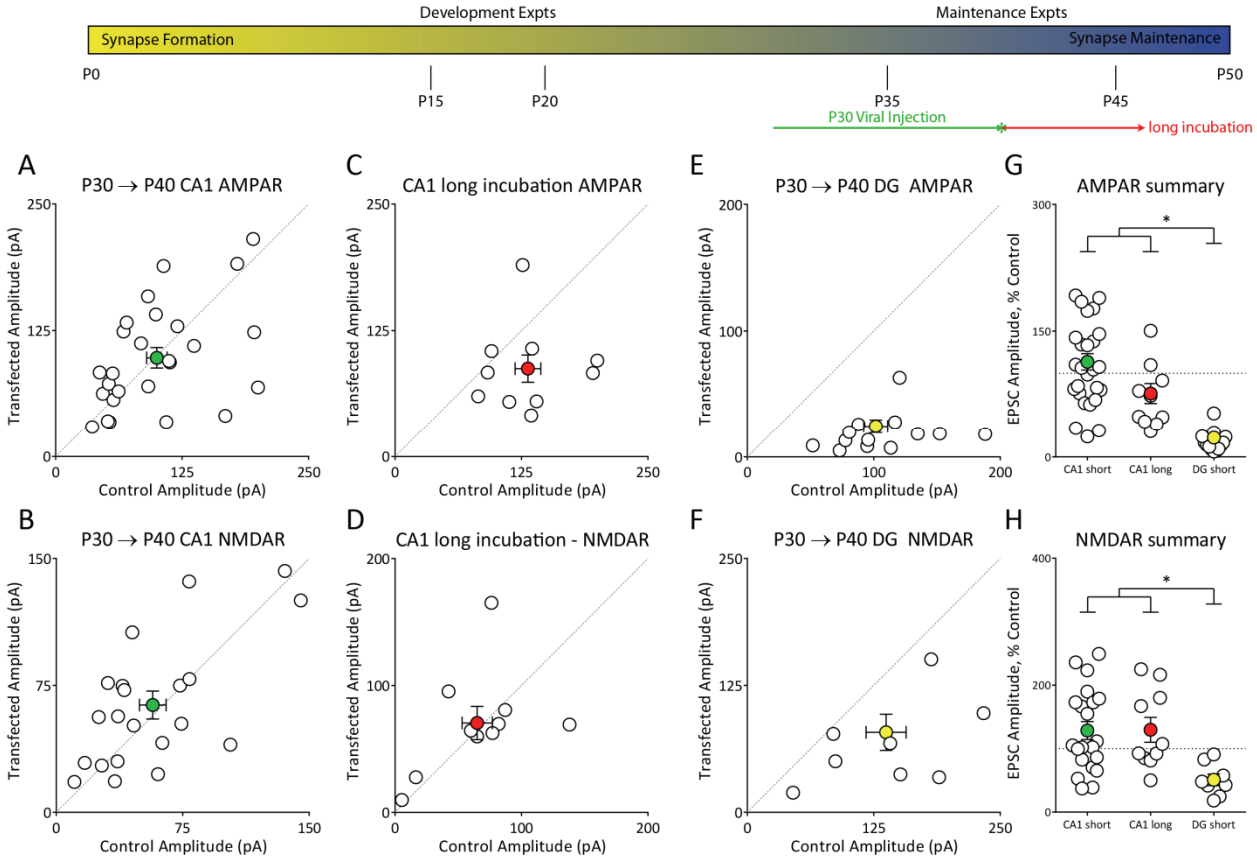
Development Expts
Maintenance Expts
Synapse Formation
Synapse Maintenance
P0
P15
P20
P35
P45
P50
P30 Viral Injection
long incubation
A
P30 → P40 CA1 AMPAR
B
P30 → P40 CA1 NMDAR
C
CA1 long incubation AMPAR
D
CA1 long incubation - NMDAR
E
P30 → P40 DG AMPAR
F
P30 → P40 DG NMDAR
G
AMPAR summary
H
NMDAR summary
Transfected Amplitude (pA)
Control Amplitude (pA)
EPSC Amplitude, % Control
CA1 short
CA1 long
DG short
*

Figure 21: MAGUK knockdown in young animals reduces AMPAR and NMDAR EPSCs. (A) MAGUK knockdown by viral infection at P8 reduces AMPAR EPSCs at P16 (24.49 ± 5.74% control, $p < 0.001$, $n = 18$). (B) MAGUK knockdown at P8 causes no change to NMDAR EPSCs at P16 (91.21 ± 17.15% control, $p > 0.05$, $n = 10$). (C) MAGUK knockdown at P8 increases the paired-pulse ratio (control 1.25 ± 0.07, miRNA 1.64 ± 0.15, $p < 0.05$, $n = 10$). (D) MAGUK knockdown by *in utero* electroporation at E17.5 reduces AMPAR EPSCs at P16 (22.62 ± 5.86% control, $p < 0.001$, $n = 15$). (E) MAGUK knockdown by in utero electroporation at E17.5 reduces NMDAR EPSCs at P16 (69.92 ± 11.66% control, $p < 0.05$, $n = 15$). (F) MAGUK knockdown at P8 increases the paired-pulse ratio (control 1.37 ± 0.07, miRNA 1.68 ± 0.12, $p < 0.01$, $n = 12$). Open circles indicate individual data points, filled circles indicate dataset mean ± SEM.

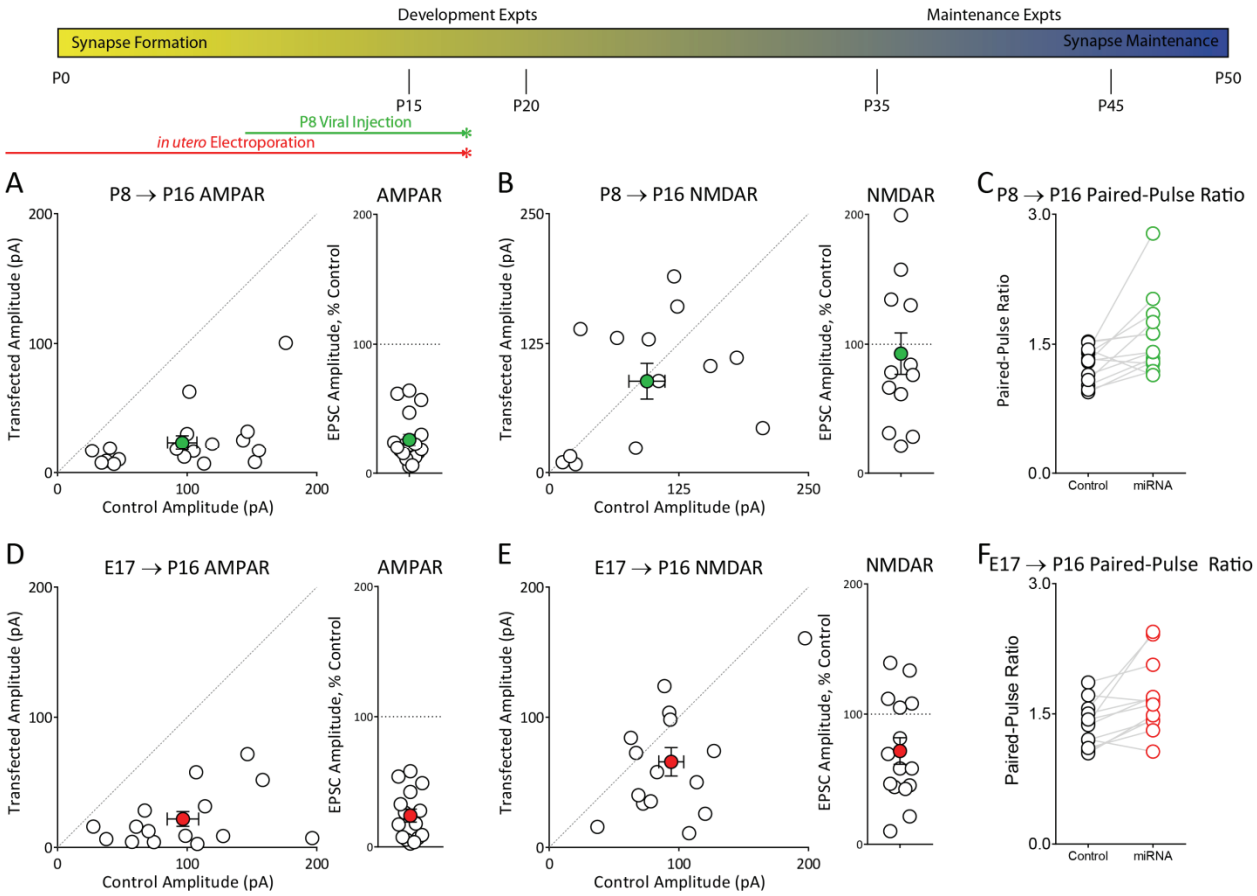
Development Expts
Maintenance Expts
Synapse Formation
Synapse Maintenance
P0
P15
P20
P35
P45
P50
P8 Viral Injection
in utero Electroporation
A
P8 → P16 AMPAR
AMPAR
Transfected Amplitude (pA)
Control Amplitude (pA)
EPSC Amplitude, % Control
B
P8 → P16 NMDAR
NMDAR
C
P8 → P16 Paired-Pulse Ratio
Paired-Pulse Ratio
Control
miRNA
D
E17 → P16 AMPAR
E
E17 → P16 NMDAR
F
E17 → P16 Paired-Pulse Ratio

Figure 22: PSD-95 overexpression increases AMPAR EPSCs in only in young animals. (A) Infection of slices cultures with lentivirus expressing PSD-95::GFP causes an increase in AMPAR EPSC with no change in NMDAR EPSC (AMPAR 288.07 ± 50.28% control, $p < 0.05$, n = 7; NMDAR 117.14 ± 16.34% control, $p > 0.05$, n =7). (B) Stereotaxic injection of P8 rats with lentivirus expressing PSD-95 causes an increase in AMPAR EPSC with no change in NMDAR EPSC (AMPAR 353.98 ± 51.73% control, $p < 0.01$, n = 11; NMDAR 114.32 ± 19.49% control, $p > 0.05$, n =11). (C) Stereotaxic injection of P34 rats with lentivirus expressing PSD-95 and recording at P40 causes a slight increase in AMPAR EPSC with no change in NMDAR EPSC (AMPAR 136.42 ± 22.16% control, $p < 0.05$, n = 9; NMDAR 85.62 ± 26.12% control, $p > 0.05$, n =8). (D) *In utero* electroporation of E17.5 rats with lentivirus expressing PSD-95 causes no change in either AMPAR or NMDAR EPSC (AMPAR 137.31 ± 13.15% control, $p > 0.05$, n = 9; NMDAR 73.60 ± 14.20% control, $p > 0.05$, n = 9). (E) Summary graphs. PSD-95 overexpression at P8 causes significantly larger increase in AMPAR EPSCs than overexpression at P34 or E17 followed by recording at P40 ($p < 0.05$). No difference in NMDAR EPSCs. Open circles indicate individual data points, filled circles indicate dataset mean ± SEM.

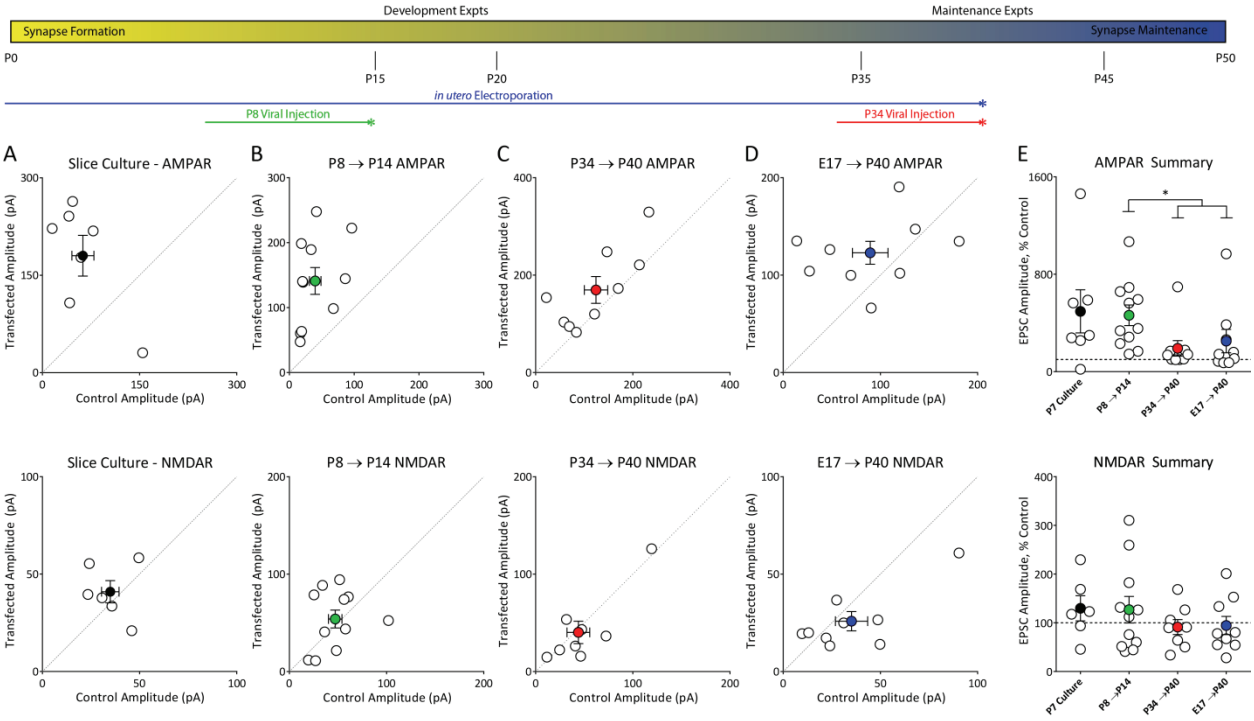
Development Expts
Maintenance Expts
Synapse Formation
Synapse Maintenance
P0
P15
P20
P35
P45
P50
in utero Electroporation
P8 Viral Injection
P34 Viral Injection
A
Slice Culture - AMPAR
B
P8 → P14 AMPAR
C
P34 → P40 AMPAR
D
E17 → P40 AMPAR
E
AMPAR Summary
Transfected Amplitude (pA)
Control Amplitude (pA)
EPSC Amplitude, % Control
*
P7 Culture
P8 → P14
P34 → P40
E17 → P40
Slice Culture - NMDAR
P8 → P14 NMDAR
P34 → P40 NMDAR
E17 → P40 NMDAR
NMDAR Summary

Figure 23: Early MAGUK knockdown has lasting effect. (A) P8 viral infections of MAGUK miRNA cause AMPAR and NMDAR EPSC reductions at P35-P40 (AMPAR 30.42 ± 5.79% control, $p < 0.01$, $n = 8$; NMDAR 37.82 ± 5.77% control, $p < 0.01$, $n = 8$). (B) E17.5 *in utero* electroporations of MAGUK miRNA causes AMPAR EPSC reduction at P35-P40 (AMPAR 55.60 ± 11.06% control, $p < 0.01$, $n = 9$; NMDAR 110.11 ± 10.64% control, $p > 0.01$, $n = 9$). (C) Summary graph showing AMPAR and NMDAR EPSCs for all MAGUK miRNA manipulations. (D) Summary data showing AMPAR and NMDAR EPSCs datasets. Long CA1 incubation (P28 – P49) is significantly different from P0-P16 and P8-P35 datasets ($p < 0.05$). Open circles indicate individual data points, filled circles indicate dataset mean ± SEM.

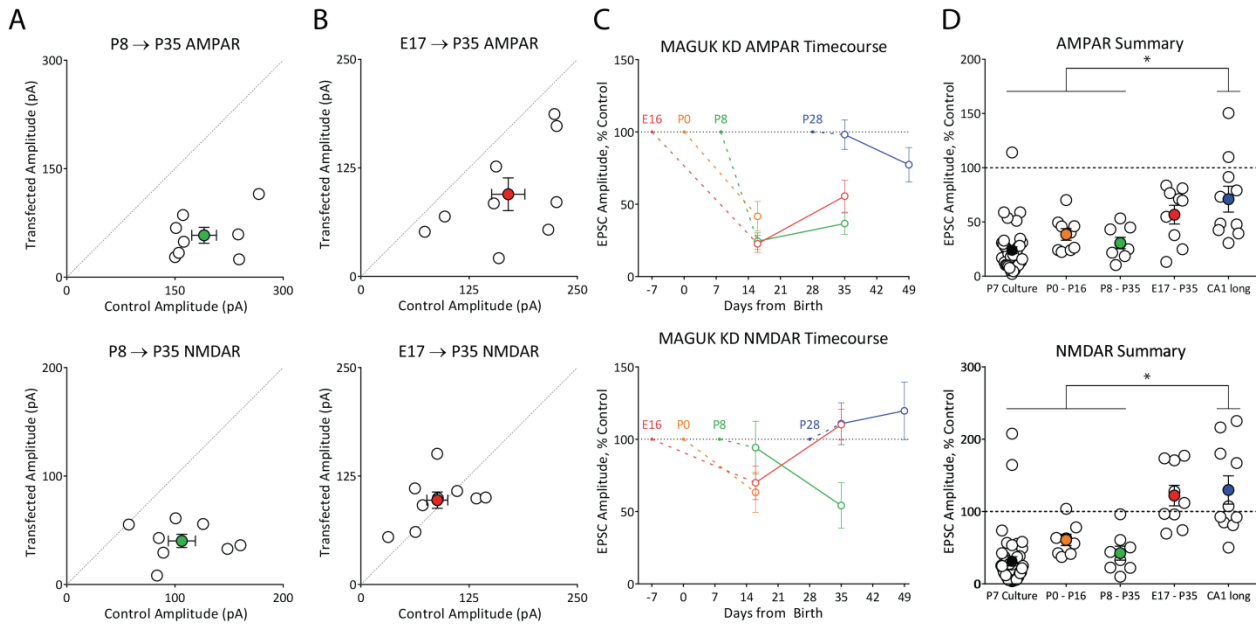
A
P8 → P35 AMPAR
Transfected Amplitude (pA)
Control Amplitude (pA)
B
E17 → P35 AMPAR
Transfected Amplitude (pA)
Control Amplitude (pA)
C
MAGUK KD AMPAR Timecourse
EPSC Amplitude, % Control
E16
P0
P8
P28
Days from Birth
D
AMPAR Summary
EPSC Amplitude, % Control
P7 Culture
P0 - P16
P8 - P35
E17 - P35
CA1 long
P8 → P35 NMDAR
Transfected Amplitude (pA)
Control Amplitude (pA)
E17 → P35 NMDAR
Transfected Amplitude (pA)
Control Amplitude (pA)
MAGUK KD NMDAR Timecourse
EPSC Amplitude, % Control
E16
P0
P8
P28
Days from Birth
NMDAR Summary
EPSC Amplitude, % Control
P7 Culture
P0 - P16
P8 - P35
E17 - P35
CA1 long

CHAPTER 6: General Discussion

Synapse-intrinsic regulation of synaptic strength

The data presented in Chapter 3 suggests that individual synapses have intrinsic set points which can be read by the homeostatic machinery. Any sensor for activity at individual synapses must be sensitive to sub-threshold depolarization, as release at single synapses will not cause action potentials or dendritic spikes (Losonczy and Magee, 2006). Interestingly, we identified the L-type calcium channel as the calcium source of the physiological set point. In hippocampal neurons, two L-type channels are expressed: CaV 1.2 and CaV 1.3. Both are expressed in dendrites (Hall et al., 2013), and experiments with calcium-sensitive dyes suggest that L-type channels localize to spines (Bloodgood and Sabatini, 2007). Might these local L-type channels underlie synapse-specific homeostasis?

Both L-type channels only open at depolarized potentials, though CaV1.3 activates at somewhat more hyperpolarized potentials than CaV1.2. The half-maximal activation of CaV1.3 occurs at -36.8mV, versus -8.8mV for CaV1.2 (Xu and Lipscombe, 2001). Although CaV1.3 begins to open at sub-threshold potentials, around -55mV, it is not clear that single release events will register with these channels. It may be that the threshold is carefully tuned such that activation does not occur via neurotransmitter release at weak synapses, but synapses of physiological synaptic strength can barely depolarize dendrites to open CaV1.3. Further experimentation is required to determine whether CaV1.2 or CaV1.3 might individually underlie local homeostasis.

Alternatively, it is possible that L-type channels are simply permissive on a global level, with a downstream local component. In support of this idea, we have identified CaMKK as a member of the local homeostatic pathway. The identified role of CaMKK is in regulating transcription, and activated CaMKK is localized to the nucleus. It is therefore difficult to

construct a pathway where subthreshold L-type signaling in spines and dendrites is directly linked to nuclear CaMKK transcriptional regulation, although it is possible that local L-type signaling can act through intermediates to regulate CaMKK. In this global-permissiveness model, L-type signaling and CaMKK would act to transcribe genes that are later required for local homeostasis.

Rules for local homeostasis

Although we have demonstrated a synapse-specific competitive homeostasis, we have not uncovered the rules that determine the winner. Manipulation of individual pre-synaptic neurons demonstrates that inhibition of release at individual synapses increases AMPAR localization (Hou et al., 2008), while increased activity decreases it (Hou et al., 2011). These pre-synaptic manipulations, however, which entail a synaptic strength change at individual synapses, could be fundamentally different from our post-synaptic manipulation in which synaptic strength is conserved, not increased or decreased. It is therefore worthwhile determining the effect of pre-synaptic changes on our post-synaptic local competition.

Specifically, in CA1 neurons, it is possible to inject ChR2-expressing virus in CA3, such that a small percentage of CA3 neurons are infected. This setup should allow for isolation of post-synaptic responses from neurons that have been chronically excited, increasing firing rate at individual synapses. Following MAGUK miRNA transfection into CA1 to induce synapse-specific homeostasis, dual whole-cell recordings in CA1 could be performed. Electrical and optogenetic stimulation of CA3 could then be performed. Electrical stimulation should be unbiased, and result in a normalized EPSC in the MAGUK miRNA-expressing neuron of roughly 25% of control EPSC. Optogenetic stimulation should trigger only neurons that have been chronically excited, allowing for isolation of the effects of chronic excitation. For example,

if following MAGUK knockdown and CA3 chronic excitation, electrical stimulation results in a normalized EPSC of 25% but optogenetic stimulation results in a much larger normalized EPSC, chronic pre-synaptic excitation would then have biased the post-synaptic competition towards active synapses.

Although synaptic activity could be the determining factor for 'winning' synapses, there are many other possibilities. For example, NMDARs are always lost in an all-or-none manner, suggesting synapses that retain NMDARs might end up as 'winners', potentially due to NMDARs allowing for induction of dendritic spikes (Smith et al., 2013). This possibility could be tested, for example, by blocking NMDARs with APV. If NMDARs confer the 'winning' signal, we might expect that consolidation would not occur in the presence of APV, analogously to, consolidation not occurring in the presence of nifedipine, which blocks the 'winning' signal conferred by L-type channels. Finally, synapses that contain more AMPARs may 'win' the competition since they will be more depolarized following individual release events. To determine whether AMPAR distribution affects the competition, NBQX could be added to block these receptors.

Beyond determining the rules for post-synaptic consolidation, we can use these experimental paradigms to look at single-synapse plasticity following pre-synaptic activity changes. Although cell-autonomous homeostatic plasticity induced by increased spike rate has been characterized (Goold and Nicoll, 2010), the effect on neurons post-synaptic to the chronically active neuron has not been examined. Furthermore, although single-synapse plasticity after pre-synaptic manipulations has been described, the underlying mechanisms are unknown. One useful paradigm could be injection of mixture of virus into CA3, allowing for equal infections by ChR2 and a variant sensitive to red light, such as VChR1 (Zhang et al.,

2008). After chronic excitation by only one wavelength, CA1 neurons could be patched and a ratio of ChR2/VChR1-induced EPSC could be obtained. This ratio would be changed by pre-synaptic activity, and amenable to pharmacological manipulations that might modulate single-synapse homeostasis. These two techniques – dual whole-cell recording of transfected neurons post-synaptic to chronically excited neurons, and stimulation of two separable sets of pre-synaptic neurons, might help elucidate the molecular mechanisms of local homeostasis.

Potential functions of synapse-level homeostasis

Homeostatic mechanisms, in general, are thought to act to return systems to pre-existing set points. At the synaptic level, returning to a pre-existing set point suggests counteracting synaptic plasticity that has previously occurred. The long time course of our manipulation, 4 days in culture, and longer than that *in vivo*, suggests that it does not act acutely to counteract changes in synaptic strength, unlike previous findings of synapse-level homeostasis induced as quickly as 30 minutes (Hou et al., 2011), with the caveat that our time course was determined in post-synaptic neurons have undergone a reduction in activity, and any activity-dependent process could be artificially slowed by this reduction.

A homeostatic program with a very slow time course could play a number of roles. One possible function of this slow time course could be a reversal of LTP. Cell-level homeostasis is proposed to adjust firing rate while keeping relative synaptic weights intact, meaning it likely does not adjust individual synaptic weights. LTD is proposed to adjust individual weights, but dependent on uncorrelated activity in the pre-synaptic neuron. We propose that synapse-level homeostasis could counteract LTP and act to normalize synaptic weight over longer time scales, in the absence of any signals. Thus, it could act to return potentiated synapses to baseline in the absence of further activity over long time scales, which cell-level homeostasis and LTD cannot

do. This activity could serve as a natural mechanism for 'forgetting' and facilitate the hippocampus's role in memory formation, not storage. The maintenance of synaptic strength at individual synapses would then be a balance between coordinated activity that maintains deviations from baseline strength, counteracted over time by a process that works to return synapses to baseline synaptic strength. In light of recent data arguing that spine dynamics are dramatically different in hippocampus and cortex (Attardo et al., 2015), it would be interesting to determine whether the time course of single-synapse homeostasis differed in hippocampus and areas more important for memory storage, such as the cortex.

Multiple pathways for homeostasis

The synapse-level homeostatic program we describe here shares its components with the previously-described 'homeostatic pathway' for cell-wide homeostasis. In fact, the components of this pathway are used for many baseline functions, including distance-dependent scaling (Shipman et al., 2013). It is clear that although cell-wide scaling up was the first function described for these proteins, including the L-type channel, CaMKK and CaMK4, and GluA2, their roles should be broadened to include synapse-level homeostasis and distance-dependent scaling, which can be thought of as a local homeostatic program driven by activity (Andrasfalvy et al., 2008). Although synapse-level and cell-level homeostasis share components, it is possible to specifically block only one pathway. Knockdown of the MAGUKs blocks cell-level scaling up (Sun and Turrigiano, 2011). Consolidation, however, occurs after MAGUK knockdown, and is only blocked by removal of additional homeostatic pathway members. These results indicate that although the homeostatic pathways may share components, they are not fully redundant.

Synapse-level regulation of quantal size by MAGUKs

Although synaptic consolidation functions to return weak synapses to physiological synaptic strength, the rules governing the opposite correction, preventing synapses from becoming too strong, have not been determined. In this context, one intriguing finding is that overexpression of PSD-95 increases AMPAR-containing synapse number rather than synaptic strength. This finding alone suggests that MAGUKs do not play a role in setting synaptic strength, and increases or decreases (as in the MAGUK miRNA) in the number of available MAGUKs do not change synaptic strength. Simultaneous overexpression of PSD-95 and knockdown of endogenous MAGUKs, though, as done in Chapter 4, causes a large increase in synaptic strength and forces a reconsideration of the role of MAGUKs. In this context, it is clear that changes in MAGUK abundance can change synaptic strength.

It is possible that the MAGUK scaffold itself maintains quantal size, and disruptions to this scaffold allow quantal size changes. It is known that the PSD size is highly correlated with the number of AMPARs present. Furthermore, the MAGUKs are required for maintenance of the PSD; loss of the MAGUKs reduces PSD size and eliminates some PSDs. Therefore, it is likely that the PSD size determines the number of AMPARs at the synapse. In support of this idea, data from photoactivatable-GFP experiments finds that during glutamate uncaging-induced potentiation, the PSD-95 scaffold at synapses must transiently break and re-form for structural plasticity to occur. Expression of PSD-95 mutants that do not transiently leave the spine head following uncaging blocks structural plasticity (Steiner et al., 2008). These data imply that changes in quantal size require changes to the size of the PSD, and in fact require complete reformation of the existing MAGUK scaffold, rather than simple addition or subtraction of pieces. In agreement, the MAGUK scaffold at individual PSDs has remarkably low diffusion

within the PSD, suggesting it exists as a rigid lattice rather than a freely-diffusible structure (Blanpied et al., 2008).

PSD-95 overexpression in the presence of endogenous MAGUKs is not able to increase quantal size, then, because the size of the PSD is tightly controlled. Endogenously-expressed MAGUKs maintain PSD size, while recombinant PSD-95 does not. It is unlikely this is due to PSD-95 playing a specific role, since overexpressed PSD-93 also increases quantal size on the background of the MAGUK miRNA. Further experiments are required to determine how overexpressed and endogenous MAGUKs might differ.

Functional heterogeneity within the MAGUK family

The overexpression experiments in Chapter 4 demonstrate that important functional differences exist between PSD-93 and PSD-95. Although both proteins are thought to be present at virtually all synapses, it would be interesting to determine how their abundance at individual synapses might be actively regulated. There has been one report that activity level changes during synaptic scaling cause inversely correlated changes in the relative abundance of PSD-95 at synapses – activity block increases PSD-95, while elevated activity reduces it (Sun and Turrigiano, 2011). These relative changes could have important implications for metaplasticity. For example, since synapses lacking PSD-95 cannot undergo LTD (Carlisle et al., 2008), increases in the relative amount of PSD-93 present at individual synapses might bias these synapses towards subsequent potentiation.

There are several possibilities for the co-existence of PSD-93 and PSD-95 at synapses. Although it is possible that they are homogenously distributed, recent super-resolution imaging studies have found that PSD-95 exhibits clustering within synapses (Fukata et al., 2013; MacGillavry et al., 2013). These clusters co-localize with AMPAR clusters and are thought to

represent nanodomains within PSDs. It would be of interest to determine whether PSD-93 and SAP102 co-localized in clusters with PSD-95, or formed clusters in the regions of low PSD-95 abundance.

Role of the MAGUKs *in vivo*

Many of the experiments conducted for this thesis have been conducted in reduced preparations at a young age. The experiments in Chapter 5 explore the role of the MAGUKs in more intact systems. As might be expected, the MAGUKs play differing roles depending on the specific region in which they are expressed. In dentate gyrus, MAGUK knockdown appears identical to that in CA1 from cultured slices. In post-adolescent CA1, however, it appears that acute MAGUK knockdown has little effect. This could be due to increased stability of the proteins themselves, meaning longer miRNA incubations are required for existing protein to turn over, or increased stability of the synapses such that loss of the MAGUKs is offset by other proteins that can compensate. Although no studies exist of adult virus injections knocking down the MAGUKs in CA1, one recent study knocked down PSD-95 in adult visual cortex, finding a decrease in AMPAR/NMDAR ratio as would be expected from PSD-95 knockdown in culture (Huang et al., 2015; Schluter et al., 2006).

Although knockdown studies are complicated by possible changes in protein turnover in different contexts, we have performed overexpression studies that avoid these issues. Overexpression of GFP-tagged PSD-95 dramatically increases AMPAR EPSCs in cultured slices and young CA1, but has little effect in aged CA1, although the overexpressed protein is localized to synapses in all cases. These results are in agreement with the idea that PSD-95 primarily unsilences synapses, since silent synapses are not thought to exist in large numbers in aged animals. It may be that in the absence of silent synapses, endogenous MAGUKs form stable

synapses that cannot be modified by overexpressed PSD-95, as is seen in cultured slices. Further experimentation is required to determine the physiological role played by the MAGUKs during development and aging *in vivo*.

CHAPTER 7: References

Akbik, F.V., Bhagat, S.M., Patel, P.R., Cafferty, W.B., and Strittmatter, S.M. (2013). Anatomical plasticity of adult brain is titrated by Nogo Receptor 1. Neuron *77*, 859-866.

Altimimi, H.F., and Stellwagen, D. (2013). Persistent synaptic scaling independent of AMPA receptor subunit composition. J. Neurosci. *33*, 11763-11767.

Andrasfalvy, B.K., and Magee, J.C. (2001). Distance-dependent increase in AMPA receptor number in the dendrites of adult hippocampal CA1 pyramidal neurons. J. Neurosci. *21*, 9151-9159.

Andrasfalvy, B.K., Makara, J.K., Johnston, D., and Magee, J.C. (2008). Altered synaptic and non-synaptic properties of CA1 pyramidal neurons in Kv4.2 knockout mice. The Journal of physiology *586*, 3881-3892.

Arellano, J.I., Benavides-Piccione, R., Defelipe, J., and Yuste, R. (2007). Ultrastructure of dendritic spines: correlation between synaptic and spine morphologies. Front. Neurosci. *1*, 131-143.

Attardo, A., Fitzgerald, J.E., and Schnitzer, M.J. (2015). Impermanence of dendritic spines in live adult CA1 hippocampus. Nature *523*, 592-596.

Avery, R.B., and Johnston, D. (1996). Multiple channel types contribute to the low-voltage-activated calcium current in hippocampal CA3 pyramidal neurons. J. Neurosci. *16*, 5567-5582.

Bats, C., Groc, L., and Choquet, D. (2007). The interaction between Stargazin and PSD-95 regulates AMPA receptor surface trafficking. Neuron *53*, 719-734.

Bekkers, J.M., and Stevens, C.F. (1990). Presynaptic mechanism for long-term potentiation in the hippocampus. Nature *346*, 724-729.

Bito, H., Deisseroth, K., and Tsien, R.W. (1997). Ca2+-dependent regulation in neuronal gene expression. Curr. Opin. Neurobiol. *7*, 419-429.

Blanpied, T.A., Kerr, J.M., and Ehlers, M.D. (2008). Structural plasticity with preserved topology in the postsynaptic protein network. Proceedings of the National Academy of Sciences of the United States of America *105*, 12587-12592.

Bloodgood, B.L., and Sabatini, B.L. (2007). Nonlinear regulation of unitary synaptic signals by CaV(2.3) voltage-sensitive calcium channels located in dendritic spines. Neuron *53*, 249-260.

Bredt, D.S., and Nicoll, R.A. (2003). AMPA receptor trafficking at excitatory synapses. Neuron *40*, 361-379.

Carlisle, H.J., Fink, A.E., Grant, S.G., and O'Dell, T.J. (2008). Opposing effects of PSD-93 and PSD-95 on long-term potentiation and spike timing-dependent plasticity. The Journal of physiology *586*, 5885-5900.

Chen, X., Nelson, C.D., Li, X., Winters, C.A., Azzam, R., Sousa, A.A., Leapman, R.D., Gainer, H., Sheng, M., and Reese, T.S. (2011). PSD-95 is required to sustain the molecular organization of the postsynaptic density. J. Neurosci. *31*, 6329-6338.

Chen, X., Winters, C., Azzam, R., Li, X., Galbraith, J.A., Leapman, R.D., and Reese, T.S. (2008). Organization of the core structure of the postsynaptic density. Proc. Natl. Acad. Sci. USA *105*, 4453-4458.

Chih, B., Engelman, H., and Scheiffele, P. (2005). Control of excitatory and inhibitory synapse formation by neuroligins. Science *307*, 1324-1328.

Del Castillo, J., and Katz, B. (1954). Quantal components of the end-plate potential. J. Physiol. (Lond.) *124*, 560-573.

Dolmetsch, R.E., Pajvani, U., Fife, K., Spotts, J.M., and Greenberg, M.E. (2001). Signaling to the nucleus by an L-type calcium channel-calmodulin complex through the MAP kinase pathway. Science *294*, 333-339.

Ehrlich, I., Klein, M., Rumpel, S., and Malinow, R. (2007). PSD-95 is required for activity-driven synapse stabilization. Proc. Natl. Acad. Sci. USA *104*, 4176-4181.

Ehrlich, I., and Malinow, R. (2004). Postsynaptic density 95 controls AMPA receptor incorporation during long-term potentiation and experience-driven synaptic plasticity. J. Neurosci. *24*, 916-927.

El-Husseini, A.E., Schnell, E., Chetkovich, D.M., Nicoll, R.A., and Bredt, D.S. (2000). PSD-95 involvement in maturation of excitatory synapses. Science *290*, 1364-1368.

El-Husseini Ael, D., Schnell, E., Dakoji, S., Sweeney, N., Zhou, Q., Prange, O., Gauthier-Campbell, C., Aguilera-Moreno, A., Nicoll, R.A., and Bredt, D.S. (2002). Synaptic strength regulated by palmitate cycling on PSD-95. Cell *108*, 849-863.

Elias, G.M., Elias, L.A.B., Apostolides, P.F., Kriegstein, A.R., and Nicoll, R.a. (2008). Differential trafficking of AMPA and NMDA receptors by SAP102 and PSD-95 underlies synapse development. Proc. Natl. Acad. Sci. USA *105*, 20953-20958.

Elias, G.M., Funke, L., Stein, V., Grant, S.G., Bredt, D.S., and Nicoll, R.A. (2006). Synapse-specific and developmentally regulated targeting of AMPA receptors by a family of MAGUK scaffolding proteins. Neuron *52*, 307-320.

Elias, G.M., and Nicoll, R.A. (2007). Synaptic trafficking of glutamate receptors by MAGUK scaffolding proteins. Trends Cell Biol. *17*, 343-352.

Fukata, Y., Dimitrov, A., Boncompain, G., Vielemeyer, O., Perez, F., and Fukata, M. (2013). Local palmitoylation cycles define activity-regulated postsynaptic subdomains. The Journal of cell biology *202*, 145-161.

Futai, K., Kim, M.J., Hashikawa, T., Scheiffele, P., Sheng, M., and Hayashi, Y. (2007). Retrograde modulation of presynaptic release probability through signaling mediated by PSD-95-neuroligin. Nat. Neurosci. *10*, 186-195.

Gainey, M.A., Hurvitz-Wolff, J.R., Lambo, M.E., and Turrigiano, G.G. (2009). Synaptic scaling requires the GluR2 subunit of the AMPA receptor. J. Neurosci. *29*, 6479-6489.

Goold, C.P., and Nicoll, R.A. (2010). Single-cell optogenetic excitation drives homeostatic synaptic depression. Neuron *68*, 512-528.

Granger, A.J., Shi, Y., Lu, W., Cerpas, M., and Nicoll, R.A. (2013). LTP requires a reserve pool of glutamate receptors independent of subunit type. Nature *493*, 495-500.

Gray, J.A., Shi, Y., Usui, H., During, M.J., Sakimura, K., and Nicoll, R.A. (2011). Distinct modes of AMPA receptor suppression at developing synapses by GluN2A and GluN2B: single-cell NMDA receptor subunit deletion in vivo. Neuron *71*, 1085-1101.

Hafner, A.S., Penn, A.C., Grillo-Bosch, D., Retailleau, N., Poujol, C., Philippat, A., Coussen, F., Sainlos, M., Opazo, P., and Choquet, D. (2015). Lengthening of the Stargazin Cytoplasmic Tail Increases Synaptic Transmission by Promoting Interaction to Deeper Domains of PSD-95. Neuron *86*, 475-489.

Hall, D.D., Dai, S., Tseng, P.Y., Malik, Z., Nguyen, M., Matt, L., Schnizler, K., Shephard, A., Mohapatra, D.P., Tsuruta, F.*, et al.* (2013). Competition between alpha-actinin and Ca(2)(+)-calmodulin controls surface retention of the L-type Ca(2)(+) channel Ca(V)1.2. Neuron *78*, 483-497.

Harris, K.M., and Kater, S.B. (1994). Dendritic spines: cellular specializations imparting both stability and flexibility to synaptic function. Annu. Rev. Neurosci. *17*, 341-371.

Harris, K.M., and Stevens, J.K. (1989). Dendritic spines of CA 1 pyramidal cells in the rat hippocampus: serial electron microscopy with reference to their biophysical characteristics. J. Neurosci. *9*, 2982-2997.

He, M., Bodi, I., Mikala, G., and Schwartz, A. (1997). Motif III S5 of L-type calcium channels is involved in the dihydropyridine binding site. A combined radioligand binding and electrophysiological study. J. Biol. Chem. *272*, 2629-2633.

Hengen, K.B., Lambo, M.E., Van Hooser, S.D., Katz, D.B., and Turrigiano, G.G. (2013). Firing rate homeostasis in visual cortex of freely behaving rodents. Neuron *80*, 335-342.

Hou, Q., Gilbert, J., and Man, H.Y. (2011). Homeostatic regulation of AMPA receptor trafficking and degradation by light-controlled single-synaptic activation. Neuron *72*, 806-818.

Hou, Q., Zhang, D., Jarzylo, L., Huganir, R.L., and Man, H.Y. (2008). Homeostatic regulation of AMPA receptor expression at single hippocampal synapses. Proceedings of the National Academy of Sciences of the United States of America *105*, 775-780.

Howard, M.A., Elias, G.M., Elias, L.A., Swat, W., and Nicoll, R.A. (2010). The role of SAP97 in synaptic glutamate receptor dynamics. Proc. Natl. Acad. Sci. USA *107*, 3805-3810.

Hsia, A.Y., Malenka, R.C., and Nicoll, R.A. (1998). Development of excitatory circuitry in the hippocampus. J. Neurophysiol. *79*, 2013-2024.

Huang, X., Stodieck, S.K., Goetze, B., Cui, L., Wong, M.H., Wenzel, C., Hosang, L., Dong, Y., Lowel, S., and Schluter, O.M. (2015). Progressive maturation of silent synapses governs the duration of a critical period. Proceedings of the National Academy of Sciences of the United States of America *112*, E3131-3140.

Hung, A.Y., Futai, K., Sala, C., Valtschanoff, J.G., Ryu, J., Woodworth, M.A., Kidd, F.L., Sung, C.C., Miyakawa, T., Bear, M.F*., et al.* (2008). Smaller dendritic spines, weaker synaptic transmission, but enhanced spatial learning in mice lacking Shank1. J. Neurosci. *28*, 1697-1708.

Ibata, K., Sun, Q., and Turrigiano, G.G. (2008). Rapid synaptic scaling induced by changes in postsynaptic firing. Neuron *57*, 819-826.

Jia, Z., Agopyan, N., Miu, P., Xiong, Z., Henderson, J., Gerlai, R., Taverna, F.A., Velumian, A., MacDonald, J., Carlen, P., *et al.* (1996). Enhanced LTP in mice deficient in the AMPA receptor GluR2. Neuron *17*, 945-956.

Ke, M.T., Fujimoto, S., and Imai, T. (2013). SeeDB: a simple and morphology-preserving optical clearing agent for neuronal circuit reconstruction. Nat. Neurosci. *16*, 1154-1161.

Kessels, H.W., Kopec, C.D., Klein, M.E., and Malinow, R. (2009). Roles of stargazin and phosphorylation in the control of AMPA receptor subcellular distribution. Nat. Neurosci. *12*, 888-896.

Kim, E., Cho, K.O., Rothschild, A., and Sheng, M. (1996). Heteromultimerization and NMDA receptor-clustering activity of Chapsyn-110, a member of the PSD-95 family of proteins. Neuron *17*, 103-113.

Kim, E., and Sheng, M. (2004). PDZ domain proteins of synapses. Nat. Rev. Neurosci. *5*, 771-781.

Kirov, S.A., Goddard, C.A., and Harris, K.M. (2004). Age-dependence in the homeostatic upregulation of hippocampal dendritic spine number during blocked synaptic transmission. Neuropharmacology *47*, 640-648.

Kornau, H.C., Schenker, L.T., Kennedy, M.B., and Seeburg, P.H. (1995). Domain interaction between NMDA receptor subunits and the postsynaptic density protein PSD-95. Science *269*, 1737-1740.

Kruger, J.M., Favaro, P.D., Liu, M., Kitlinska, A., Huang, X., Raabe, M., Akad, D.S., Liu, Y., Urlaub, H., Dong, Y.*, et al.* (2013). Differential roles of postsynaptic density-93 isoforms in regulating synaptic transmission. J. Neurosci. *33*, 15504-15517.

Lambo, M.E., and Turrigiano, G.G. (2013). Synaptic and intrinsic homeostatic mechanisms cooperate to increase L2/3 pyramidal neuron excitability during a late phase of critical period plasticity. J. Neurosci. *33*, 8810-8819.

Lee, K.F., Soares, C., and Beique, J.C. (2014). Tuning into diversity of homeostatic synaptic plasticity. Neuropharmacology *78*, 31-37.

Levy, J.M., Chen, X., Reese, T.S., and Nicoll, R.A. (2015). Synaptic Consolidation Normalizes AMPAR Quantal Size following MAGUK Loss. Neuron *87*, 534-548.

Losonczy, A., and Magee, J.C. (2006). Integrative properties of radial oblique dendrites in hippocampal CA1 pyramidal neurons. Neuron *50*, 291-307.

Lu, W., Bushong, E.A., Shih, T.P., Ellisman, M.H., and Nicoll, R.A. (2013). The cell-autonomous role of excitatory synaptic transmission in the regulation of neuronal structure and function. Neuron *78*, 433-439.

Lu, W., Shi, Y., Jackson, A.C., Bjorgan, K., During, M.J., Sprengel, R., Seeburg, P.H., and Nicoll, R.A. (2009). Subunit composition of synaptic AMPA receptors revealed by a single-cell genetic approach. Neuron *62*, 254-268.

MacGillavry, H.D., Song, Y., Raghavachari, S., and Blanpied, T.A. (2013). Nanoscale scaffolding domains within the postsynaptic density concentrate synaptic AMPA receptors. Neuron *78*, 615-622.

Magee, J.C., and Cook, E.P. (2000). Somatic EPSP amplitude is independent of synapse location in hippocampal pyramidal neurons. Nature neuroscience *3*, 895-903.

Malinow, R., and Tsien, R.W. (1990). Presynaptic enhancement shown by whole-cell recordings of long-term potentiation in hippocampal slices. Nature *346*, 177-180.

Martinez-Tellez, R.I., Hernandez-Torres, E., Gamboa, C., and Flores, G. (2009). Prenatal stress alters spine density and dendritic length of nucleus accumbens and hippocampus neurons in rat offspring. Synapse *63*, 794-804.

Matsuzaki, M., Ellis-Davies, G.C., Nemoto, T., Miyashita, Y., Iino, M., and Kasai, H. (2001). Dendritic spine geometry is critical for AMPA receptor expression in hippocampal CA1 pyramidal neurons. Nat. Neurosci. *4*, 1086-1092.

Matsuzaki, M., Honkura, N., Ellis-Davies, G.C., and Kasai, H. (2004). Structural basis of long-term potentiation in single dendritic spines. Nature *429*, 761-766.

Migaud, M., Charlesworth, P., Dempster, M., Webster, L.C., Watabe, A.M., Makhinson, M., He, Y., Ramsay, M.F., Morris, R.G., Morrison, J.H.*, et al.* (1998). Enhanced long-term potentiation and impaired learning in mice with mutant postsynaptic density-95 protein. Nature *396*, 433-439.

Miledi, R. (1966). Strontium as a substitute for calcium in the process of transmitter release at the neuromuscular junction. Nature *212*, 1233-1234.

Muller, D., Buchs, P.A., and Stoppini, L. (1993). Time course of synaptic development in hippocampal organotypic cultures. Brain research. Developmental brain research *71*, 93-100.

Norrholm, S.D., and Ouimet, C.C. (2000). Chronic fluoxetine administration to juvenile rats prevents age-associated dendritic spine proliferation in hippocampus. Brain Res. *883*, 205-215.

Nusser, Z., Lujan, R., Laube, G., Roberts, J.D., Molnar, E., and Somogyi, P. (1998). Cell type and pathway dependence of synaptic AMPA receptor number and variability in the hippocampus. Neuron *21*, 545-559.

Oliet, S.H., Malenka, R.C., and Nicoll, R.A. (1996). Bidirectional control of quantal size by synaptic activity in the hippocampus. Science *271*, 1294-1297.

Opazo, P., Sainlos, M., and Choquet, D. (2012). Regulation of AMPA receptor surface diffusion by PSD-95 slots. Current opinion in neurobiology *22*, 453-460.

Penzes, P., Johnson, R.C., Sattler, R., Zhang, X., Huganir, R.L., Kambampati, V., Mains, R.E., and Eipper, B.A. (2001). The neuronal Rho-GEF Kalirin-7 interacts with PDZ domain-containing proteins and regulates dendritic morphogenesis. Neuron *29*, 229-242.

Price, J.C., Guan, S., Burlingame, A., Prusiner, S.B., and Ghaemmaghami, S. (2010). Analysis of proteome dynamics in the mouse brain. Proceedings of the National Academy of Sciences of the United States of America *107*, 14508-14513.

Rao, A., Kim, E., Sheng, M., and Craig, A.M. (1998). Heterogeneity in the molecular composition of excitatory postsynaptic sites during development of hippocampal neurons in culture. J. Neurosci. *18*, 1217-1229.

Sans, N., Petralia, R.S., Wang, Y.X., Blahos, J., Hell, J.W., and Wenthold, R.J. (2000). A developmental change in NMDA receptor-associated proteins at hippocampal synapses. J. Neurosci. *20*, 1260-1271.

Schluter, O.M., Xu, W., and Malenka, R.C. (2006). Alternative N-terminal domains of PSD-95 and SAP97 govern activity-dependent regulation of synaptic AMPA receptor function. Neuron *51*, 99-111.

Schnell, E., Sizemore, M., Karimzadegan, S., Chen, L., Bredt, D.S., and Nicoll, R.A. (2002). Direct interactions between PSD-95 and stargazin control synaptic AMPA receptor number. Proc. Natl. Acad. Sci. USA *99*, 13902-13907.

Sheng, M., and Hoogenraad, C.C. (2007). The postsynaptic architecture of excitatory synapses: a more quantitative view. Annu. Rev. Biochem. *76*, 823-847.

Shi, S., Hayashi, Y., Esteban, J.A., and Malinow, R. (2001). Subunit-specific rules governing AMPA receptor trafficking to synapses in hippocampal pyramidal neurons. Cell *105*, 331-343.

Shin, S.M., Zhang, N., Hansen, J., Gerges, N.Z., Pak, D.T., Sheng, M., and Lee, S.H. (2012). GKAP orchestrates activity-dependent postsynaptic protein remodeling and homeostatic scaling. Nat. Neurosci. *15*, 1655-1666.

Shipman, S.L., Herring, B.E., Suh, Y.H., Roche, K.W., and Nicoll, R.A. (2013). Distance-Dependent Scaling of AMPARs Is Cell-Autonomous and GluA2 Dependent. J. Neurosci. *33*, 13312-13319.

Shipman, S.L., and Nicoll, R.A. (2012). A subtype-specific function for the extracellular domain of neuroligin 1 in hippocampal LTP. Neuron *76*, 309-316.

Shipman, S.L., Schnell, E., Hirai, T., Chen, B.S., Roche, K.W., and Nicoll, R.A. (2011). Functional dependence of neuroligin on a new non-PDZ intracellular domain. Nat. Neurosci. *14*, 718-726.

Smith, M.A., Ellis-Davies, G.C., and Magee, J.C. (2003). Mechanism of the distance-dependent scaling of Schaffer collateral synapses in rat CA1 pyramidal neurons. The Journal of physiology *548*, 245-258.

Smith, S.L., Smith, I.T., Branco, T., and Hausser, M. (2013). Dendritic spikes enhance stimulus selectivity in cortical neurons in vivo. Nature *503*, 115-120.

Soderling, T.R. (1999). The Ca-calmodulin-dependent protein kinase cascade. Trends Biochem. Sci. *24*, 232-236.

Song, I., and Huganir, R.L. (2002). Regulation of AMPA receptors during synaptic plasticity. Trends Neurosci. *25*, 578-588.

Stein, V., House, D.R.C., Bredt, D.S., and Nicoll, R.a. (2003). Postsynaptic density-95 mimics and occludes hippocampal long-term potentiation and enhances long-term depression. J. Neurosci. *23*, 5503-5506.

Steiner, P., Higley, M.J., Xu, W., Czervionke, B.L., Malenka, R.C., and Sabatini, B.L. (2008). Destabilization of the postsynaptic density by PSD-95 serine 73 phosphorylation inhibits spine growth and synaptic plasticity. Neuron *60*, 788-802.

Sun, Q., and Turrigiano, G.G. (2011). PSD-95 and PSD-93 play critical but distinct roles in synaptic scaling up and down. J. Neurosci. *31*, 6800-6808.

Takumi, Y., Ramirez-Leon, V., Laake, P., Rinvik, E., and Ottersen, O.P. (1999). Different modes of expression of AMPA and NMDA receptors in hippocampal synapses. Nat. Neurosci. *2*, 618-624.

Tatavarty, V., Sun, Q., and Turrigiano, G.G. (2013). How to scale down postsynaptic strength. J. Neurosci. *33*, 13179-13189.

Thiagarajan, T.C., Lindskog, M., and Tsien, R.W. (2005). Adaptation to synaptic inactivity in hippocampal neurons. Neuron *47*, 725-737.

Thiagarajan, T.C., Piedras-Renteria, E.S., and Tsien, R.W. (2002). alpha- and betaCaMKII: Inverse regulation by neuronal activity and opposing effects on synaptic strength. Neuron *36*, 1103-1114.

Tokumitsu, H., Inuzuka, H., Ishikawa, Y., Ikeda, M., Saji, I., and Kobayashi, R. (2002). STO-609, a specific inhibitor of the Ca(2+)/calmodulin-dependent protein kinase kinase. J. Biol. Chem. *277*, 15813-15818.

Tokumitsu, H., Inuzuka, H., Ishikawa, Y., and Kobayashi, R. (2003). A single amino acid difference between alpha and beta Ca2+/calmodulin-dependent protein kinase kinase dictates sensitivity to the specific inhibitor, STO-609. J. Biol. Chem. *278*, 10908-10913.

Tonnesen, J., Katona, G., Rozsa, B., and Nagerl, U.V. (2014). Spine neck plasticity regulates compartmentalization of synapses. Nat. Neurosci. *17*, 678-685.

Turrigiano, G.G., Leslie, K.R., Desai, N.S., Rutherford, L.C., and Nelson, S.B. (1998). Activity-dependent scaling of quantal amplitude in neocortical neurons. Nature *391*, 892-896.

Wang, H.L., Zhang, Z., Hintze, M., and Chen, L. (2011). Decrease in calcium concentration triggers neuronal retinoic acid synthesis during homeostatic synaptic plasticity. J. Neurosci. *31*, 17764-17771.

Wayman, G.A., Lee, Y.S., Tokumitsu, H., Silva, A.J., and Soderling, T.R. (2008). Calmodulin-kinases: modulators of neuronal development and plasticity. Neuron *59*, 914-931.

Xu-Friedman, M.A., and Regehr, W.G. (2000). Probing fundamental aspects of synaptic transmission with strontium. J. Neurosci. *20*, 4414-4422.

Xu, W., and Lipscombe, D. (2001). Neuronal Ca(V)1.3alpha(1) L-type channels activate at relatively hyperpolarized membrane potentials and are incompletely inhibited by dihydropyridines. J. Neurosci. *21*, 5944-5951.

Zhang, F., Prigge, M., Beyriere, F., Tsunoda, S.P., Mattis, J., Yizhar, O., Hegemann, P., and Deisseroth, K. (2008). Red-shifted optogenetic excitation: a tool for fast neural control derived from Volvox carteri. Nature neuroscience *11*, 631-633.

Publishing Agreement

It is the policy of the University to encourage the distribution of all theses, dissertations, and manuscripts. Copies of all UCSF theses, dissertations, and manuscripts will be routed to the library via the Graduate Division. The library will make all theses, dissertations, and manuscripts accessible to the public and will preserve these to the best of their abilities, in perpetuity.

Please sign the following statement:

I hereby grant permission to the Graduate Division of the University of California, San Francisco to release copies of my thesis, dissertation, or manuscript to the Campus Library to provide access and preservation, in whole or in part, in perpetuity.

Author Signature

11/17/15

Date